MINISTRY OF EDUCATION AND SCIENCE OF UKRAINE

NATIONAL AVIATION UNIVERSITY

FACULTY OF AIR NAVIGATION, ELECTRONICS AND TELECOMMUNICATIONS

AIR NAVIGATION SYSTEMS DEPARTMENT

PERMISSION FOR DEFENCE

Head of the Department

Doctor of Sciences (Engineering),

prof. _____V.Yu. Larin

"_____" _____ 2023

MASTER'S THESIS

ON THE EDUCATIONAL PROFESSIONAL PROGRAM
"SYSTEMS OF AIR NAVIGATION SERVICE"
(EXPLANOTARY NOTE)

Theme: "Optimizing and improving the efficiency of satellite systems in the aviation sector"

Performed by: **_____ A. V. Shtefan**

Supervisor: Cand. of Sc. (Engineering) **_____ O.S. Pogurelskiy**

Standard inspector **_____ G.F. Argunov**

KYIV 2023

МІНІСТЕРСТВО ОСВІТИ І НАУКИ УКРАЇНИ

НАЦІОНАЛЬНИЙ АВІАЦІЙНИЙ УНІВЕРСИТЕТ

ФАКУЛЬТЕТ АЕРОНАВІГАЦІЇ, ЕЛЕКТРОНІКИ ТА ТЕЛЕКОМУНІКАЦІЙ

КАТЕДРА АЕРОНАВІГАЦІЙНИХ СИСТЕМ

ДОПУСТИТИ ДО ЗАХИСТУ
Завідувач кафедри
д-р техн. наук, проф.
_____В.Ю. Ларін
«__»_____2023 р.

ДИПЛОМНА РОБОТА
(ПОЯСНЮВАЛЬНА ЗАПИСКА)

ВИПУСКНИКА ОСВІТНЬОГО СТУПЕНЯ МАГІСТРА
ЗА ОСВІТНЬО-ПРОФЕСІЙНОЮ ПРОГРАМОЮ
«СИСТЕМИ АЕРОНАВІГАЦІЙНОГО ОБСЛУГОВУВАННЯ»

Тема: «Задача оптимізації та підвищення ефективності супутникових систем в авіаційній сфері»»

Виконав: **_____ А.В. Штефан**

Керівник: к.т.н., доцент **_____ О.С. Погурельський**

Нормоконтролер, д.т.н., проф. **_____Г.Ф. Аргунов**

Київ 2023
НАЦІОНАЛЬНИЙ АВІАЦІЙНИЙ УНІВЕРСИТЕТ
Факультет: аеронавігації, електроніки та телекомунікацій_____
Кафедра: кафедра аеронавігаційних систем_____
Освітній ступінь: магістр_____
Спеціальність: 272 «Авіаційний транспорт»_____

Освітньо-професійна програма: Організація повітряного руху_____

ЗАТВЕРДЖЕНО
Начальник відділу
В. Ларін
«____»_____2023 р

Завдання магістерської роботи

Ім'я студента: Артем Штефан

1. Тема дисертації: «**Задача оптимізації та підвищення ефективності супутникових систем в авіаційній сфері**»
затверджено наказом ректора від 22 серпня 2023 року № 1443/ст.
2. Дипломна робота повинна бути виконана з: 23.10.2023 по 31.12.2023
3. Вихідні дані: теоретичні відомості керівних документів Міжнародної організації цивільної авіації та національних документів України у сфері забезпечення та виконання польотів цивільних повітряних суден.

4. Зміст пояснювальної записки (перелік питань до розгляду): Вступ; теоретичні основи супутникових систем в авіації; аналіз факторів, що впливають на ефективність супутникових систем в авіації; оптимізація супутникових систем для авіації; розробка та впровадження оптимізованих супутникових систем у сфері авіації; ефективність і переваги оптимізованих супутникових систем; висновки; посилання
5. Перелік обов'язкових графічних матеріалів: схема дослідження, графічний (ілюстративний) матеріал: малюнки, таблиці, формули.
Для графічної підтримки та презентації слід використовувати Microsoft office Excel, Power Point.

6. Календарний графік виконання магістерської роботи.

Завдання	Термін виконання робіт	записка про виконання
Підготовка огляду літератури	23.10.23 – 30.10.23	
Збір та аналіз інформації про супутникові системи	01.11.23 - 08.11.23	

Вивчення ролі супутників в авіації	09.11.23 – 16.11.23	
Дослідження впливу типу орбіт на працездатність	17.11.23 – 24.11.23	
Аналіз викликів погодних умов на супутниковий зв'язок	25.11.23 – 31.11.23	
Дослідження перешкод сигналу та забезпечення безперебійного зв'язку	01.12.23 – 05.12.23	
Розробка алгоритмів штучного інтелекту для оптимізації супутникових систем	06.12.23 – 11.12.23	
Аналіз та порівняння результатів тестування	12.12.23 - 15.12.23	
Написання пояснювальної записки	16.12.23 – 19.12.23	
Підготовка та оформлення презентації	20.12.23 – 22.12.23	
Допуск на можливі зміни та виправлення	23.12.23 – 25.12.23	

8. Дата випуску: «25» жовтня 2023 року.

Керівник магістерської роботи _____ Олексій ПОГУРЕЛЬСЬКИЙ

Виключив завдання _____ Артем ШТЕФАН

NATIONAL AVIATION UNIVERSITY

Faculty: *Air Navigation, Electronics and Telecommunications*
Department: *Air Navigation Systems Department*
Educational degree: *Master*
The specialty: *272 "Aviation Transport"*
Educational Professional Program: *Air Traffic Management*

APPROVED BY

Head of the Department
_____ V. Larin
"____" _____2023

Master's Thesis Assignment

Student`s name: Artem Shtefan

1. The thesis theme: "***Optimizing and improving the efficiency of satellite systems in the aviation sector"***
approved by the Rector's order *of "22" August 2023 № 1443/cm*

2. The thesis should be performed from : *23.10.2023 to 31.12.2023*

3. Initial data: *theoretical data of the International Civil Aviation Organization's governing documents and national documents of Ukraine in the field of ensuring and performing civil aircraft flights.*

4. The content of the explanatory note (the list of problems to be considered): *Introduction; theoretical foundations of satellite systems in aviation; analysis of factors affecting the effectiveness of satellite systems in aviation; optimization of satellite systems for aviation; development and implementation of optimized satellite systems in the field of aviation; efficiency and advantages of optimized satellite systems; conclusions; references*

5. The list of mandatory graphic materials*: research scheme, graphic (illustrative) material: drawings, tables, formulas.*
Microsoft office Excel, Power Point should be used to provide graphic support and presentation.

6. Calendar Schedule of Performing the Master's thesis.

Tasks	Period of works execution	execution note
Preparation of a literature review	23.10.23 – 30.10.23	
Collection and analysis of information about satellite systems	01.11.23 - 08.11.23	
Study of the role of satellites in aviation	09.11.23 – 16.11.23	
Study of the influence of the type of orbits on performance	17.11.23 – 24.11.23	

Analysis of the challenges of weather conditions on satellite communications	25.11.23 – 31.11.23	
Study of signal interference and ensuring uninterrupted communication	01.12.23 – 05.12.23	
Development of artificial intelligence algorithms for optimization of satellite systems	06.12.23 – 11.12.23	
Analysis and comparison of test results	12.12.23 - 15.12.23	
Writing an explanatory note	16.12.23 – 19.12.23	
Preparation and design of the presentation	20.12.23 – 22.12.23	
Allowance for possible changes and corrections	23.12.23 – 25.12.23	

8. Date of issue: «25» October 2023.

Supervisor of master's thesis _____ Olexiy POGURELSKIY

Excepted the task _____ Artem SHTEFAN

ABSTRACT

The purpose of the thesis -analysis and optimization of satellite systems in the context of aviation in order to improve their efficiency and ensure the safety and reliability of air transportation. The work is aimed at revealing the potential of satellite technologies to improve various aspects of the aviation industry.

Object of study - satellite systems used in aviation. Satellite systems are an integral part of air transport infrastructure and have a significant impact on the safety, efficiency and reliability of aviation services. The research is aimed at analyzing, optimizing and improving these systems in order to ensure better quality of aviation operations.

Subject of study -the process of optimizing and improving the efficiency of satellite systems in the field of aviation. This includes the analysis of technical, technological and functional aspects of satellite systems, as well as the study of the impact of various factors on their performance and reliability in the context of aviation operations.

Research methods -Analysis of literary sources, statistical analysis, use of computer programs, experiments and testing, mathematical modeling, empirical methods

Relevance -the relevance of the research lies in the possibility of improving aviation operations, making them safer, more efficient and environmentally sustainable through the development and optimization of satellite systems.

The result of the thesis is recommended to be used for Aviation Industry: The developed strategies for optimization and improvement of satellite systems can be used by airlines, airports and aircraft equipment manufacturers to increase the efficiency of air transport, ensure the accuracy of navigation and improve communication between aircraft.

AIR TRAFFIC SERVICEOPTIMIZATION, IMPROVEMENT OF EFFICIENCY, SATELLITE SYSTEMS, IMPROVEMENT, ARTIFICIAL INTELLIGENCE

REMARKS SHEET

CONTENT

List of conventional abbreviations

ACC - Aviation satellite systems

AG - Aviation industry

ANS - Aviation Navigation System

GNSS - Global Navigation Satellite System

SSP - Satellite positioning system

TSO - Operator connection point

NSS - Ground Segmented System

PSS - Air segmented satellite communication

ICT - Information and communication technologies

AI - Artificial Intelligence

MN - Machine learning

PZ - Software

TP - Telecommunication services

PO - Air Ocean

NASA - National Aerospace Agency

ICAO - International Civil Aviation Organization

RLS - Radar system

RS - Radio system

STS - Specialized telecommunication system

DNS - Long-range navigation satellite

Terms and definitions

1. Satellite system: A complex of technical means, which includes satellites, ground equipment and software, designed to provide communication, navigation, telemetry and other functions over long distances.

2. Aviation Satellite System (ASA): A satellite system specially designed and configured for aviation tasks, including navigation, communication and monitoring.

3. Navigation Satellite System (NSS): A system that uses satellites to determine the location, coordinates, and paths of objects, including aircraft.

4. Satellite positioning: The process of determining the geographical position of an object using signals sent by satellites and their processing at the receiver.

5. Global Navigation Satellite System (GNSS): A navigation system that consists of a collection of satellites located in space and ground-based receivers designed to determine a precise position on the Earth's surface.

6Satellite Communication: A form of wireless communication in which signals are transmitted from aircraft to satellites and vice versa, providing a communication network even in remote and hard-to-reach regions.

7. Artificial Intelligence (AI): A branch of computer science that studies the creation of programs and systems that perform tasks that normally require human intelligence, including learning, language understanding, and decision-making.

8. Machine Learning: A subfield of AI that explores the development of algorithms and models that allow computers to learn from data and improve their performance over time.

9. Communication stability: The property of a satellite system to provide continuous and reliable data exchange even in conditions of limitations or obstacles.

10. Bandwidth: The maximum amount of data that can be transmitted through a satellite system per unit of time.

INTRODUCTION

Satellite communication is a popular and important means of data transmission in the world. It is used to create networks of national and international level, as well as for television broadcasting and individual reception. Satellite systems are usually more expensive to install and operate than their terrestrial counterparts. Overcoming technical challenges in the form of creation and maintenance of satellites, antennas and receiving devices requires high technologies and space resources.

From an economic point of view, satellite systems are massive and can serve millions of users. Therefore, it is important to ensure the efficient and cost-effective operation of the entire infrastructure.

Finally, national satellite systems often affect neighboring countries and other international satellite systems. Therefore, international coordination and regulation are important aspects that ensure interoperability and electromagnetic compatibility between different satellite systems and other

CHAPTER 1. BASIC INFORMATION ABOUT MODERN SATELLITE COMMUNICATION SYSTEMS

1.1 Introduction to satellite communications

Satellites are specially designed for telecommunication purposes. They are used for mobile applications such as communications with ships, automobiles, aircraft, handheld terminals, and television and radio broadcasting. They are responsible for providing these services in a certain region (area) on Earth. The power and bandwidth of these satellites depend on the desired footprint size, the complexity of traffic management schemes, and the cost of earth stations.

The satellite works most efficiently when the transmissions are aimed at the desired area. If the area is directional, then the radiation does not go beyond the defined

area, thereby minimizing interference with other systems. This contributes to a more efficient use of the spectrum.

Satellite antenna directional patterns play an important role and must be designed to best cover a defined geographic area (which is typically irregular in shape).

Satellites must be designed to be usable for short- and long-term effects throughout their lifetime. The ground station must be able to control the satellite if it moves out of orbit or is subject to any kind of resistance from external forces.

- Application of satellites:
- Weather forecasts
- Radio and television broadcasting
- Military satellites
- Navigation satellites
- Global phone
- Connection with remote areas
- Global mobile communication

1.2 Information on satellite parameters

If we assume that the Earth has an ideal spherical shape and the Earth's gravitational force is the only one acting on the satellite, then the motion of the satellite will correspond to Kepler's well-known laws. The orbit of the satellite will have the shape of an ellipse, where one of the foci of the ellipse is located in the center of the Earth (see Fig. 1.1), and the plane of the orbit passes through the center of the Earth and remains unchanged. Since the movement of the satellite takes place in airless space, it will not be affected by air resistance. In orbits with high apogees, the motion of the satellite can continue for hundreds of years. Practically, the service life of a satellite is determined by the duration of the functioning of its electronic equipment for communication and control, as well as the efficiency of solar batteries. It may also be limited by the amount of fuel for engines that periodically adjust the satellite's orbit due to the influence of other celestial bodies, gravitational deviations from the spherical shape of the Earth, and other factors. As the distance from the Earth increases, the speed

of the satellite decreases (the period of rotation increases), and as it approaches the Earth, the speed of the movement increases.

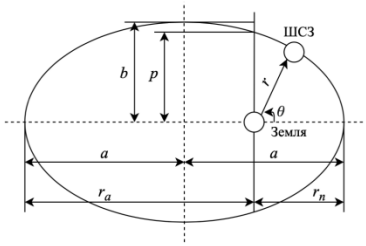

Figure. 1.1. The SHSZ orbit and its main parameters

The equation describing the elliptical orbit of the satellite in the polar coordinate system can be written as follows:

$$r = \frac{p}{1 + e \cdot cos(\theta)}$$

Where:

r- radius vector module, i.e. the distance from the satellite to the center of the Earth;

θ- the angular coordinate of the radius vector, which is also called the true anomaly;

e- eccentricity of the orbit, which can be in the range from 0 to 1;

$p$is the focal parameter, which is calculated as$p = \frac{b^2}{a} = a(1 - e^2)$

$a$and b are the semi-major and minor axes of the ellipse.

Eccentricity e can take different values in the interval from 0 to 1. When e=0, the orbit becomes circular, the foci merge with the center, and r=p. The perigee of the orbit corresponds to the minimum distance from the satellite to the center of the Earth (i.e. r=rn), and the apogee is the maximum distance (i.e. r=ra).

The parameters of the elliptical orbit a and b are interconnected by the following relations:

$a = \frac{ra+rn}{2}$- the average value of the semi-major axis;

$b^2 = a^2(1 - e^2)$ - the square of the minor semi-axis;

$e = \sqrt{1 - \frac{b^2}{a^2}}$- eccentricity;

$r_{a=} \frac{p}{1-e}$- apogee;

$r_{a=} \frac{p}{1+e}$- perigee

The distance between the foci of the ellipse and the center of the Earth is ae, and the height of the satellite above the surface of the Earth H can be expressed as

H=r−R,

where R is the radius of the Earth.

The line where the plane of the orbit intersects the plane of the equator is called the "nodal line," and the angle i between the plane of the orbit and the plane of the equator is known as the "inclination of the orbit."

The formula for the potential of the central gravitational field has the form:

$$U = \frac{fM}{r}$$

Where=6.672f·1011 $м^3 \cdot кг \cdot сек^{-2}$- gravitational constant attraction; M=5.947·10^{24}kg - mass of the Earth; r is the distance from the center of the Earth to the point where the gravitational potential is calculated.

The quantity μ=fM=398,600.5() is known as the "gravitational constant of the Earth." This quantity is related to the field potential and represents the force that acts on a material point (for example, a satellite) in the gravitational field during movement.$км^3/сек^2$

Determining the parameters of the unforced motion of a material point (for example, a satellite) in the gravitational field of a central body (for example, the Earth) is called the "two-body problem."

1.3 Kepler's laws

1.3.1 Introduction to Kepler's laws

Satellites (spacecraft) orbiting the Earth obey the same laws that govern the motion of the planets around the Sun.

Kepler's laws apply quite generally to any two bodies in space interacting through gravity. The more massive of the two bodies is called primary, the other - secondary or satellite.

1.3.2 Kepler's first law

Kepler's first law states that the path along which the satellite moves around the primary body will be an ellipse. The ellipse has two focal points, marked as F1 and F2 in Fig. 1.2. The center of mass of two bodies, called the barycenter, is always at the center of the foci. The semi-major axis of the ellipse is denoted as a, and the semi-minor axis is denoted as b. Eccentricity e is calculated by the formula:

$$e = \frac{\sqrt{a^2 - b^2}}{a}$$

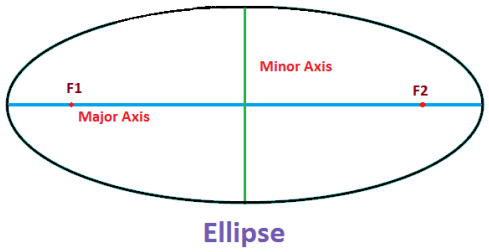

Figure. 1.2 F1 and F2 foci, semimajor axis a and semiminor axis b of the ellipse.

1.3.3 Kepler's second law

Kepler's second law states that for equal periods of time the satellite will pass equal areas in its orbital plane centered around the barycenter. Referring to Fig. 1.3,

suppose that the satellite covered distances S1 and S2 meters in 1 second, then the areas A1 and A2 will be equal. The average speed in each case is S1 and S2 m/s, and because of the law of equal areas, it follows that the speed at S2 is less than at S1.

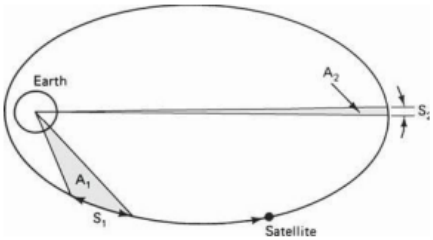

Figure. 1.3 Kepler's second law. Areas A1 and A2 traveled per unit time are equal.

1.3.4 Kepler's third law

Kepler's third law states that the square of the period of rotation is proportional to the cube of the average distance between the two bodies. The average distance is equal to the semimajor axis a. For artificial satellites of the Earth, Kepler's third law can be written in the following form:

$$a^3 = \mu/n^2$$

where n is the average movement of the satellite in radians per second, and μ is the Earth's geocentric gravitational constant equal to 3.986005 x 10^14 m^3/s^2.

1.4. Newton's laws:

1.4.1 Newton's first law

An object that is at rest will remain at rest unless acted upon by an unbalanced force. An object in motion continues to move at the same speed and in the same direction unless acted upon by an unbalanced force. This law is often called the "law of inertia".

1.4.2 Newton's second law

Acceleration occurs when a force acts on a mass. The greater the mass (of the object being accelerated), the greater the force required (to accelerate the object).

1.4.3 Newton's third law

For every action there is an equal and opposite reaction. This means that for every force there is a reaction force that has the same magnitude but opposite direction. In other words, when an object pushes on another object, it receives a corresponding pressure in the opposite direction.

1.5. Orbital parameters:

- Apogee: The point in a satellite's orbit that is farthest from Earth. Denoted as ha.
- Perigee: The point of a satellite's orbit closest to Earth. Denoted as hp.
- Line of apsides: A line connecting perigee and apogee through the center of the Earth. This is the main axis of the orbit. Half the length of this line is the semimajor axis and corresponds to the average distance of the satellite from the Earth.
- Ascending node: The point where the orbit crosses the equatorial plane going from north to south.
- Descending node: The point where the orbit crosses the equatorial plane going from south to north.
- Inclination: The angle between the orbital plane and the equatorial plane of the Earth. It is measured at the ascending node from the equator to the orbit, in the direction of east to north. Also, this angle is often denoted as i.
- Line of nodes: The line that connects the ascending and descending nodes through the center of the Earth.
- Prograde orbit: An orbit in which the satellite moves in the same direction as the Earth's rotation. The inclination is always in the range from 0 to 90 degrees. Many

satellites follow this trajectory because of the high speed of the Earth's rotation, which makes them easier to launch.

- Retrograde orbit: An orbit in which the satellite moves in the direction opposite to the Earth's rotation.

- Perigee argument: The angle from the perigee point in the orbital plane, calculated at the center of the Earth, in the direction of the satellite's motion.

- Direct relation of lifting node: Determination of orbit in space, position of lifting node is determined. But since the Earth rotates, the elevation longitude of the node changes and cannot be used for reference. Therefore, for the practical determination of the orbit, the longitude and time of crossing the ascent node are used. An absolute measurement requires a fixed point in space. It can also be defined as "the direct relation of the elevation of the node; the direct relation is the angular position calculated due east along the celestial equator from the vernal equinox to the hour circle of the object".

- Average anomaly: It provides the average value of the angular position of the satellite relative to the perigee.

- True anomaly: This is the angle from the perigee point to the position of the satellite, measured at the center of the Earth.

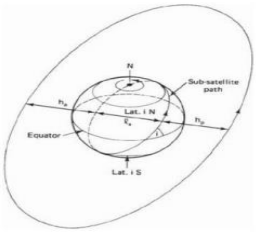

Figure. 1.4 shows the height of apogee (ha), height of perigee (hp) and slope (i). The line marked "L" represents the line of apses.

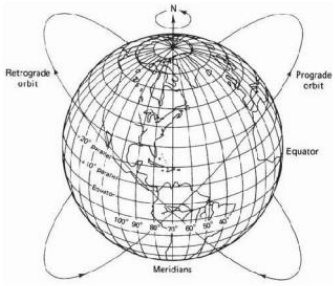

Figure. 1.5 Clockwise and reverse orbits.

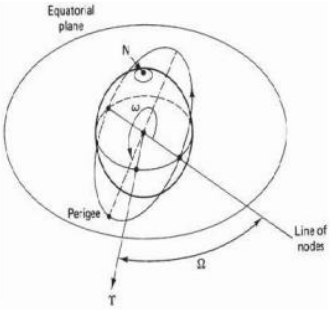

Figure. 1.6 The perigee argument (w) and the direct relation of the node elevation (Ω).

1.6. Orbital deviations

Theoretically, the orbit described by Kepler is ideal because the Earth is considered to be a perfect sphere and the force acting around the Earth is a centrifugal force. This force is assumed to balance the Earth's gravitational pull.

In reality, other forces also play an important role and affect the satellite's motion. These forces are the gravitational forces of the Sun and the Moon along with atmospheric drag. The influence of the Sun and the Moon is more pronounced on satellites in geostationary orbits, while the effect of atmospheric drag is more pronounced on satellites in low orbits around the Earth.

1.6.1 Influence of the non-spherical shape of the Earth

Since the shape of the Earth is not a perfect sphere, this leads to some variation in the path the satellites take around the primary object. Since the Earth protrudes from the equatorial belt, and given that the orbit is not a physical entity, but the forces arising from the orbiting Earth act on the satellite and change the orbital parameters. This leads to a displacement of the satellite due to the regression of the nodes and the latitude of the perigee point (the point closest to the Earth). This leads to the rotation of the apse line.

As the orbit itself moves relative to the Earth, changes occur in the values of the perigee argument and the direct ratio of the elevation of the node. As a result of the non-

spherical shape of the Earth, there is another effect known as the "Satellite Graveyard". The non-spherical shape leads to a small value of eccentricity (10^-5) in the equatorial plane. This creates a gravitational gradient on satellites in geostationary orbits and causes them to drift toward one of two stable points that coincide with the minor axes of the equatorial ellipse.

1.6.2 Atmospheric resistance

For satellites that rotate in low orbits around the Earth, the effect of atmospheric resistance is more pronounced. The influence of this resistance is maximal at the point of perigee. Drag (attraction to the Earth) affects the speed of the satellite (the speed decreases). This leads to the fact that the satellite does not reach the height of the apogee in successive revolutions. This leads to a change in the value of the semimajor axis and the eccentricity. Satellites in service are adjusted by the ground station to return to their original orbit.

1.7 Station support

In addition to orientation control, it is important that the geostationary satellite remains in its correct orbital slot. The equatorial ellipticity of the Earth causes the geostationary satellites to slowly drift along the orbit to one of two stable points located at 75° East and 105° West longitude. To compensate for this drift, the satellite is given a rotating component of speed by means of jet engines that are fired once every 2 or 3 weeks. These maneuvers are called east-west station-keeping maneuvers. Satellites in the 6/4 GHz band must remain within 0.1° of the assigned longitude, and in the 14/12 GHz band within 0.05°.

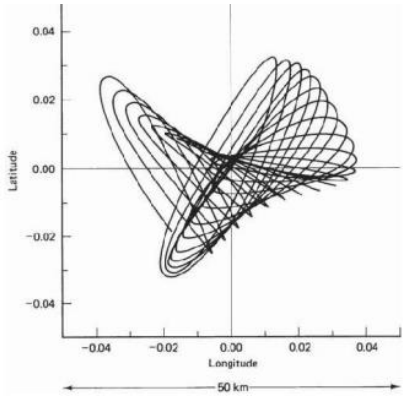

Figure. 1.7 Typical satellite movement.

1.8. Geostationary and non-geostationary orbits

1.8.1. Geostationary

A geostationary orbit is an orbit in which the satellite revolves around the Earth with accuracy to the same speed of the Earth's rotation and at the same latitude, specifically - zero, the latitude of the equator. A satellite in geostationary orbit appears to be suspended in the same place in the sky and is directly above the same area of the Earth's surface at all times.

A geosynchronous orbit is an orbit in which the satellite is synchronized with the Earth's rotation, but the orbit is tilted relative to the plane of the equator. A satellite in geosynchronous orbit will move up and down in latitude, although it will remain above the same line of longitude. Although the terms "geostationary" and "geosynchronous" are sometimes used interchangeably, they are not technically identical; geostationary orbit is a subset of all possible geosynchronous orbits.

The person most credited with developing the concept of geostationary orbits is science fiction author Arthur C. Clarke (books "Islands in the Sky", "Childhood", "A Meeting with Rama" and the film "2001: A Space Odyssey"). Others had previously indicated that bodies that had traveled a certain distance above the Earth on the equatorial plane remained motionless relative to the Earth's surface. But Clark published an article in the magazine "Wireless World" in 1945, where he took the step from the German government's rocket research to the idea of creating permanent artificial satellites that could serve as communication relays.

Objects in geostationary orbit must be at a certain distance from the Earth's surface; closer to the Earth, the orbit will deteriorate, and further they will be forced by the Earth's gravity altogether. This distance is 35,786 kilometers (22,236 miles) from the surface.

The first geosynchronous orbit satellite was launched in 1963, and the first geostationary one the following year. Since there is only one geostationary orbit in the plane with the equator at a distance of 35,786 kilometers, there is only one circle around the world where these conditions are met.

This means that the "real estate" in geostationary orbit is limited. Although the satellites are not in danger of colliding with each other, they must be positioned along this circle so that their frequencies do not interfere with the work of their nearest neighbors.

1.8.2 Geostationary satellites

There are two types of artificial satellites in the sky: one type orbits the Earth once or twice a day, and the other type is called a communication satellite and is stationary 22,300 miles (35,900 km) above the equator of the fixed Earth.

Satellites orbiting the Earth include the Space Shuttle and the International Space Station, which are in Low Earth Orbit (LEO) to avoid the deadly Van Allen radiation belts.

The most prominent satellites in the Mean Earth Orbit (MEO) are the satellites that make up the GLOBAL POSITIONING system, or GPS, as it is called. Global Positioning System (GPS)

The Global Positioning System was developed by the US military and then opened up for civilian use. It is used today to track planes, ships, trains, cars, or literally anything that moves. Anyone can buy a receiver and track their exact location using a GPS receiver.

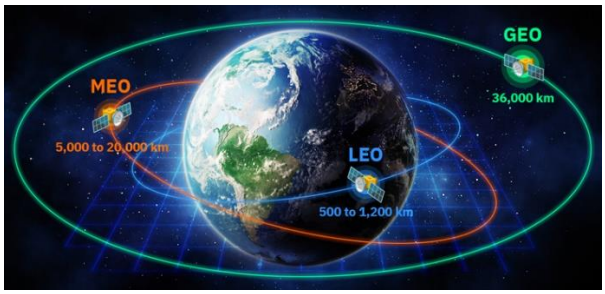

Figure. 1.8 Geostationary and non-geostationary orbits.

1.9 Artificial satellites and their types

An artificial satellite is any artificial object launched into orbit with the help of rockets. These spacecraft are equipped with sensitive instruments and cameras to study Earth and other planets, facilitate communication, and even observe the distant universe. Thanks to their wide field of view and improved spatial resolution, they can collect information much faster than ground-based sensors. Also, unlike ground-based observatories, the view from space is not obstructed by any type of atmospheric obscuration such as clouds and dust.

Each spacecraft goes into space for a different type of mission, be it communications, scientific research, weather forecasting, or field observation. The purpose of the satellite will determine its size, orbit type and general location. Although there are different types of artificial satellites and their orbits, they all follow the same physical laws and mathematical calculations when they reach space.

1.9.1 Types of satellites by orbit

In most cases, after launch, the satellite is placed in one of several predetermined orbits around the Earth. But in some cases, it can be directed on an interplanetary journey, following a path around the Sun until it reaches its final destination.

Satellites are usually classified based on their orbital altitude (distance from Earth's surface), which directly affects their coverage and the speed at which they travel around the planet. When choosing an orbit type, spacecraft designers must consider its

intended purpose, the data it receives and the services it offers, as well as cost, coverage, and the ability to use different orbits. 5 main types of satellites depending on their orbits:

- low earth orbit (LEO);
- mean Earth orbit (MEO);
- geostationary orbit (GEO);
- Sun-synchronous orbit (SSO);
- geostationary transfer orbit (GTO).

1.9.2 Low Earth Orbit (LEO) Satellites.

Satellites in low Earth orbit move at an altitude of approximately 160–1500 kilometers above the Earth's surface. They have a short orbital period of 90 to 120 minutes, meaning they can travel around the planet up to 16 times a day. This makes them particularly suitable for all types of remote sensing, high-resolution earth observation and scientific research, as data can be acquired and transmitted quickly.

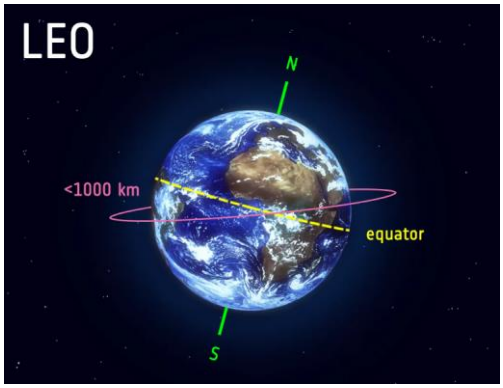

Figure. 1.9 Low Earth Orbit (LEO) Satellites

All types of satellites in LEO can change the angle of inclination of their plane relative to the Earth's surface. The type of low Earth orbit is very common because it provides more potential paths for spacecraft. However, due to their proximity to Earth, they have a smaller coverage area than other types of satellites. Often groups of LEO spacecraft, known as satellite constellations, are launched together to form a type of network encircling the Earth. This allows them to cover huge areas at the same time, working together.

1.9.3 Satellites in the mean Earth orbit (MEO).

Medium-Earth orbit is located between low-Earth and geostationary orbits, typically at an altitude of approximately 5,000 to 20,000 kilometers. Positioning and navigation services such as GPS make extensive use of MEO-type satellites. MEO's high-throughput satellites (HTS) have recently been commissioned to provide low-latency data transmission to service providers, commercial and government organizations.

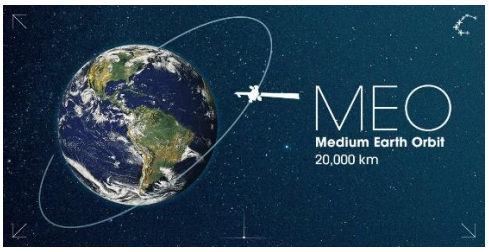

Figure. 1.10 Satellites in the medium Earth orbit (MEO)

With a longer orbital period (typically 2 to 12 hours), this type of satellite offers the best trade-off between coverage area and data rate. Compared to low-Earth orbit spacecraft, MEOs require fewer devices to provide worldwide coverage, but their latency is longer and their signals are weaker.

1.9.4 Satellites in Geostationary Orbit (GEO)

Spaceships in geostationary orbit are located at an altitude of 35,786 kilometers above the Earth's surface, exactly above the equator. The three evenly spaced machines in GEO can provide near-global coverage due to the vast area they cover on Earth.

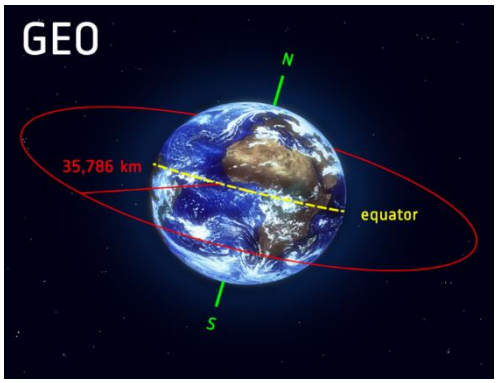

Figure. 1.11 Satellites in Geostationary Orbit (GEO)

Objects in GEO appear stationary from Earth because their orbital period is identical to Earth's rotation of 23 hours 56 minutes and 4 seconds. This allows the ground antenna to always point to the same device in space. This is why this type of satellite is ideal for always-on communications services such as television and telephones.

In addition, this type can be used in meteorology to monitor the weather in specific regions and track the development of local patterns. The disadvantage of GEO-type spacecraft for real-time communication is a longer signal delay caused by their great distance from Earth.

1.9.5 Satellites in sun-synchronous orbit (SSO).

Satellites of the sun-synchronous orbit type pass from north to south through the polar regions at an altitude of 600 to 800 km above the Earth. The orbital inclination and altitude of the SSO spacecraft are calibrated so that they always cross any given location at exactly the same local solar time. Thus, the lighting conditions are suitable for image acquisition, making this type of satellite ideal for Earth observation and environmental monitoring.

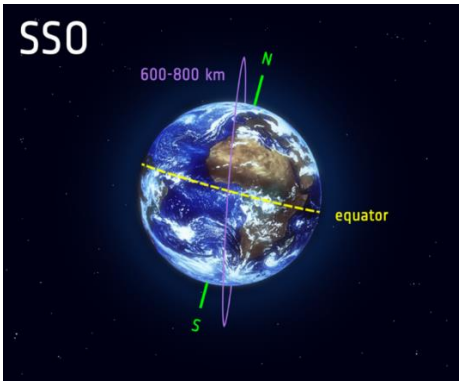

Figure. 1.12 Satellites in Sun-Synchronous Orbit (SSO)

This also means that current and past SSO satellite images are well suited for change detection. Scientists use these image sequences to learn about developing weather patterns, predict cyclones, monitor and prevent wildfires and floods, and gather information about long-term problems such as deforestation and shoreline changes. But

due to the lower orbital altitude, SSO-type spacecraft can only cover a smaller region at a time, requiring more vehicles.

1.9.6 Satellites in geostationary orbit (GTO).

The most common type of satellite orbit is geostationary, which is used to transition from a transition orbit to a GSO. Spacecraft are not always launched directly into a final orbit when they are launched from Earth into space by launch vehicles such as the Falcon 9. Rockets carrying payloads to GEO drop them into intermediate orbits that are halfway to their final position. The satellite's engine is then fired to reach the destination orbit and adjust its inclination. This shortcut allows the vehicle to enter geostationary orbit with minimal resources.

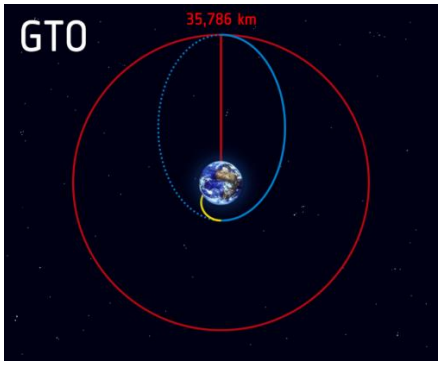

Figure. 1.13 Satellites in Geostationary Orbit (GTO)

Other, less common types of orbits include a highly elliptical orbit (HEO), a polar orbit, and a Lagrange point (L-point). The goals and objectives of the spacecraft will dictate the type of orbit chosen. Because of this, you should think more about the types of satellites according to the programs.

1.10 Satellites and their functions

The provision of telecommunications and television services is only the tip of the iceberg when it comes to the use of space technology. Many types of satellites have been launched in recent years for a variety of scientific purposes, including Earth observation, meteorological research, navigation, studying the effects of spaceflight on living organisms, and gaining insight into space. Today, the most common are four types of satellites according to their application:

- communication;
- Earth observation;
- navigation;
- astronomical.
- Communication satellites

A communications spacecraft, usually located at GEO and equipped with a transponder—an integrated radio signal receiver and transmitter—can receive signals from Earth and relay them back to the planet. As a result, communication channels are opened between regions that previously could not communicate with each other due to long distances or other obstacles. Different types of communications satellites facilitate different forms of media transmission, such as radio, television, telephone, and the Internet.

Using the spacecraft type of communication, you can relay many signals simultaneously. Space vehicles for broadcasting and distributing the television signal to ground stations usually have individual repeaters for each carrier. However, in most cases, several operators will be relayed by one transponder. Due to compatibility with mobile terminals, this type of satellites is ideal for long-distance communication.

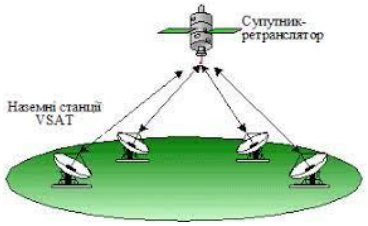

Figure. 1.14 Satellites and their functions

1.10.1 Earth observation satellites

Earth observation satellites are designed to observe our planet from space and report any changes they observe. This type of space technology enables continuous and repeatable monitoring of the environment, as well as rapid analysis of events during emergencies such as natural disasters and armed conflicts.

The objectives of the observation mission determine the type of satellite sensors used to observe the Earth. The information collected depends on the type of sensor used and the available frequency ranges.

Figure. 1.14 Jan-2-30

Earth observation spacecraft can be divided into the following types:

- Weather satellites are used to monitor and forecast weather trends and provide actual weather data. GEO is ideal for various types of weather satellites because it provides a constant vantage point that allows scientists to track cloud structure and predict cloud movement.
- The main application of remote sensing satellites is all kinds of environmental monitoring and geographic mapping. Machines used for various types of remote sensing orbit the Earth in one of three orbits: polar, non-polar LEO, or GEO. Geographic Information System (GIS) satellites are a type of remote sensing spacecraft whose primary function is to provide images suitable for GIS mapping and subsequent spatial analysis.

1.10.2 Navigation satellites

The constellations of the navigation system are located at a distance of 20,000 to 37,000 kilometers from the Earth's surface. This type of satellite sends signals that show their time, position in space, and health status. There are two main types of space navigation systems:

- Global Navigation Satellite System (GNSS) spacecraft broadcast signals that GNSS receivers receive and use for geolocation purposes, providing global

coverage. Galileo in Europe, GPS in the United States, and the BeiDou navigation satellite system in China are all examples of GNSS.

- The Regional Navigation Satellite System (RNSS) is an autonomous regional navigation system that provides coverage on a regional scale. For example, India's IRNSS project aims to provide a reliable location-based service to Indian citizens.

Figure. 1.15 Navigation satellites

1.10.3 Astronomical satellites

Essentially, an astronomical satellite is a giant telescope in orbit. It is able to see well unobstructed by the Earth's atmosphere, and its infrared imaging technology can work properly without misleading the planet's surface temperature. A type of satellite used in astronomy has a vision ten times better than the most powerful telescope on Earth.

Spaceships used in astronomy can be divided into several different types:

- Astronomical satellites are used to study various types of celestial bodies and phenomena in space, from mapping the surfaces of stars and planets and obtaining images of the planets in our solar system to studying black holes.
- Using climate research satellites equipped with specific types of sensors allows scientists to collect comprehensive, multifaceted data about the world's oceans and ice, land, biosphere, and atmosphere.
- Space studies of cells and structures of plants and animals are possible thanks to biosatellites. Because they allow scientists from different regions to work together, this type of spacecraft plays a crucial role in the advancement of medicine and biology.

The vast majority of satellites can perform more than one function at a time. However, it is a general recommendation that researchers diversify the types of satellites

they use to obtain more complete and accurate results from their research. EOSDA LandViewer is a useful tool for this, as it integrates images collected in space (including high resolution) from many sources and provides a convenient interface for searching and downloading the images you need.

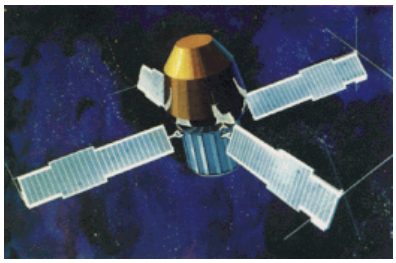

Figure. 1.16Small Astronomical Satellite 2, also known as SAS-2, SAS B or Explorer 48

1.11 Recent achievements of space technology and its future prospects

All types of satellites, classified by orbit or function, have become vital to our daily lives. In addition to facilitating communication, navigation, spatial analysis, weather forecasting, disaster management, and astronomical knowledge, these types of space devices also help us gain a deeper knowledge of our place on Earth and in the universe.

Advances in technology, including shrinking computers and other components, have made it easier to launch various types of remote sensing satellites. In 2022, 6,905 active satellites orbited the Earth, which is 43.8% more than in the previous year. Of course, this number will continue to grow, eventually giving people on Earth opportunities they could only dream of before.

We must continue to pour resources into space technology because it can greatly improve human life. Satellites enable real-time monitoring and data collection from inaccessible regions, allowing us to make informed decisions about pressing issues such as climate change and natural disasters. By expanding connectivity to rural and underdeveloped areas, they can drive economic growth and help bridge the digital divide, leading to a fairer and more sustainable future for all.

Conclusions regarding the first chapter:

1. Satellite communication is widely used for various purposes and for various types of communication.

2. The need for satellite communication arose in order to improve the efficiency of information transmission due to the lack of direct radio communication between points.

3. The variety of applications of artificial satellites requires a certain level of adaptability on the part of telemetry data transmission and reception systems.

4. The complexity of satellite systems implies the need to achieve very high accuracy.

CHAPTER 2. ADVANTAGES OF AVIATION OVER SATELLITE NAVIGATION

Retreat

Global Navigation Satellite Systems (GNSS) are useful for aviation because they allow aircraft to fly directly from their point of departure to their destination, using the most economical routes and navigating difficult low-altitude terrain. Satellite navigation provides the opportunity to develop new procedures that allow aircraft to fly closer together to increase arrival and departure speeds and perform constant takeoffs and descents to minimize fuel consumption, noise and carbon emissions. In the language of the aviation community, HSSN allows for performance-based navigation, which includes area navigation (RNAV) and mandatory navigation performance (RNP). Both RNAV and RNP allow unlimited point-to-point routes. RNP differs from RNAV in that it also provides a monitoring and alert function to alert the pilot of the need for correction, allowing aircraft to fly more precisely. HSSN is the only source of navigation approved for RNP operations.

Introduction

Global Navigation Satellite Systems (GNSS) serve a large number of users in the air, on land, at sea and in space. These users around the world have the ability to receive location accuracy at the level of 5 meters at any hour and in any weather. If even greater precision is required, there are differential techniques that make it possible to achieve precision in decimeters or even centimeters.

Figures 2.1 and 2.2 show the satellites that provide this global utility. In particular, Figure 1 shows the Global Positioning System (GPS) satellites in orbit at the end of 2014. The GPS satellites are in the Mean Earth Orbit (MEO), and seven satellites in the Geostationary Orbit (GEO) complement this core constellation, broadcasting safety information for aviation. GPS was the backbone of the HSSN, but new constellations are being deployed by China and Europe. Figure 2.2 shows all HSSN satellites in orbit at

the end of 2014. As can be seen, this superset is located in MEO, GEO and inclined geosynchronous orbits.

HSSN is a passive system; the signal travels from the satellites to the users without the user emitting any signals. These satellite signals are in the L-band of the radio spectrum (1.0-2.0 GHz) and are designed to allow users to measure signal time of arrival (ToA) very precisely. With four such ToA measurements, users can estimate their latitude, longitude, altitude and time offset relative to satellite system time. In short, four (or more) equations are used to estimate these four unknowns. HSSN resolves the user's time offset relative to HSSN system time, which in turn is related to Coordinated Universal Time (UTC). For this reason, the GPSN is called the Space Positioning, Navigation and Timing (PNT) system.

Figure 2.3 shows the main operation associated with one of the HSSN satellites. Each satellite sends out a signal created with special care, which allows the receiving equipment to accurately measure the range. The signal from each HSSN satellite has two components. First, each satellite sends a unique code that creates sharp radio signatures that the receiver can easily distinguish from background noise and signals from other satellites. This code has special correlation properties that allow the user to accurately measure its ToA to within a few billionths of a second.

Second, each satellite adds the necessary data to these codes using a so-called navigation message. This data includes the location of the satellite and the time of transmission of the signal. Together, these two components allow the receiver to accurately measure the arrival time of a signal from several HSSN satellites.

The HSSN signal travels at a speed very close to the speed of light, but on its way from orbit to the user, it passes through the ionosphere and troposphere, and these interferences slow the wave down a bit. These speed deviations are intelligently modeled and can be corrected as explained later.

The user equipment (ie, the GPSN receiver) measures the ToA of the signal, the correlation of the satellite codes with the code replicas stored in the receiver. As mentioned above, the satellite provides transmission time and location by sending a

navigation message, in addition to a radio tag to determine distance. The user subtracts the transmission time from the arrival time, and this time difference is denoted below as $t_{rcv} - t_{tmt}$.

$$\rho = c(t_{rcv} - t_{tmt})$$
$$= \text{range} + cb_{rcv}$$
$$= \sqrt{(x_{rcv} - x^{(sat)})^2 + (y_{rcv} - y^{(sat)})^2 + (z_{rcv} - z^{(sat)})^2} + cb_{rcv}$$

t_{rcv} = arrival time measured by receiver
t_{tmt} = broadcast time marked by satellite
range = range from satellite to receiver
c = speed of light
b_{rcv} = receiver clock time difference from GNSS time
$\{x_{rcv}, y_{rcv}, z_{rcv}\}$ user location
$\{x^{(sat)}, y^{(sat)}, z^{(sat)}\}$ satellite location

When converted to distance, this time difference is known as the pseudorange (q) because it is equal to the geometric distance from the satellite to the user plus the additional offset (brcv) due to the time difference between the receiver clock and the GNSS time.

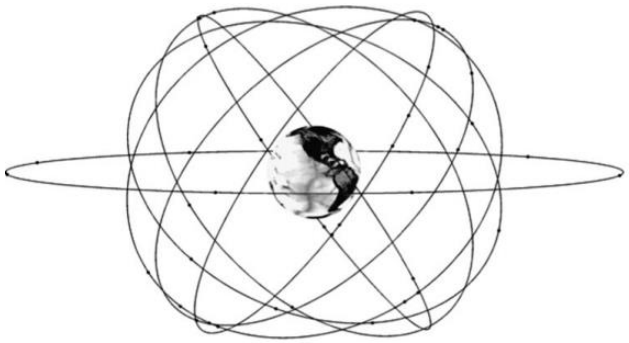

Figure. 2.1 Global Positioning System (GPS) satellites in orbit in May 2014.

Today, GPS has approximately 32 satellites in the Mean Earth Orbit (MEO). Also shown are the seven Geostationary Orbit (GEO) satellites that complement GPS; they broadcast error limits in real time to support aviation use.

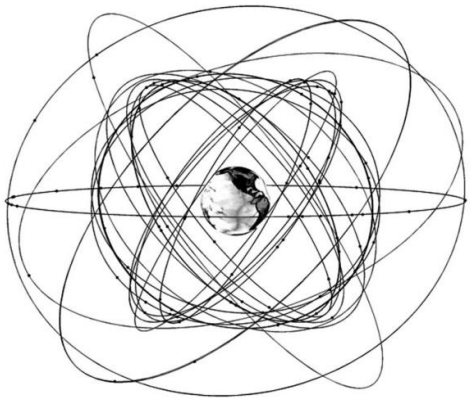

Figure. 2.2 Global Navigation Satellite System (GNSS) satellites in orbit in May 2014.

This figure includes satellites from the GPS systems, Beidou's GLONASS (China), Galileo (Europe), the Quasi-Zenit Satellite System (QZSS, Japan), and the Indian Regional Navigation Satellite System (IRNSS). As shown, these constellations include satellites in MEO, GEO, and inclined geosynchronous orbits.

Each pseudorange measurement is sensitive to receiver location (xrcv, yrcv, zrcv) and receiver clock bias, brcv. These four quantities (xrcv, yrcv, zrcv, brcv) are known as estimanda or custom condition. The other variables in this equation are generally well known. Recall that the satellite sends its location as part of the navigation message. Thus, four such pseudorange measurements are required to estimate a four-dimensional user state.

Although four satellites are definitely necessary for user condition estimation, four satellites may not be sufficient. The satellites must have good geometry relative to each other; they should be spread across the sky and not clustered together or in the same plane. Figure 2.3 shows a typical distribution of HSSN receiver errors in 2013. A two-dimensional scatter diagram characterizes the operation of the receiver. The reported locations are scattered around the origin (0, 0), where the receiver actually is. As shown, the errors are typically less than 5 meters. As noted earlier and discussed in detail later, differential positioning relative to a known receiver can improve this accuracy and provide decimeter or centimeter accuracy.

By the way, the North-South scattering orientation in Figure 2.3 is specific to this data set and is not a general feature of satellite navigation.

The data set shown in Figure 2.3 is based on the GPS system, which is currently the most widely used satellite constellation within the HSSN. GPS was developed by the US Department of Defense in the 1970s. At the time, planners predicted that GPS would serve a total of 40,000 military users, with some additional civilian use. Today, the public community has already deployed more than 3 billion GPS receivers.

The civilian tail is now GPS driven, and the civil aviation community is already enjoying a growing array of GPS applications aimed at increasing efficiency, conserving fuel and reducing the environmental impact of aviation.

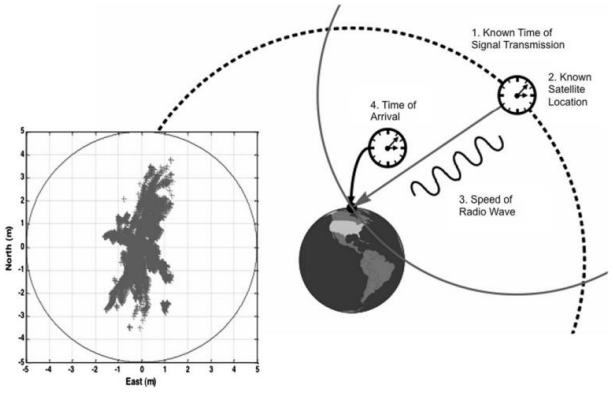

Figure. 2.3 The basic principle of operation of a GNSS satellite showing the key components of pseudorange measurement.

These include (1) the known time of transmission of the unique satellite spectral unfolding, (2) the known location of the satellite at the time of transmission, (3) the known speed of propagation of the radio wave, and (4) the precise measurement of the arrival time of the signal. Typical GNSS receiver accuracy is shown in the scatter plot.

As stated earlier, GPS is not the only one. GLONASS has relaunched its satellite navigation system, which as of December 2013 has 24 satellites. Europe has launched the first prototype satellites for its Galileo system, which will eventually consist of 24 satellites. China is expanding its regional BeiDou system to provide global coverage.

Japan and India have also launched satellites for regional systems. Figure 2.2 shows the current melange of satellites in this system of systems. Over time, these national constellations will create a powerful HSSN with more than 100 satellites.

The multitude of satellites described above will provide geometric diversity with signals coming from almost every direction overhead. Importantly, the new satellites will also provide frequency diversity for civilian users. Each new satellite will transmit civilian signals on three frequencies, rather than the single civilian frequency that was available until 2010.

Figure 2.4 shows the spectrum for the new HSSN signals that will be commissioned over the next 10 years. All these signals are located in the parts of the radio spectrum that have been allocated for satellite radio navigation systems. Some of them are also located in the bands designated for aeronautical radio navigation systems (ARNS). As shown, GPS satellites transmit signals on three civilian frequencies called L1 (1575.42 MHz), L2 (1227.60 MHz), and L5 (1176.45 MHz). L1 is home to the so-called open-access (C/A) signal, which is the basis for most civilian applications to this day. This C/A signal is superimposed on military signals in the same band. L2 also carries the civil signal on the seven latest GPS satellites. L5 is the location for the third civilian signal and is included on the last four GPS satellites. L5 has a wider spectrum than civil signals on L1 and L2 and is therefore the most stable civil signal.

Together, L1, L2, and L5 provide redundancy to combat random radio frequency interference (RFI) and a means of removing dispersion delay through the ionosphere. Both of these functions are important. RFBI is becoming increasingly common in the GPS bands, and the ionosphere is the largest natural source of error. These two issues will be described in more detail later in this article. L1 and L5 are particularly important for aviation because they both belong to the ARNS bands in the radio frequency spectrum. As such, they have greater aeronautical utility because they enjoy greater institutional protection than L2.

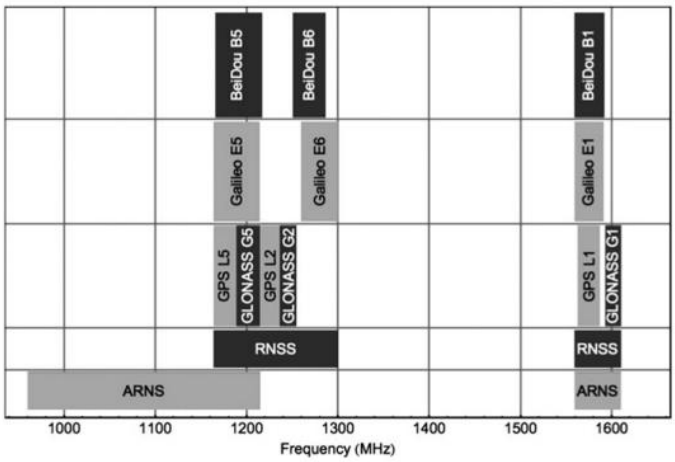

Figure. 2.4 Signal spectra for GPS, Galileo, BeiDou and GLONASS. On the left, the new GPS satellites emit signals at frequencies L5 (1176.45 MHz), L2 (1227.60 MHz) and L1 (1575.42 MHz).

Signals for Galileo and Compass are also shown in Figure 2.4. As shown, they are not located exactly in the same places as the GPS signals. However, they share common features: ternary frequency diversity with at least two signals in the ARNS bands, around L1 and L5.

As mentioned earlier, GPS user equipment serves many applications. For example, every new Boeing or Airbus aircraft is equipped with a GPS receiver to navigate the airspace during flight and during landing. GPS is also used to guide aircraft when approaching airports. In some cases, it provides the most critical vertical location parameter at altitudes up to 200 feet. Aviation GPS receivers are expensive due to the costs associated with design and testing for such a safety-critical application.

On the other hand, most new cell phones come with GPS/GLONASS receivers with a list of materials around $1. These receivers are used for navigation while walking and driving. They also automatically provide our location to emergency services when we make such a call.

2.1 Benefit in efficiency and environmental benefits

As mentioned earlier, satellite navigation saves aviation fuel and reduces the environmental impact of air travel. In order to tell this story, we begin by discussing a parallel development: green car routing.

Green routing for cars Recently, Ford and Hyundai, together with TeleNav and Navtech, are working to improve the efficiency of cars by implementing so-called green navigation systems or 'green GPS' in their cars. Like other car navigation systems, these systems use distance and average speed to calculate the 'shortest' and 'fastest' route from point A to point B. However, they also consider additional factors to provide the 'greenest' or most fuel-efficient route. Some of these eco-factors include .

Traffic lights and stop signs: avoid stops. Traffic: Avoid stopping and moving in heavy traffic, idle and very low speed. Curves: avoid slowing down and overtaking . Climbs: Avoid going uphill A study of one such eco-routing system found that choosing the 'greenest' route resulted in an average fuel economy of 10%. This estimate is conservative as these savings are compared to the existing 'fastest route' provided by standard navigation systems, which is already significantly more fuel efficient than the average route without the use of a navigation system.

Given that highway CO2 emissions account for 26% of total US CO2 from all sources, eco-routing for all US road trips has the potential to reduce total US CO2 emissions by 2.6%, an impressive impact for such a simple solution. Meanwhile, while automotive eco-routing can save 2.6% of US CO2 emissions, US aviation in general is only responsible for 2.6% of total US CO2 emissions. Even so, aviation remains one of the most difficult sectors to reduce emissions. This stability is explained by aviation's need for fuels with the highest energy density (joules per kilogram and joules per volume). Thus, as total emissions decrease in the future, the contribution of aviation will increase. As the relative impact of aviation grows, so does the importance of finding effective ways to reduce its growing share of global CO2 emissions. In recent aviation history, innovations in the design of airframes and propulsion systems have led to significant reductions in aircraft fuel consumption. Between 1960 and 2008, the average fuel consumption of new aircraft more than halved due to improvements in engine and aerodynamic efficiency and more efficient use of power.

With the introduction of the Boeing 787, which was designed to be 20% more efficient than similar aircraft, this reliable trend will continue. This article does not deal

with the details of aerodynamics and propulsion systems, but focuses on the use of navigation technology to create more efficient routes and procedures for aircraft. In this section, we examine several of these operational improvements, each made possible by improved air navigation systems, primarily GNSS. It is important to note, however, that the efficiency improvements brought about by navigation and those brought about by airframe design and propulsion systems are additive.

2.2 Juneau, Alaska, and Jackson Hole, Wyoming

As aircraft approach airports, especially in severe weather and challenging terrain, navigation becomes extremely important. This is especially true for airports in Alaska.

Alaska has a rugged landscape and unpredictable weather that complicates aviation operations, including airport approaches and departures. GPS is extremely important in Alaska because it provides navigational signals that surround the entire airport and allow unrestricted area-based navigation (RNAV). RNAV allows aircraft to fly directly between any two points without flying the less efficient conventional routes between two ground navigation stations. For example, Alaska Air has started using GPS when flying into Alaska's state capital, Juneau. This city is accessible only by air and water, and air routes require several turns and significant security negotiations.

Figure 5 shows a cost-effective route for aircraft arriving at or approaching Juneau Airport. As shown, this route follows the Gastineau Canal and the aircraft flies northwest to approach Runway 26 at the Juneau Airport. Cliffs border both sides of this channel, and often the Alaskan weather blocks the view of these borders. Fortunately, Alaska Airlines worked with the FAA and the Boeing Company to determine the path shown in Figure 5. Precise Positioning GPS with Receiver Autonomy Monitoring (RAIM), which we discuss in the safety section, allowed Alaska Airlines to navigate the channel in conditions of limited visibility. Prior to these opportunities, aircraft were forced to avoid Juneau if the cloud minimum was below 1,000 feet or en-route visibility was less than 2 miles. With GPS support for navigating the Gastineau Channel, the minimum cloud height dropped to 337 feet and visibility on course was 1 mile.

Figure. 2.5 Departures and arrivals at Juneau Airport (JNU) via the Gastineau Canal.

The left turn at the end of the channel, close to the airport, requires area navigation (RNAV) capability. Such a turn cannot be supported by a linear radio beam coming from the ground.

In 1996, Alaska Airlines began using the Gastineau Canal in earnest. They flew through the narrow Gastineau Channel in 2011 5,683 times thanks to GPS navigation. Of these flights, 831 were salvaged, meaning they would have been canceled or diverted due to weather conditions if not equipped with GPS.

Alaska Airlines estimates annual savings of approximately $1 million thanks to GPS navigation in Juneau.

Today, Alaska Airlines uses GPS to navigate 30 airports in Alaska and the continental United States. They operate a fleet of 117 Boeing 737 aircraft with this capability, and their sister airline Horizon Air also has similar capabilities on Bombardier Q400 turboprops. According to Alaska Air, they handled 12,700 arrivals and departures in 2011, avoiding the diversion of 1,545 flights thanks to GPS navigation. That year, the airline used GPS to help reduce fuel consumption by 210,000 gallons and save more than $15-19 million across their fleet and operations.

Jackson Hole, Wyoming also has a unique airport that makes good use of GPS. Figure 6 shows the approach path from above. The airport (JAC) is located at the bottom left of the figure. As shown, a conventional landing requires two straight segments based

on the limitations of traditional ground radionavigation systems. The first segment flies west and the second segment flies south to the airport.

The new path uses RNAV waypoints for a curvilinear path that avoids the sharp turn and noise-sensitive area near Grand Teton National Park. This new route is a shorter 14 mile and 3 minute flight.

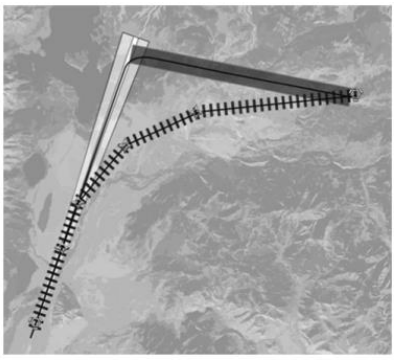

Figure. 2.6 Arrival at Jackson Hole Airport (JAC) using GPS-enabled RNAV. The RNAV route is curvier and shorter, and avoids the major hazards of Grand Teton National Park.

2.3 Optimized Decline Profile

In the Juneau and Jackson Hole cases, the approach designers optimized the horizontal track on the ground. However, it is also possible to fly more efficient vertical profiles using an optimized descent profile (OPZ), which allows qualified aircraft to reduce fuel consumption, noise and carbon emissions. Currently, standard terminal arrivals use a number of mandatory altitudes along the arrival route, which gradually lower the aircraft towards the airport. The advantage of this approach is that it is easy to standardize and it minimizes the amount of protected airspace around the airport.

However, in terms of fuel, time, and noise pollution, the step-down approach is not ideal because airplanes use high power adjustments to maintain steady flight.

An ideal OPS is a continuous descent operation where the aircraft descends from cruise altitude to the runway in a smooth glide path at low power, which conserves time and fuel, and reduces noise and emissions (see Figure 7). Some of these descending aircraft may be idling, while others may require a little more power for anti-icing

capability. These ADRs are published procedures and the controller may authorize the aircraft to fly the ADRs. When the aircraft is cleared, it can safely descend from near cruise altitude to near runway at near idle thrust.

The first OPZ flights were conducted approximately ten years ago at Louisville Airport (SDF). Descent in SDF resulted in average fuel economy of approximately 200 kg per approach B737-300 test aircraft. The peak noise level has also been significantly reduced.9

In December 2007, Los Angeles Airport (LAX) implemented the first publicly-charted airport terminal. All aircraft using this fully-functional airbase at LAX save an average of 25 gallons (76 kg) and 200 kg of CO2 emissions per approach. In total, LAX's OPZ saves approximately 2 million gallons (6 million kg) of fuel each year and reduces annual CO2 emissions by 19 million kg. OPZ also saves time by reducing the average flight time by 44 s and reducing ground noise around LAX.10

Significant fuel savings have been demonstrated during flight tests at other airports. For example, OPZ flight tests with B757s and B737-800s to Miami Airport (MIA) showed average fuel savings of 49 gallons (150 kg) of fuel per approach, and tests with B767s to Atlanta Hartsfield-Jackson Airport (ATL) showed average fuel savings of of 37 gallons (113 kg) per flight.11

OPZ savings depend on the efficiency of the OPZ trajectory, the inefficiency of the conventional approach, the type of aircraft and the weather conditions. Currently, the FAA is developing new means of association and location for aircraft sequencing controllers at the airfield. These improved tools will allow controllers to locate aircraft hundreds of miles from aircraft and in the terminal area.

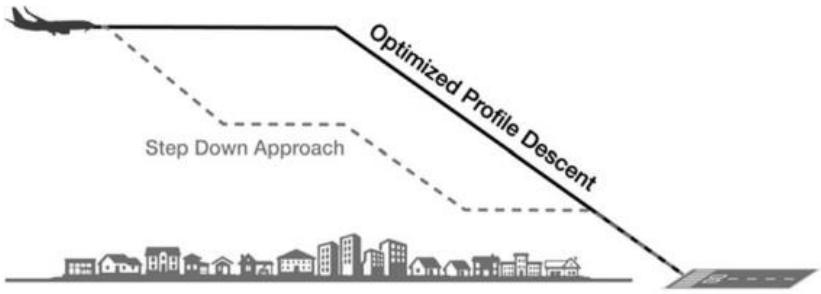

Figure. 2.7 Optimized profile descents (OPZ) compared to step approaches (move and dive).

OPZ offers a close approximation of the optimal glide slope with idle thrust and can save hundreds of kilograms of fuel per flight.

If you have a smartphone or tablet, you may have played Flight Control, an amazingly addictive game where the goal is to guide planes to their pre-assigned runways while avoiding potential collisions. It starts off easy, with one plane, then two, and in such low air traffic conditions you are free to take any path you wish. But as the difficulty of the game increases, with the number of planes on the screen increasing, your choice of paths becomes much more limited. If your strategy for the game is anything like ours, then as the difficulty increases, you play it safe by creating an orderly queue of planes for each runway and sending each new plane to the end of the queue, even if it means following a much longer path than you could do otherwise.

Although working as an air traffic controller in the real world requires a lot more skill than this simple game, the basic strategy is similar. When the skies are clear, cost-effective flight paths are great. When there's traffic in the sky, conflict avoidance becomes a top priority, to the detriment of fuel efficiency. Of course, this means that the potential benefits of an optimized route often fail to be realized in real-world circumstances. Fortunately, fuel efficiency and safety don't always have to be at odds.

With the help of individual arrivals, we can simultaneously increase fuel efficiency, reduce the burden on air traffic controllers and increase safety.

Custom arrivals allow you to customize arrival routes for individual flights based on current air traffic conditions. The basic idea is this: accurately measure the position and speed of each aircraft at all times. Use this information along with current meteorological data to accurately predict each aircraft's future location.

Optimize all arrival (and departure) routes simultaneously, while reducing fuel consumption and flight time for each aircraft, maintaining distance and avoiding conflicts. See the example in Figure 2.8.

How it works: An incoming aircraft transmits its data to air traffic control, which uses a computer program such as NASA's En Route Descent Advisor to create an optimal descent path. This trajectory calculation takes into account the state of the aircraft, the predicted trajectories of other aircraft in the airspace and the weather. This optimal approach path is then transmitted to the aircraft and loaded into the flight control system. Although the technological capabilities to develop and execute these individual landings are not yet widely operational (on the ground or in the air), several promising tests of the concept have already been conducted.

In 2006, United partnered with the FAA to test the concept on 40 flights from Honolulu to San Francisco (SFO) in various air traffic conditions. In low-traffic conditions, landings using an individual approach with an optimized descent profile at SFO resulted in average fuel savings of approximately 110 kg, which is similar to the conventional optimized descent profile tests described above. In heavy traffic conditions, the average fuel savings were 1,460 kg per arrival.

This dramatic increase in savings can be attributed to the ineffectiveness of the traditional conditional load approach at SFO, which includes a 30-mile low-altitude lift path. Traditionally, during heavy traffic, any given flight went around the back row. Individual approaches allow the flight to smoothly integrate into the middle of the queue as the aircraft continues to travel its own most efficient approach path.

As a result, the tests at SFO showed that individual approaches can save more fuel during heavy traffic, since traditional approaches during heavy traffic are often much less efficient than approaches during low traffic. (Note: Benefits shown after 25% penalty based on the assumption that in heavy traffic conditions some forward structural stretch would still be necessary to properly coordinate arrival times. The real savings from a true ideal approach compared to a traditional approach in heavy traffic would be 1.896 kg.)

In a later trial period at SFO, the four airlines testing individual arrivals at SFO saved more than 500,000 kg of fuel over the course of a year. Trials of individual arrivals in Melbourne and Sydney showed average fuel savings of 100-200kg per

arrival, and later trials in Brisbane saved 200,000kg of fuel and 650,000kg of CO2 emissions over the course of a year.

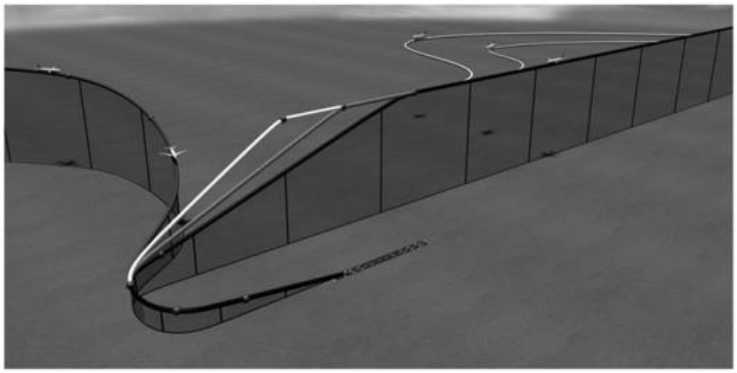

Figure. 2.8 Individual arrivals.

These aircraft operate advanced terminal arrival procedures. Each of the aircraft approaching from the right uses a descent angle that minimizes fuel consumption for their aircraft. Also, aircraft approaching from the left join the approach path they share with the first three aircraft that have left the open flight pile.

2.4 Flight optimization along the route

GNSS also allows the implementation of advanced procedures for aircraft flying en route or over water, taking into account distance, winds and convective weather. While eco-routing on the road is limited to choosing the best route based on existing highways, eco-routing in the air can go even further by choosing efficient routes that deviate from traditional air travel. With GNSS, aircraft can now safely fly routes that deviate from fixed flight routes and realize significant fuel savings and reduced emissions, while saving time and reducing conflicts. Figure 2.9 shows the hierarchy of such possibilities.

Flexible track systems. The simplest form of optimized routes in the air is flexible track systems. Operators design and fly an optimized trajectory between a pair of cities, a route predicted to be more efficient than a traditional ATS flight route based on general meteorological forecasts and a representative aircraft performance model. This optimized trajectory becomes the route for all flights between twin cities and is updated annually. Demonstrating the potential inefficiencies of legacy fixed routes and the

potential savings to be gained by switching to flexible route systems, a trial of 592 Emirates Airlines flights between Dubai and Melbourne/Sydney resulted in an average fuel saving of 1000kg per flight and an average time saving of 6 minutes for each flight.

User-selectable routes (UPR). User-selectable routes are similar to flexible route systems, but they are updated for individual flights based on short-term, specific forecasts. They take into account the characteristics of the specific aircraft to be flown (eg B737 and A380) and the most recent wind and convective weather information for the specific date and time the aircraft will be flying (eg 17 Oct 2013 at 09:25 PST) . User-selectable routes optimize the track for an individual flight, which may differ significantly from the optimal track for the same flight operated by another aircraft at a different time of the same day.

Dynamic Air Redistribution Procedure (DARP). Dynamic air reassignment routines are similar to flexible track systems and user-selectable routes, but can be updated in flight based on short-term, specific forecasts. DARP flights start with a user-selected route route, but update that route during flight based on current weather. Based on the results of DARP flights between Auckland (AKL) and SFO, Air New Zealand reports that 58% of their AKL-SFO flights can benefit from DARP, and that for AKL-SFO flights using DARP, the average fuel savings is 450kg.

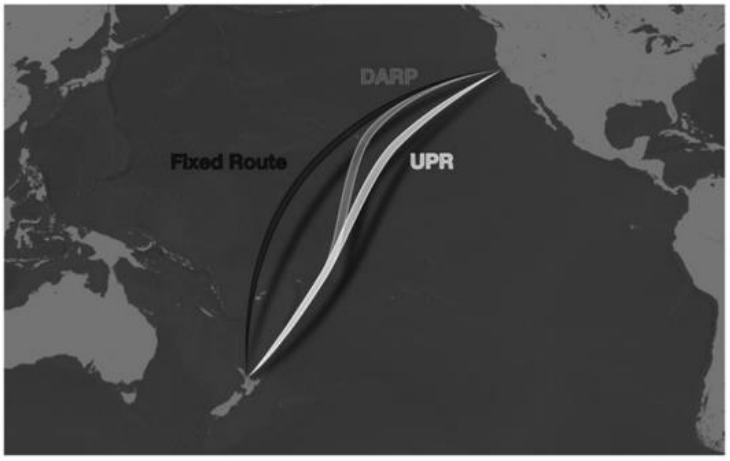

Figure. 2.9 Three routing protocols for the airborne phase of flight: (1) fixed routing, (2) user-selected routing (UPR), and (3) dynamic airborne redistribution procedures (DARP).

2.4.1 Security

As described above, satellite navigation is of great importance for improving flight efficiency and reducing fuel consumption and greenhouse gas emissions. GNSS does this by enabling RNAV. Aircraft will no longer be restricted from flying point-to-point defined by ground navigation aids or excessively restricted air traffic zones. Aircraft will not have to descend and climb when approaching airports; they will continuously descend to the airport, maximizing aerodynamic efficiency. Over time, planes will also be able to make turns in time to join the queue of planes approaching the airport. They will adapt their speed in flight to synchronize this coordinated merger with their flying counterparts. Also, their flights in the flight phase will be optimized based on the weather, which can be forecast or current.

2.4.2 Mandatory navigation level

Satellite navigation supports RNAV, but it is not enough. To take full advantage of GNSS, RNP must also be provided. The RNP includes four closely related flight safety requirements:

1. Accuracy describes the daily or nominal error rate of the system. As described below, it is measured at the 95% level and has two components: Navigation Sensor Error (NSE) and Flight Technical Error (FTE). NSE measures the performance of the navigation sensor and FTE measures the performance of the human pilot or autopilot.

2. Performance monitoring protects the navigation sensor from rare events. As opposed to precision, measured at 10^-5, 10^-7, or 10^-9. In the case of GNSS, NSE monitoring should detect human-made faults, space weather and bad actors. All of this is described in the following sections, along with how the escalation systems detect these events and send error information in real time.

3. The reliability of the aircraft equipment determines the ability of the navigation system to provide navigation without interruptions. Air traffic navigation systems must be reliable; the average time between failures of air equipment should be greater than

100,000 hours. Achieving such reliability is difficult to achieve with a single line of electronics, and therefore GNSS avionics are duplicated, tripled, or even arranged in a double-duplicate configuration. The avionics manufacturer and aircraft manufacturers are responsible for the resulting reliability of the aircraft equipment.

4. Signal in space indicates signals from major GNSS constellations and boost signals sent as performance monitors. Constellation service providers (eg Europe for Galileo, China for BeiDou, United States for GPS and Russia for GLONASS) are responsible for the quality of GNSS signals.

Air navigation service providers (ANSPs) are responsible for the integrity of elevation signals. For example, the ANSP in the United States is the Federal Aviation Safety Agency (FAA).

As mentioned above, accuracy is based on two error components: NSE and FTE. NSE is the difference between the true position of the aircraft and the position indicated by the navigation system. FTE is the difference between the desired attitude indicated by the navigation system and the attitude flown by the pilot or autopilot. In other words, FTE measures the ability of an aircraft (manual pilot or autopilot) to fly the route indicated by the navigation system. NSE and FTE are both significant and the total systematic error (TSE) is their statistical sum as shown below:

$$TSE = \sqrt{NSE^2 + FTE^2}$$

Flight safety requires the control of TSE, and this requirement is determined by the TSE limit, which depends on the flight operations. For example, RNP 10 is often used over oceans and means that the TSE should not exceed 10 nautical miles (NM) more than 5% of the time (ie, less than 0.05 probability). An additional interpretation is also important: the TSE must not exceed twice the TSE limit, 20 nautical miles, with a probability greater than 10^-5.

RNP 4 is often used when the aircraft is in the phase of flight over continental territories. RNP 1 is used for an aircraft arriving at a destination and crossing a busy terminal area surrounding an airport (eg New York or London). An RNP of 0.3 is often used when an aircraft is on its final approach to an airport. This requires that the TSE

does not exceed 0.3 and 0.6 nautical miles with probabilities of 0.05 and 10^-5 respectively. Obviously, the TSE limit is lower for more demanding flight operations.

The RNP does not specify how navigational performance is achieved. Instead, the RNP is the upper level of the aircraft's capability specification; this capability determines whether the measured aircraft can fly the specified operation. In addition, RNAV also has this property where a performance level is defined for an operation, but the requirement is not specific to any sensor.

As indicated above, the RNP requires that the TSE limit be fixed at two probability levels: a probability of 0.05 measures nominal or daily performance, while a level of 10^-5 measures performance under extreme conditions (ie, including extreme events). These TSE limit requirements determine both FTE and NSE controls. For these reasons, the aeronautical GNSS system community is emphasizing the monitoring of NSE performance, and this article introduces that effort.

As mentioned above, RNP should take into account navigation performance under unexpected (atypical) events. In the case of satellite navigation, these pathologies can be classified as malfunctions related to people, space weather or intruders. The "Systems or Procedures Malfunctions" section and the "Space Weather" section describe human-related malfunctions and space weather, respectively.

The section "Safety enhancement systems that monitor GNSS performance" describes safety enhancement systems that monitor these effects and protect against potentially dangerous information indication (HMI). The "Stalkers: Jammers and Communicators" section looks at attackers who attempt to intentionally disable GNSS service (stalkers) or spoof signals in space (stalkers). It also describes the aviation response to this malignancy.

2.5 Malfunctions in systems or procedures

As the name suggests, these failures involve failures in human procedures, hardware, or software. They are not intentional. The scatterplot in Figure 2.10 shows the impact of a human-related fault that occurred in April 2007. GPS ground control then

initiated a station-keeping maneuver for the GPS satellite over the Pacific Ocean. Such maneuvers are held regularly once or twice a year. In this case, however, the engines were started without the usual display to users. This resulted in large (60 m) errors for users who included this satellite in their navigation solution. In other words, this procedure malfunction affected point 2 in Fig. 2.3; the broadcast location of the satellite had large errors.

There have been other human-related failures in the history of GPS. Over time, the hardware of the satellites introduced significant malfunctions. For example, so-called clock escapes are the most common malfunctions associated with people. GNSS satellites carry atomic clocks, and they tend to be very stable. However, sometimes the clock time deviates from the GPS time quite quickly, and the clock data contained in the navigation message does not have time to catch up with this drifting event. In other cases, the signal hardware (baseline or RF) suffers a mild malfunction and the transmitted signal becomes distorted compared to the expected signal.

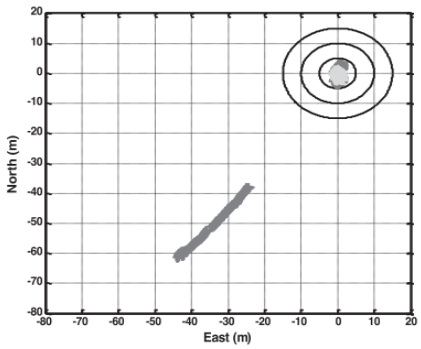

Figure. 2.10 Scatterplot showing outliers for a GNSS receiver. The 60 meter errors were caused by a change in the satellite's orbital position without alerting the user community via a navigation message.

The errors described above, related to human intervention, are potentially dangerous. In fact, the aviation community identifies them as potential sources of dangerous information because the errors can be significant compared to the requirements of critical aviation operations such as airport approach and landing. In addition, the probability of the occurrence of dangerous information is higher than the target level of security in aviation. For these two reasons, the aviation community has

developed a number of additions to GNSS that detect these errors and alert the air fleet within seconds. These additions will be described in the Security Additions Monitoring GNSS Performance section, but first let's look at another important source of insecure information: space weather.

2.6 Space weather

The ionosphere surrounds the Earth at an altitude of 70 to 1300 km and introduces an additional delay in the travel time of the GNSS signal from orbit to Earth. Figure 2.11 is an example of nominal ionospheric delay over the continental United States (CONUS). The data was collected on November 19, 2003, and the figure shows the delay a user would experience if the satellite was directly above the receiver. As shown, these vertical delays vary from 3 to 7 meters. For satellites closer to the horizon, the error can be three to four times greater than the delays shown in the figure. Nevertheless, ionospheric delays are generally uniform over large areas. Figure 2.11 shows that the vertical delay varies by only a few meters over the CONUS. Therefore, ionospheric estimates made at a fixed receiver source will be accurate for hundreds of kilometers. More precisely, if we place GNSS receivers at airports, the ionospheric delays observed at the airport will be highly correlated with the ionospheric delays experienced by the approaching aircraft.

Figure 2.12 is an example of the ionospheric delay for the next day, 20 November, which was very disturbed. As shown, the vertical delay now varies from 2 to 26 meters. This change is five times greater than in Figure 2.11, and the spatial gradients are much sharper. The delay over Ohio varies by about 20 meters over a distance of 500 km. This corresponds to a gradient of approximately 40 parts per million (ppm). In fact, gradients of up to 400 ppm were observed at the GNSS L1 frequency. Such acute events require considerable care, especially when GNSS is used to support the aircraft during approach and landing at the airport.

Figures 2.11 and 2.12 show that solar activity can lead to significant increases in ionospheric delay and associated spatial gradients. Latencies can jump from nominal

values of a few meters to tens of meters. The associated gradients can be 20 meters or more over a distance of 500 km. Two of the enhancements described in the "Security Enhancements that Monitor GNSS Performance" section are differential GNSS systems. They correct these errors by placing the sources of GNSS receivers in known locations. These measurements on the ground are broadcast to the air fleet and used to correct the measurements on board the aircraft. However, even this differential treatment is not ideal, as strong space weather events can introduce the sharp gradients mentioned above. In such cases, the ionospheric delay measured at the receiver source may not correlate strongly with the delay experienced by the avionics. Large ionospheric storms can last several hours and occur over large areas of the United States. Thus, the impact of space weather conditions on GNSS has been a significant subject of study over the past two decades.

Figure 2.13 shows the variation of space weather phenomena with the 11-year solar cycle. With greater accuracy, the figure shows the number of sunspots. Sunspots are cool events, the size of several planets, on the surface of the sun that are associated with strong magnetic phenomena on the sun. These solar events propagate through the solar system and can often cause disturbances in the ionosphere here on Earth.

A disturbed ionosphere can have another effect: scintillation. Scintillation is a rapid change in amplitude and phase of received GNSS signals. These fluctuations can cause the GNSS signal strength to drop by 10 dB or more. Such fluctuations may only last a few seconds, but they can cause disruption of the GNSS function on board the aircraft. Scintillation is especially common in equatorial and polar regions, where the entire evening can be accompanied by sporadic scintillation. Thus, the influence of scintillation on satellite navigation is also an important object of current research.

Security enhancements that monitor GNSS performance

To solve the above problems, civil aviation has supplemented GPS with systems that detect and correct errors associated with human intervention and space weather events. The probability of an error associated with human intervention in the GPS system is approximately 10 - 5 /h per satellite. The target level of safety for an aircraft

navigation system is approximately 10 - 7 /hr, or one hundred times less than the observed failure probability. Also, space weather events, especially the ionosphere, can introduce location errors that can be potentially dangerous for aircraft safety.

These storms can occur several times a year during the peak of the solar cycle. In these years, the level of such events is more than a hundred times higher than the target level of safety for aviation.

For these reasons, civil aviation has supplemented GPS with systems that detect and remove errors associated with human intervention and space weather events. There are three such supplement strategies that are now described. The Ground Differential Correction System (GBAS) is described in the next section and provides integrity by comparing GNSS measurements to the known locations of three or four receiver sources located within the airport area.

The Space Based Differential Correction System (SBAS) compares GNSS measurements with the known locations of dozens of source receivers located over continental areas. RAIM does not use ground checks; it compares each GNSS range measurement to the total solution of other satellites seen by the airborne aircraft.

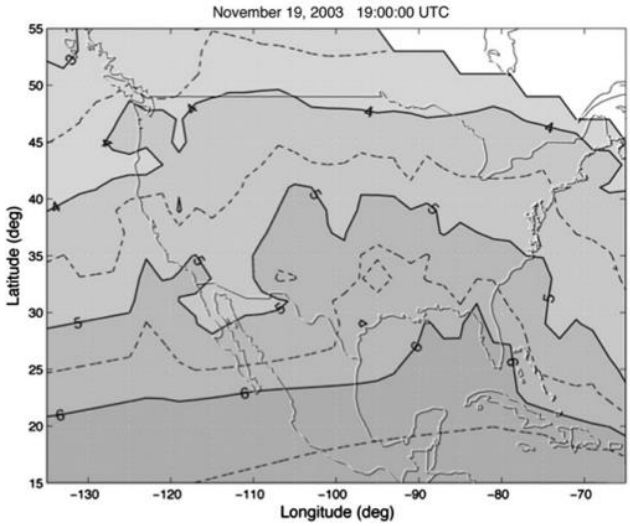

Figure. 2.11. Vertical ionospheric delay over the United States during calm space weather on November 19, 2003.

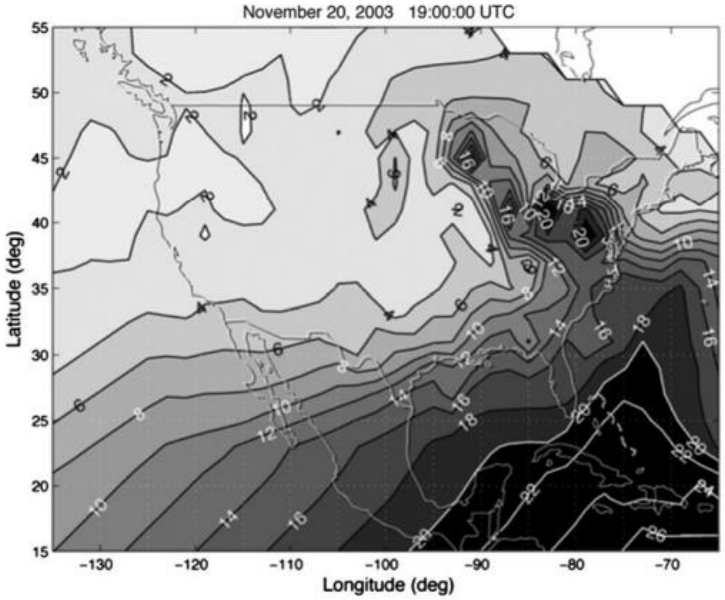

Figure. 2.12. Vertical ionospheric delay over the United States on the day of the 20 November 2003 ionospheric storm.

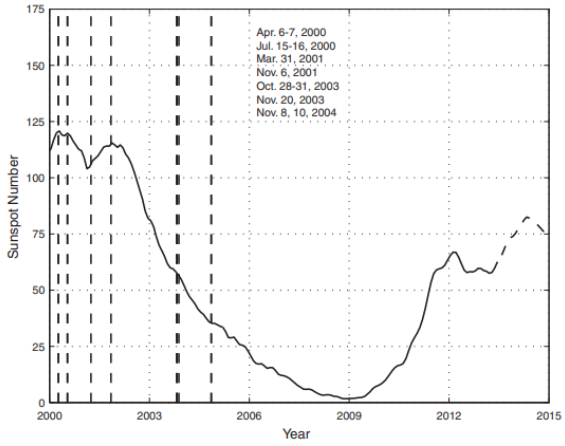

Figure. 2.13. The number of sunspots since the beginning of 2000 shows the last two peaks of the 11-year solar cycle.

Also shown are ionospheric storms that caused the vertical guidance normally provided by the Wide Area Augmentation System (WAAS) to be disabled. WAAS outages indicated by dashed vertical lines last more than 1 hour.

2.7 Augmentation system on the ground.

As shown in Figure 2.14, GBAS are located at the airport being served. Reference receivers are connected to them, which monitor GPS (or GNSS) signals. Because reference receivers are at known locations, they can provide corrections to eliminate

nominal GPS errors. They also contribute to performance monitoring by generating alarms for satellites that cannot be intelligently corrected. GBAS also provides data that allows the aircraft to continuously assess the level of protection, which should always be greater than the actual NSE error. We say that the level of protection exceeds the true error. All GBAS base receivers are located on the airport territory. Therefore, corrections and alerts are valid for approximately 100 km around the airport. They serve aircraft that land, approach or take off from the airport. GBAS is also capable of supporting aircraft maneuvering in the terminal airspace surrounding the airport. With this range of applications in mind, GBAS uses line-of-sight radio broadcasting to the air fleet. This radio transmission operates in the very high frequency (VHF) range of the radio spectrum and is called VHF radio data transmission.

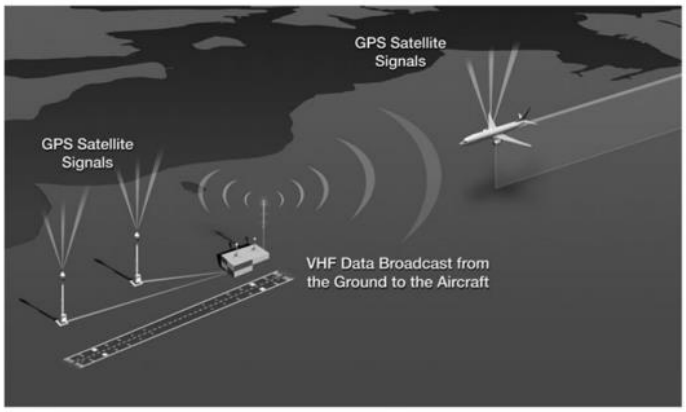

Figure. 2.14 Ground Support System (GBAS)

2.8 Space saturation subsystem.

SBAS places their receivers all over the continental area. As shown in fig. 2.15, approximately 38 stations are used to cover North America and a similar number are used to serve European airspace. As shown in the figure, these receivers send GPS measurement data to master stations that generate corrections and error-limiting data that apply to the area covered by the reference network. Since the data is valid in continental areas, SBAS uses geostationary satellites to transmit this navigational safety data to the air fleet. Figures 2.1 and 2.2 show these SBAS satellites.

The Wide Area Augmentation System (WAAS) is the SBAS for North America. Similar systems work in Europe and Japan, and are being developed in India and Russia.

WAAS has been in operation since July 2003 and is serving well. Figure 2.16 shows the cumulative distribution function (CDF) for the vertical NSE WAAS. It shows the 10 billion error measurements collected since WAAS was launched in 2003. As shown, the largest error in this history is 14 m and occurred once. We emphasize two features of this NSE distribution. First, the kernel of the distribution covers the central 95% of errors, and precision defines the width of this nominal kernel. As shown, WAAS vertical accuracy is 1.4 m. This is typical everyday WAAS performance.

The CDF tails shown in Figure 16 are also important. These NSE tails are measured at 10 - 5 , 10 - 7 , or even 10 - 9 . At these low-probability levels, the tails include the potential effects of human-made faults (see Errors in systems or procedures), space weather (see section Space Weather) and bad actors (see section Bad Actors: Blockers and Forgers). As shown, WAAS does a good job of managing these faults and thus the tails shown in Figure 2.16 are not significant.

Navigation systems that detect NSE tail events with high probability are said to have integrity, and Figure 2.17 illustrates WAAS integrity. Specifically, it provides a CDF for the ratio of WAAS vertical errors to the WAAS-provided standard deviation of those vertical errors. This standard deviation is related to the level of protection mentioned earlier. In particular, the NSE error distribution must be a known Gaussian distribution with zero mean and standard deviation provided by WAAS. Figure 2.17 also shows 10 billion data points for the ten-year period from 2003 to 2013. It shows that the performance of WAAS is much better than the Gaussian curve.

A statistician would say that the WAAS errors are leptokurtic, meaning that the errors are more concentrated towards zero than the CDF of a Gaussian distribution with the same standard deviation. The aviator would just be happy with a useful limit on the true position error. Navigational systems that comply with the RNP must have integrity and continuity. Continuity requires that the false positive rate of performance controllers be small.

This requirement competes with integrity because continuity is broken when integrity signals an error. Therefore, integrity monitors must be sensitive to real threats to navigational safety, but they must be specific to real threats; they must not give false signals and unduly interrupt continuity.

Figure. 2.15. WAAS showing links between reference receivers and the East Coast WAAS master station.

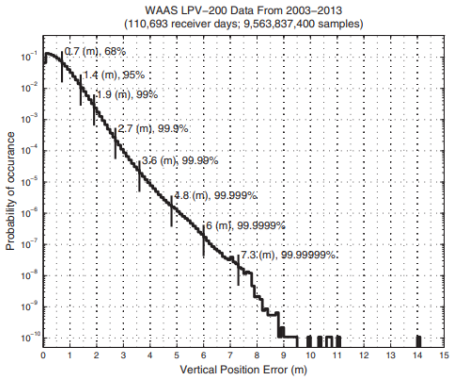

Figure. 2.16. Cumulative distribution function (CDF) for vertical errors when using WAAS.

Precision measures the width of the main part of the error distribution, while integrity controls the swing of the tails.

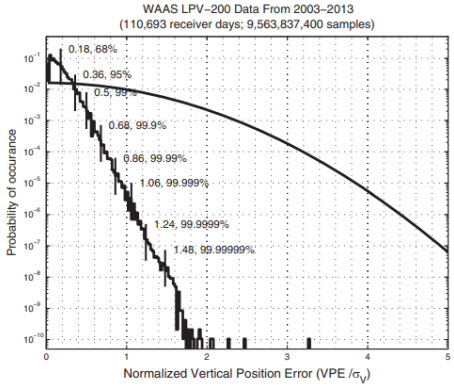

Figure. 2.17. A histogram (or cumulative distribution function) for the ratio of WAAS vertical errors to the standard deviation provided by WAAS for those vertical errors.

2.9 System of independent monitoring of receiver integrity.

Unlike SBAS and GBAS, RAIM is self-contained. In fact, RAIM belongs to a larger family of error detection techniques known as aircraft-based avionics homing systems. As already mentioned, SBAS and GBAS detect errors by comparing GPS measurements with accurate ground information. RAIM compares the GNSS measurements of each individual satellite to a consensus of other satellites in sight. Mathematically, RAIM is based on the residuals of individual GNSS measurements compared to a least-squares navigation solution based on all satellites visible to the user. RAIM is attractive because it does not require a network of base stations on the ground or an actual broadcast from the network to the aircraft.

However, error detection in RAIM is intrinsically weaker than SBAS or GBAS because it does not have access to accurate ground information. The navigation solution must be overspecified, and the geometries of the subordinate subset solutions must be robust. In principle, SBAS and GBAS can provide navigational integrity even for an aircraft with only four visible satellites. However, RAIM requires at least five satellites because the navigation solution must be retrofitted. In addition, all five subsets created by extracting one satellite at a time must have strong geometry so that the subsets have sufficiently high accuracy. This means that RAIM often needs six or even seven visible satellites to detect errors. For this reason, RAIM has not yet been used for vertical control. However, it has been approved for horizontal control, and approximately 200,000 aircraft worldwide provide RAIM support for horizontal control on enroute runways, terminal areas, and non-instrument take-off and landing phases.

As already mentioned, GNSS will ultimately be based on multiple full constellations: GPS, GL ONASS, Galileo and BeiDou. With the initiation of these new constellations, RAIM can provide support for vertical navigation. Given the geometric diversity from two or more constellations, all navigation solutions will be retooled and

the underlying subset geometries will be more robust. The air navigation community is exploring this possibility and has developed a concept known as Advanced RAIM or ARAIM. To provide vertical guidance, ARAIM includes a set of requirements for the main GNSS constellations. These requirements must be met and periodically verified if the basic constellation constant is to be included in the set of measurements used by avionics to support vertical navigation. If ARAIM can be proven safe, it could support navigation to a height of just 200 feet above the airport surface. Because ARAIM would be a multi-constellation instrument, it would be independent of the performance of any of the major GNSS constellations.

2.10 Negative Actors: Interferers and Manipulators

All GNSS satellites are in medium orbit, and signals must travel 20,000–24,000 km before they reach the Earth's surface. Thus, these signals are extremely weak when they reach the Earth's surface; their power is approximately 10 - 16 W. In principle, navigation satellites could be placed closer to Earth to increase the received power, but to ensure the presence of four (or more) satellites in the field of view of each user requires many more satellites.

Radio signals from a terrestrial source can easily exceed weak GNSS signals. If criminal signals are sent to disrupt GNSS, they are called jammers. If these signals are fakes of the GNSS signal, they are called manipulators. The latter are more insidious as they are designed to introduce a dangerous positional error without detection.

Together, jammers and manipulators are negative actors in the GNSS system.

In recent years, the GNSS community has been particularly concerned about the prevalence of personal jammers. These devices intentionally emit a signal in part of the GNSS frequency range. They are designed to interfere with GNSS navigation devices that are illegally installed on the car to secretly track the driver's location. These personal jammers certainly serve their purpose, but they also interfere with all GNSS use in the immediate vicinity of the vehicle under surveillance. Personal jammers have been particularly problematic at Newark International Airport.

The GBAS prototype was installed at this airport with antennas and measurement receivers all located within a few hundred meters of the New Jersey Turnpike. Unfortunately, the vehicles plying this route carry personal jammers and occasionally interfere with GPS receivers in Newark; the GBAS test system was a collateral casualty.

To date, the overall operational impact of interference on GNSS in aviation is limited to the availability of navigation aids that preceded GNSS. These systems include VHF omnidirectional (VOR) systems, distance determination systems (DME) and instrument landing systems (ILS). These are all terrestrial radio systems and they still work. VOR and DME support navigation for aircraft operating in national enroute and terminal airspace and for non-precision approaches at airports. ILS is used to guide aircraft when approaching and landing at airports. Together, these systems support all current conventional navigation operations. However, with the gradual transition of aviation operations to performance-based navigation, traditional systems cannot provide adequate support for the operations described in the Performance and Environmental Benefits section.

For this reason, the aviation community is developing an Alternative Positional Navigation and Time (APNT) system, which is essentially a reconfiguration of existing FAA ground transmitters to provide RNAV and RNP. If it is successful, APNT will become a key element of the air transport system of the next generation (NextGen). One modification of the APNT is the hybrid APNT, which will combine signals from the DME and radio transmitters (RTs) that will be deployed to provide dependent control of air traffic clearance. Both of these signal sources are of terrestrial origin and of high power; thus, they are difficult to thwart.

In addition, these signals will be plentiful in the United States, which already has approximately 1,100 DME stations and plans to have approximately 700 RTs. DME and RT both broadcast in the ARNS frequency range, which is located between 960 and 1215 MHz. Figure 2.18 shows this radio band, which is also shown on the left in Figure 2.4.

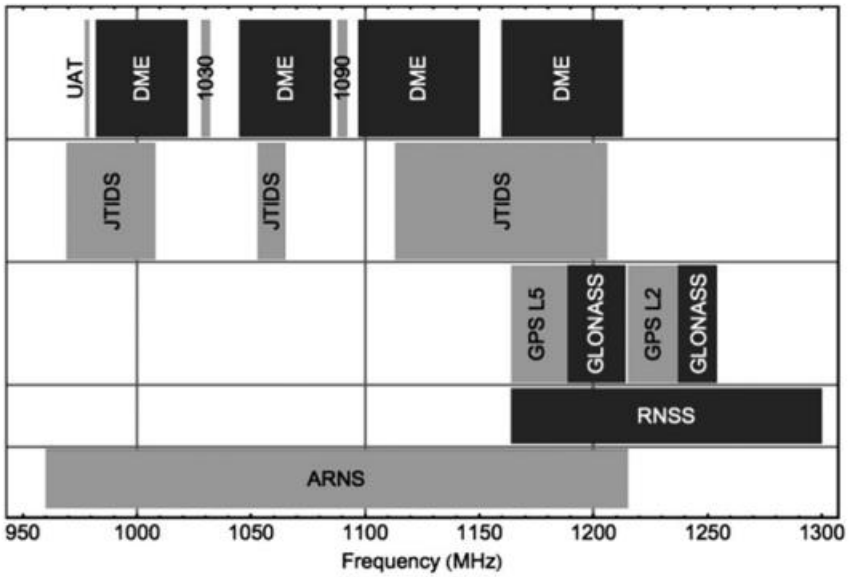

Figure. 2.18. Aeronautical Radio System (ARNS) radio spectrum, including hybrid APNT.

This band is from 960 to 1215 MHz, and is also shown on the left in Figure 4. The spectral blocks, labeled DME, contain many channels for signals from distance measuring equipment (DME). The blocks marked 978, 1030 and 1090 are used for aerial surveillance, and the blocks marked L2 and L5 are for GNSS frequencies.

Blocks marked as JTIDS are used by the military for the Joint Tactical Information Distribution System (JTIDS).

The APNT hybrid system also combines two types of range-finding measurements: one-digit and two-digit. Unambiguous measurement is synonymous with pseudorange measurement used in GNSS and described at the beginning of this section. In the case of APNT, single-digit signals are transmitted from the ground to the aircraft, and the aircraft passively receives these single-digit signals; the plane does not respond. Hybrid APNT uses baroaltimetry to estimate altitude, so an unambiguous measurement would require three APNT signals from the ground to estimate longitude, latitude and aircraft clock offset.

To reduce the number of signals from three to two, the hybrid APNT also uses two-digit measurements. Indeed, modern DME is based on ambiguous measurements. The aircraft starts by sending a signal and the ground station responds when it receives

the aircraft's signal. The aircraft measures the round trip time, subtracts the ground station turn delay and divides by two. After this processing, the measurement estimates the one-way travel time. Unlike pseudo-distance, this binary method is not passive; the aircraft must emit a signal. However, APNT will use binary measurements to a limited extent. It will track single-digit distance to all APNT transmitters in range and generate double-digit measurements from a single DME in range. Thus, the hybrid APNT will be able to estimate the avionics clock offset, and only two stations in line of sight will be needed to estimate the longitude and latitude. Thus, the hybrid APNT will not threaten the DME capacity.

In particular, the community is developing techniques to detect counterfeiting. Some are based on standalone receiver tests, others may be network based. For example, a GNSS receiver can periodically compare GNSS and APNT positions to protect against spoofing.

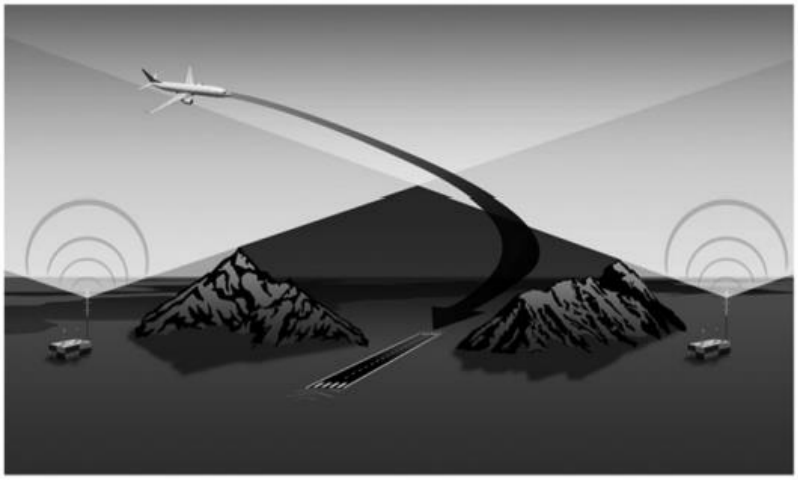

Figure 2.19. The role of inertial sensors in the system of alternative position and time navigation (APNT).

As the aircraft descends, ground signals are overlapped and the APNT will use inertial sensors to support lateral navigation as the aircraft descends from areas of strong radio coverage to areas of weak radio coverage.

Conclusion

Aviation operations that will use satellite navigation to reduce fuel costs and the negative impact on the environment of aviation were described. These operations are based on RNAV and RNP GNSS capabilities. These features allow free point-to-point routes; flights are no longer limited to trajectories imposed by ground radio navigation.

They enable aircraft to fly directly from departure to destination, using the most fuel-efficient routes and avoiding difficult low-altitude terrain.

They provide the opportunity to develop new procedures that allow aircraft to fly closer together to increase arrival and departure levels and perform continuous take-offs and landings to minimize fuel consumption, noise and carbon emissions.

Satellite navigation supports complex take-off and landing procedures that cannot be served by direct beams from ground transmitters. It also supports OPD, where the aircraft descends to the ground according to its own aerodynamics. These maneuvers save fuel and reduce ground noise. Over time, GNSS will support operations in terminal areas, which will include aircraft landing in a "descent" mode in a route pattern, rather than necessarily departing at the end of the queue. Finally, GNSS will also support aircraft that wish to use changes in wind direction, even if those changes occur after the runway.

It also tried to outline the safety basics of GNSS-based air navigation. Indeed, GNSS is being augmented to meet RNP performance monitoring requirements. GNSS complements detect known nuisance events that may threaten the safety of navigation. They broadcast defense levels to the air fleet and this information is used to exceed true positional errors in real time. Known events that cause fear include errors in GNSS systems and procedures, space weather, and "Negative Actors" (spoofs and jammers).

CHAPTER 3. EXPERIMENTAL ASSESSMENT OF THE EFFICIENCY OF SATELLITE NAVIGATION SYSTEMS

The section presents the results of a study of the criteria for the effectiveness of existing satellite navigation systems. The study is performed for single-system mode of operation of receiving equipment and multi-system processing of combinations from

several systems. Online service tools are usedgnssplanning.com and software products in the MatLab environment, developed by the satellite technology laboratory of the Department of Aeronautical Systems of the National Aviation University.

3.1Efficiency criteria of satellite navigation systems

To carry out an experimental assessment of the effectiveness of the use of satellite systems for the aviation sector, we will provide a list of criteria by which the effectiveness of satellite navigation systems is assessed. This information is contained in Annex 10 Aeronautical Communications – Volume 1 in section 3.7.3 Technical requirements for GNSS elements. The analysis of this document shows that the requirements for the characteristics of these systems are put forward according to the following criteria: accuracy, operational readiness, reliability, continuity of service and area of operation.

Precision.

When defining accuracy requirements, an approach is taken where the accuracy standards refer only to the Signal in Space (SIS) of the Standard Positioning Service (SPS) and do not take into account errors due to the atmosphere and receiver noise.

The accuracy of determining the location according to the stated requirements should not exceed the following requirements:

Error determining the location in the horizontal plane:

- the global average for 95% of the time is 8 m
- the worst place for 95% of the time is 15 m

Error determining the location in the vertical plane:

- the global average for 95% of the time is 13 m
- the worst place for 95% of the time is 33 m

The accuracy of the time data transmission in the SPS service of the GPS system does not exceed 30 ns for 95% of the time.

Operational readiness.

This performance criterion is established for users with single-frequency receivers operating on the L1 frequency with the C/A code and is the following values:

≥ 99% for service in the horizontal plane and medium location (95% threshold value 15 m);

≥ 99% for service in the vertical plane and medium location (95% threshold value 33 m);

≥ 90% for service in the horizontal plane and the worst location (95% threshold 15 m);

≥ 90% for service in the vertical plane and the worst location (95% threshold 33 m);

Reliability.

The reliability of the SPS service must meet the following requirements for the measurement error of the receiver satellite-antenna range (URE) at the level of no more than 30 m

- at least 99.94% (global average);

- not less than 99.79% (average for a separate item in the worst case).

Continuity of service.

The probability of loss of an L1 C/A signal from one of the 24 satellites of the nominal space segment due to an unplanned interruption shall not exceed one hour.$2 \cdot 10^{-4}$

Coverage.

The SPS service area of the GPS system covers the Earth's surface and extends up to an altitude of 3,000 km.

3.2 Methodology of research

To evaluate the effectiveness of satellite navigation systems, we will use the following methodology. We will download up-to-date information on the status of all active satellite navigation systems that are part of GNSS and, using a number of ready-made software products, we will evaluate the performance criteria of each system separately, as well as when using several and all of them together.

Information about the current status of the current systems GPS, Galileo, Beidou, QZSS is contained in the almanac, which is published by the Trimble receiving navigation equipment development company and is available for download on its ftp server (Fig. 3.1).

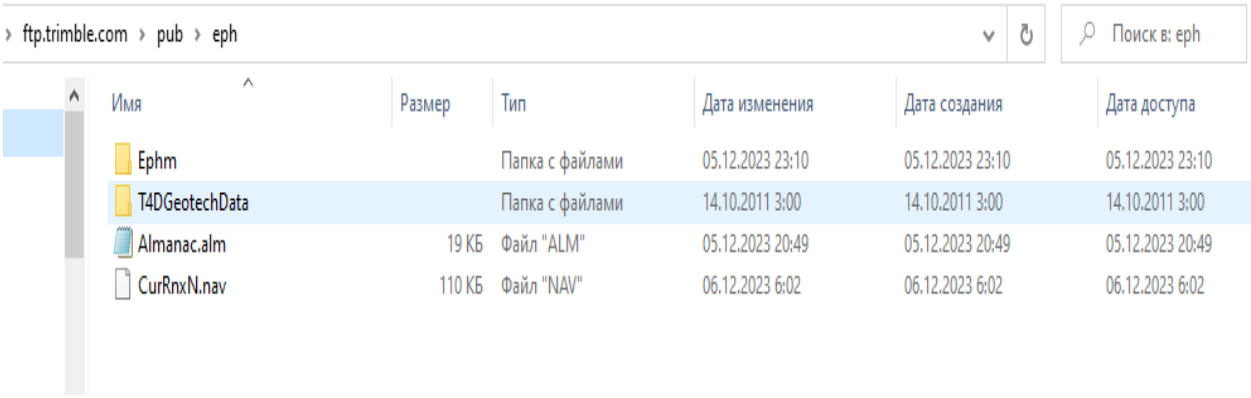

Fig. 3.1 GNSS almanac on the Trimble ftp server

After downloading, the almanac can be opened with any text editor to analyze the data it contains. Uploaded on December 5, 2023, the almanac (Fig. 3.2) contains information on a total of 152 satellites with a range of numbers from 2 to 390.

Satellites of each of the operating systems have their own range of numbers according to the table. 3.1. Data on the GLONASS system are not considered and completely ignored in the framework of the thesis, which is indicated in the table. 3.1 by crossing out its name.

Table 3.1 – Correspondence of satellite numbers to GNSS systems

The number of the satellite in the Trimble almanac file	**Satellite system**
1 ... 37	GPS
38 ... 64	~~GLONASS~~
111 ... 118	QZSS
201 ... 263	Galileo
264 ... 283	Beidou

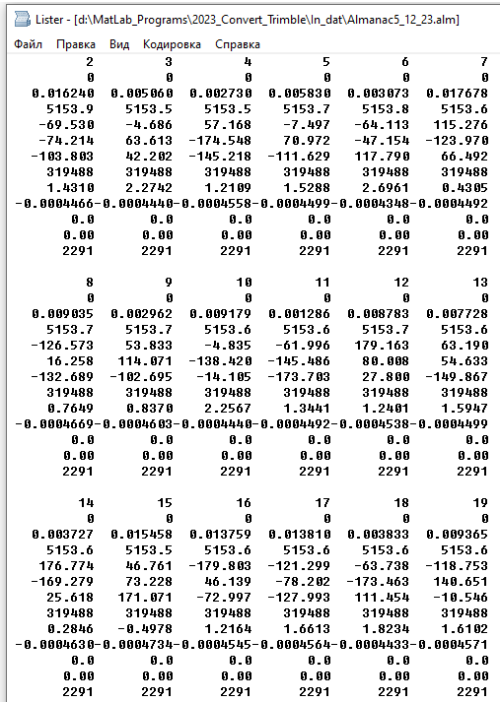

Fig. 3.2 Contents of the downloaded almanac

The data recording format in this file must be converted to the Yuma format, which is more universal in GNSS systems simulation programs.

It is advisable to use for conversionMatLab program 2023_Convert_Trimble (Fig. 3.3) developed by the Laboratory of Navigation Systems of the National Aviation University.

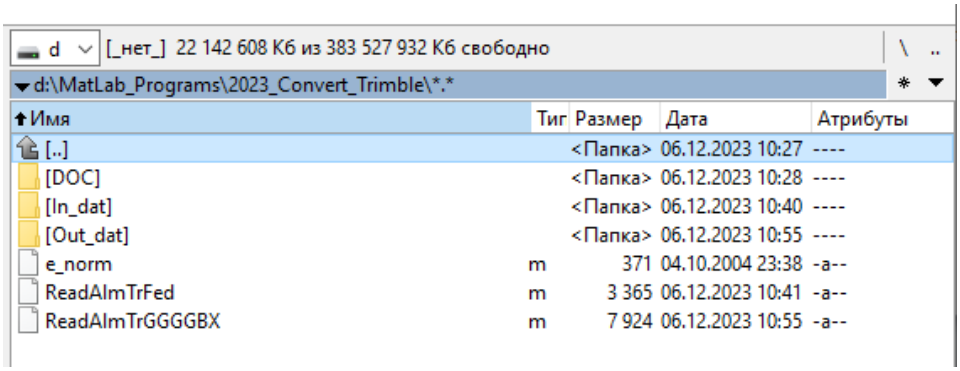

Figure. 3.3 Program folder 2023_Convert_Trimble

The main conversion steps are as follows:

The recorded almanac file must be located in the In_Dat input folder. After that, its name must be specified in the corresponding lines of code of the programs ReadAlmTrFed and ReadAlmTrGGGGBX, as shown in Fig. 3.4 and 3.5.

Figure. 3.4 Almanac file name to convert to ReadAlmTrGGGGBX

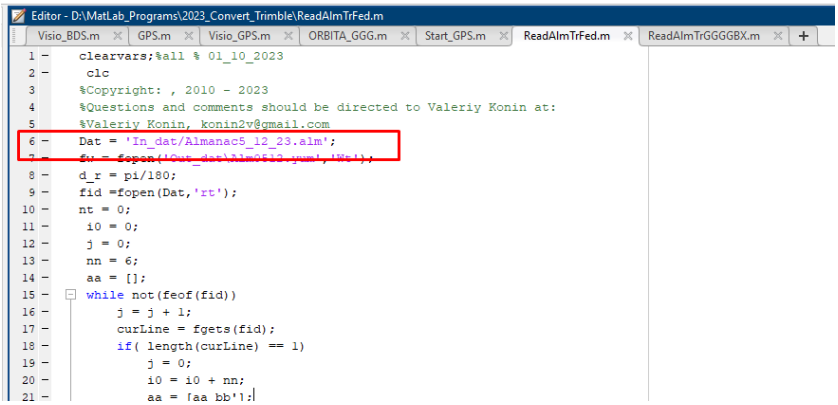

Figure. 3.5 Almanac file name to convert to ReadAlmTrFed

Also, in the text of the programs, the names of the source files are specified, in which the almanacs in Yuma format will be placed for each of the systems separately as a result of the ReadAlmTrGGGGBX program and the common almanac of all systems as a result of the ReadAlmTrFed execution. All these almanacs are placed in the Out_Dat output folder, the final content of which is shown in Fig. 3.6.

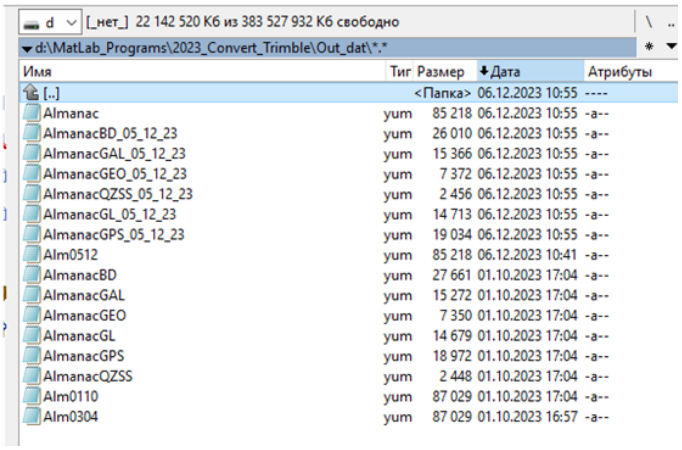

Figure. 3.6 Contents of the Out_Dat output folder

The files created as a result of the MatLab programs contain almanacs of GPS, Galileo, Beidou and QZSS satellite systems in the Yuma format, which can be opened in a text editor. For example, in fig. 3.7 shows the contents of the received Yuma almanac for the Galileo system.

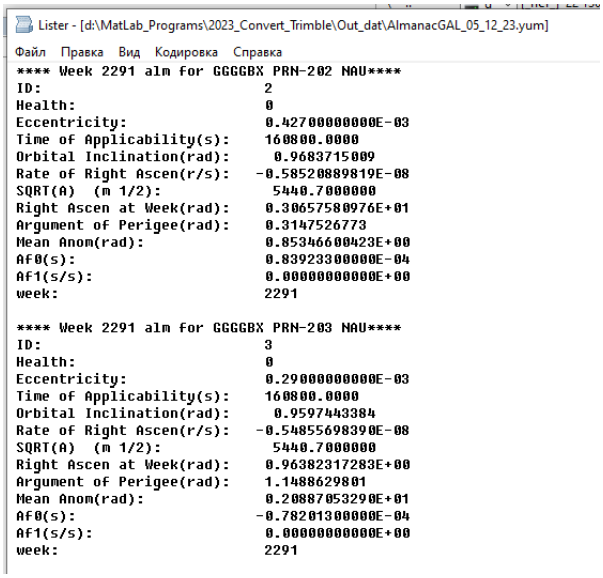

Figure. 3.7 Yuma almanac of the Galileo system

As can be seen from fig. 3.7 GPS week number corresponding to the created almanac is 2291. Let's find for which calendar dates this number is relevant. By linkhttps://www.labsat.co.uk/index.php/en/gps-time-calculatoran online calculator is available that you can use to check. The result of the calculation made with its help for the date of December 5, 2023 gives the result of GPS week 2291 (Fig. 3.8), which coincides with the week in the file and thus confirms the relevance of the received data in the almanac.

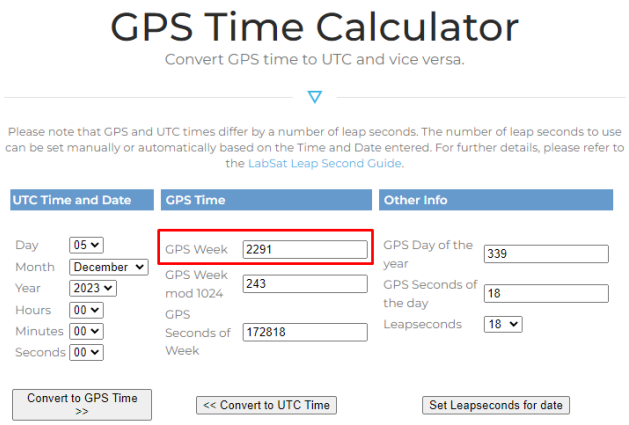

Figure. 3.8 Checking the GPS number of the week for December 5, 2023

The resulting almanacs in Yuma format will be used in the next stage of the research. For its implementation, we will use the software tool Galileo Satellite Simulation Facility (GSSF V2.1.11). It is a tool for comprehensive studies of the characteristics of the Galileo system, which works both with models of satellites that are built into it at the stage of creation, and allows updating this data by downloading almanacs of active satellite systems. We will present a step-by-step algorithm for loading current almanacs into the GSSF program environment.

At the first step, GSSF is launched using the program icon on the desktop (Fig. 3.9).

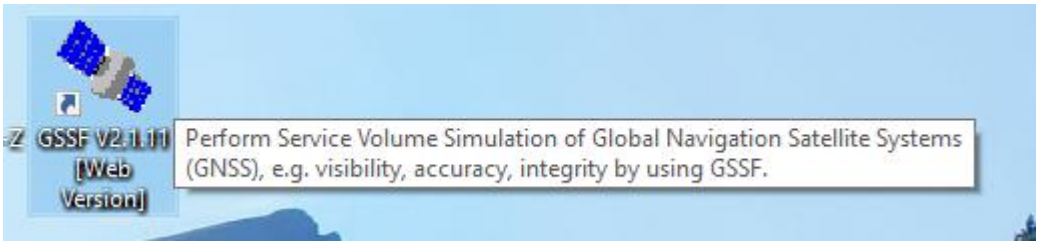

Figure. 3.9 The appearance of the GSFF launch icon

After launch, the expanded interface of the program at the beginning of work looks like that shown in Fig. 3.10

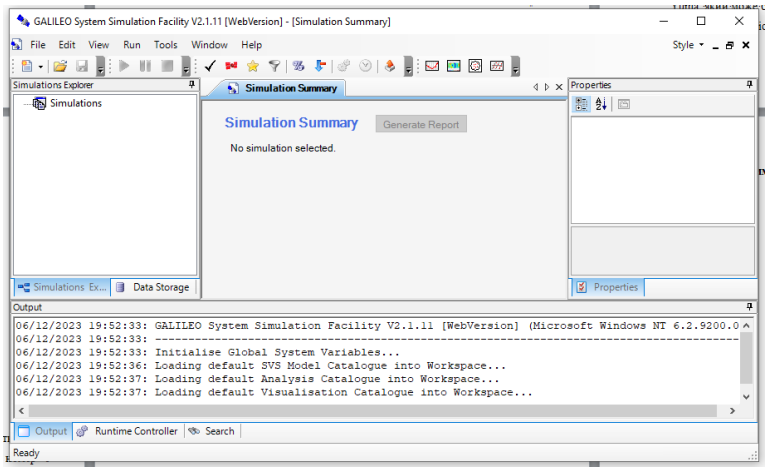

Figure. 3.10 Start view of the interface

To create a research scenario, it is necessary to perform the steps of creating a new Simulation – Empty Scenario and then filling it with components that will form the composition of the system and the type of analysis that will be performed. Some of these steps are shown in the following figures. 3.11 - 3.14.

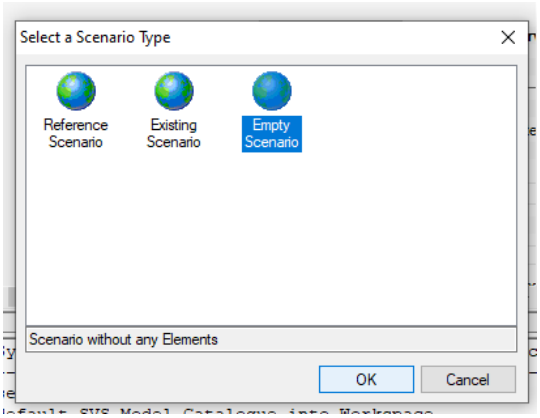

Figure. 3.11 Creating an empty script form

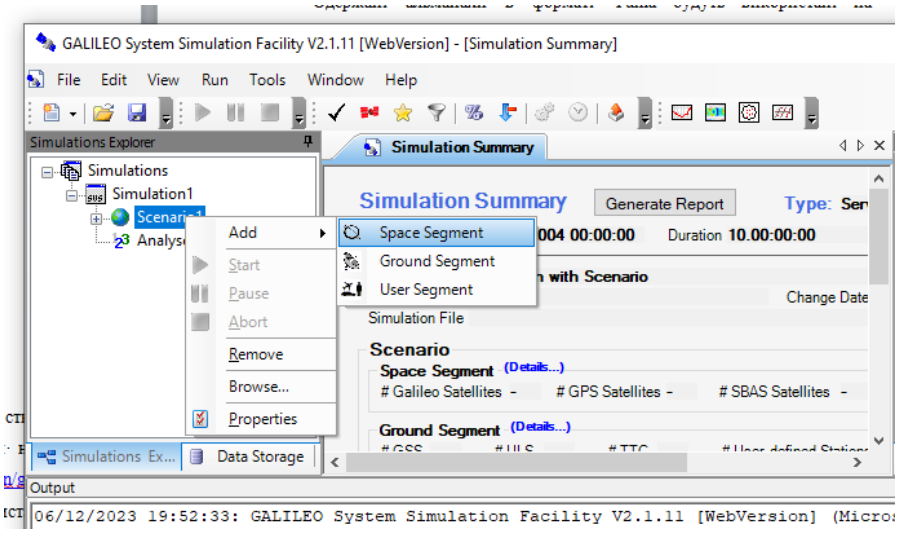

Figure. 3.12 Adding a space segment to the scenario (satellite system to be analyzed)

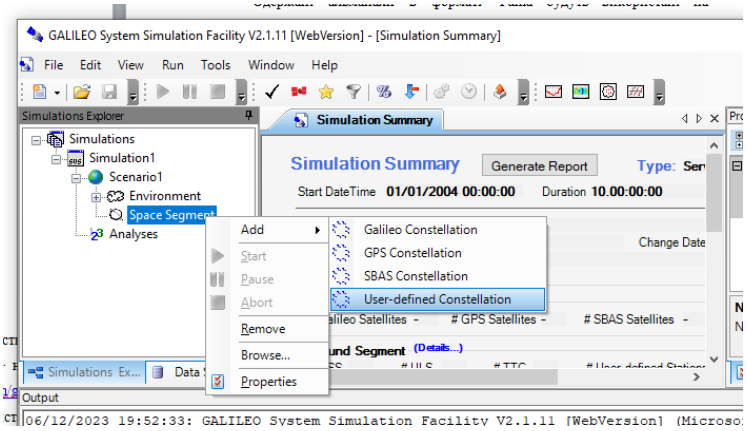

Figure. 3.13 Selecting the User-defined Constellation option

The stage reproduced in fig. 3.13 allows you to choose between several variants of satellite segments, which are already present in the GSSF program in the form of models corresponding to the nominal constellations of the GPS and Galileo systems. The possibility of switching to the use of real data is included in the selection of the last item of this menu, namely the User-defined Constellation option followed by the selection of the Constellation File Wizard (Fig. 3.14), which will offer to download the almanac file in the Yuma format.

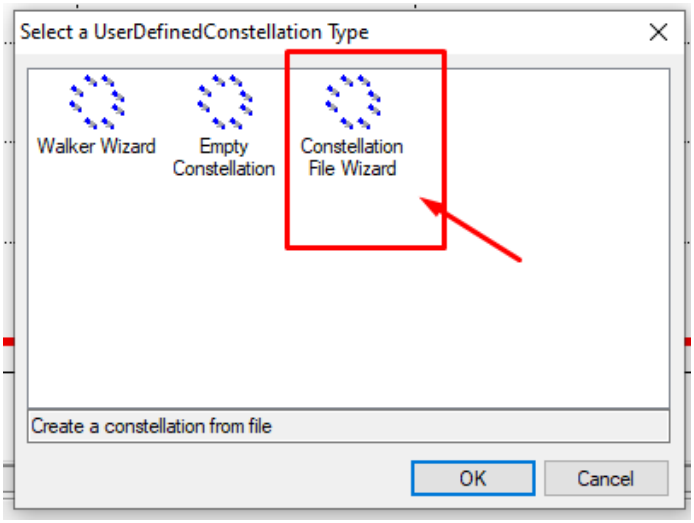

Figure. 3.14 Selection of almanac download from user file

Thus, the further selection as an almanac file of those Yuma almanacs that were previously generated by the MatLab program (Fig. 3.15) allows us to proceed to studies in the middle of the GSSF based on current data on satellite systems.

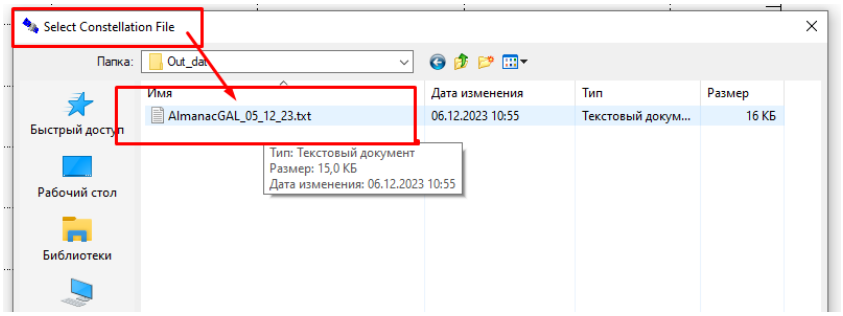

Figure. 3.15 Selecting an almanac from the Out_Dat output folder

A sign that the GSSF interface has successfully accepted the proposed almanac will be the display of the number of User-defined Satellites in the Simulation Summary form (Fig. 3.16).

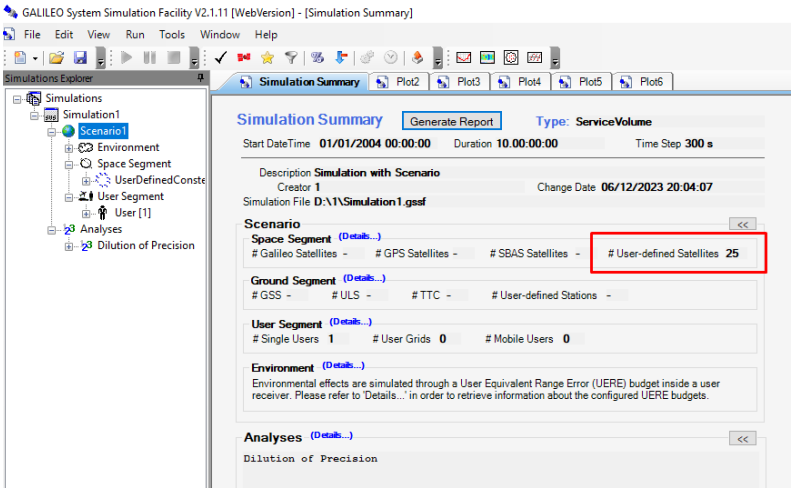

Figure. 3.16 25 satellites are connected

To check whether the number of satellites corresponds to the current situation, you can compare it with the satellite library on the gnssplanning.com service page, which shows the same number of active satellites as part of Galileo for December 6 (Fig. 3.1).

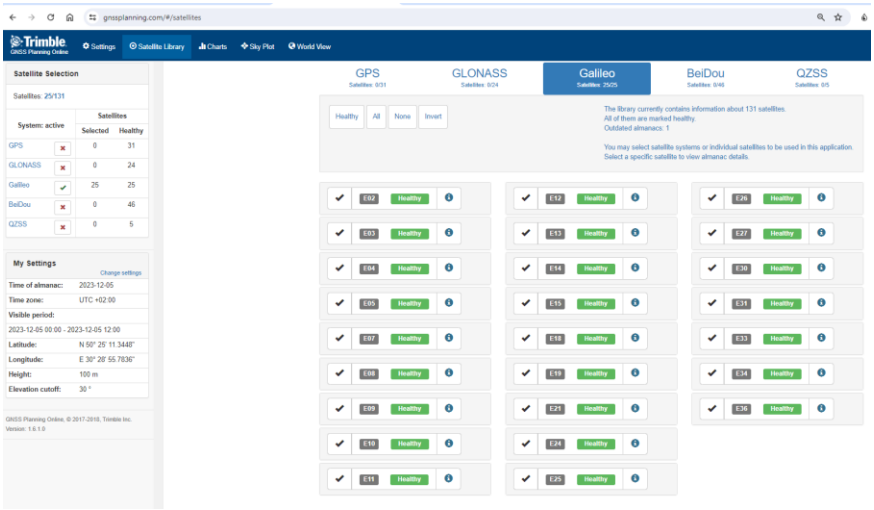

Figure. 3.17 Checking the number of Galileo satellites on the selected date 12/5/2023 on the gnssplanning.com page

3.3 Experimental evaluation of the global availability of satellite navigation systems

To assess the availability of satellite navigation services, it is necessary to create scenarios in GSSF based on the created almanacs of operating systems and select the Visibility criterion as an analysis.

The results of the assessment of the availability of the Galileo satellite system for the day of December 5, 2023 are shown in Fig. 3.19-3.21

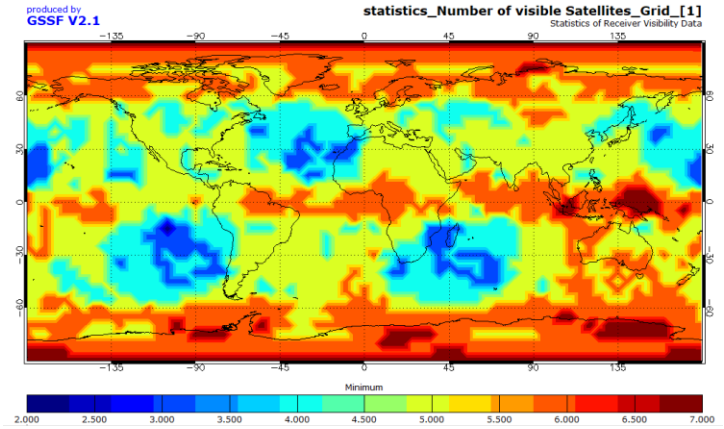

Figure. 3.18 Minimum number of visible Galileo satellites

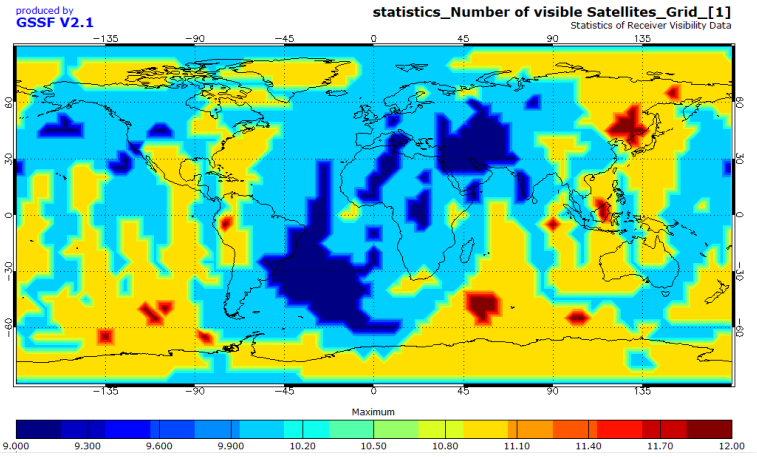

Figure. 3.19 Maximum number of visible Galileo satellites

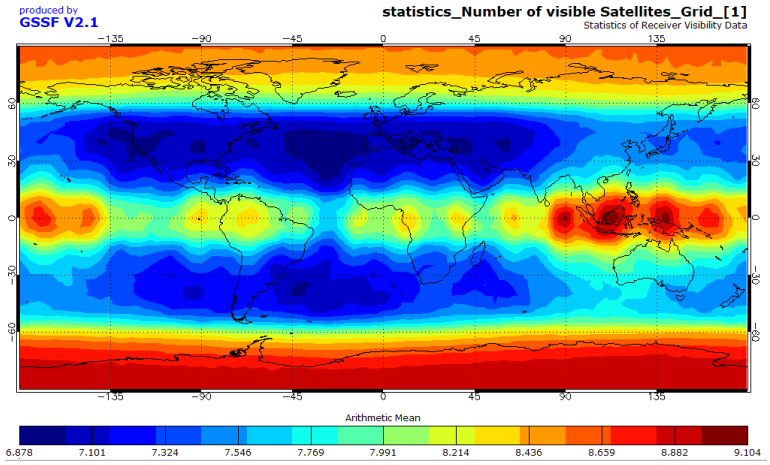

Figure. 3.20 Average number of visible Galileo satellites

The results of the assessment of the availability of the satellite systemGPS are shown in fig. 3.21 - 3.24.

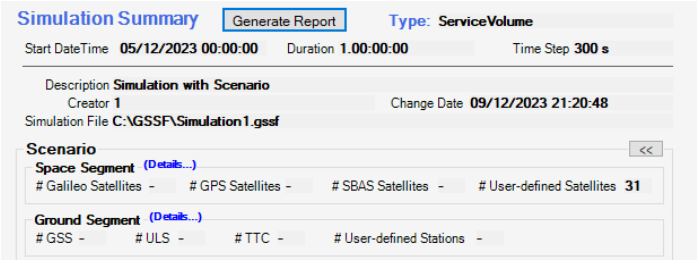

Figure. 3.21 Loading the GPS system almanac script

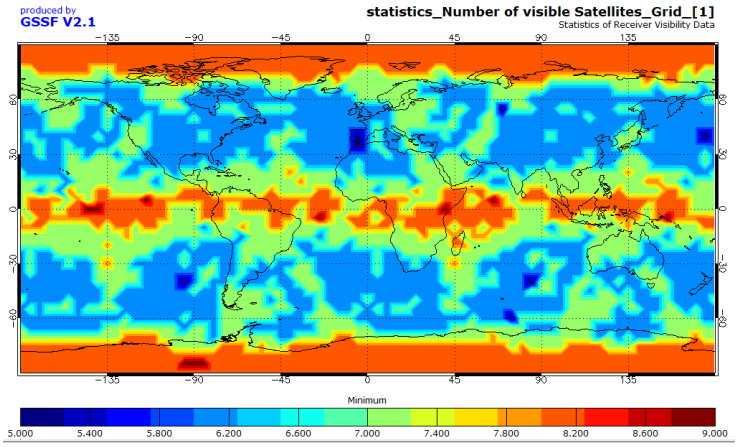

Figure. 3.22 Minimum number of visible GPS satellites

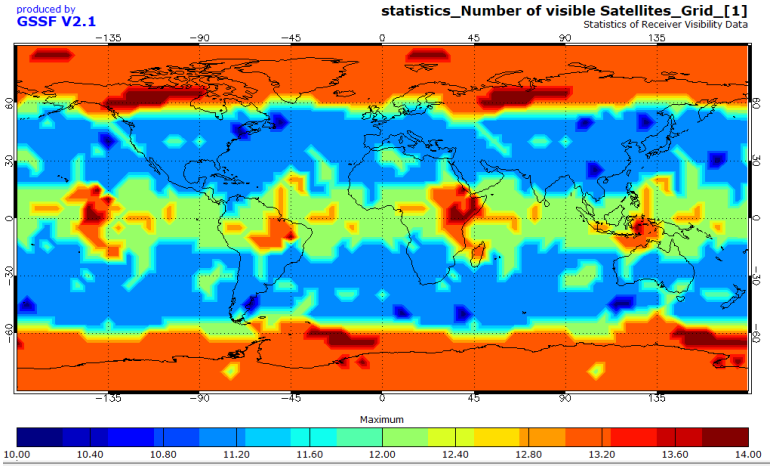

Figure. 3.23 Maximum number of visible GPS satellites

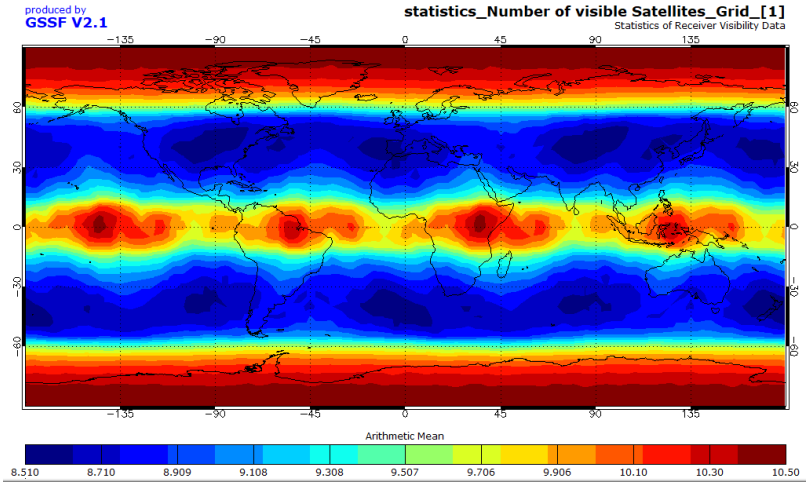

Figure. 3.24 Average number of visible GPS satellites

The results of the assessment of the availability of the Beidou satellite system are shown in Fig. 3.25 - 3.28.

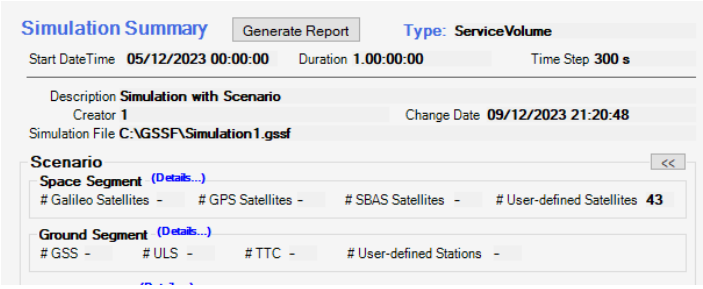

Figure. 3.25 Loading into Beidou system almanac script

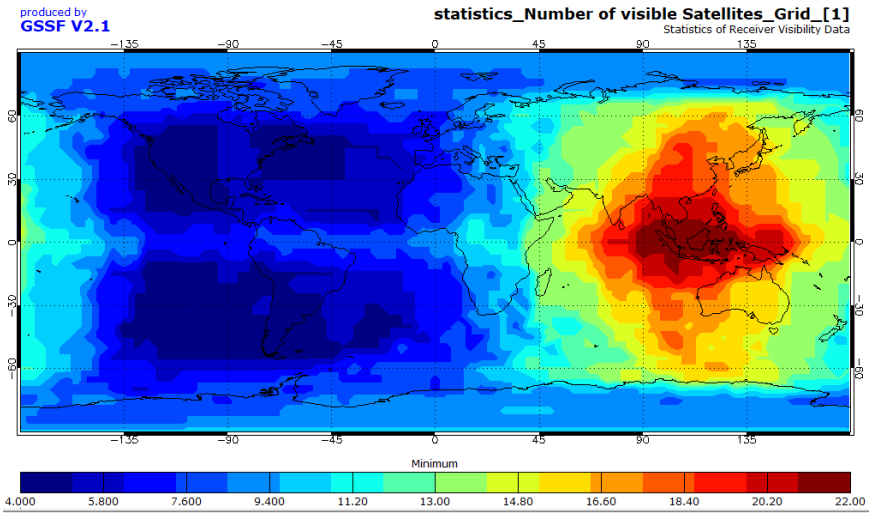

Figure. 3.26 Minimum number of visible Beidou satellites

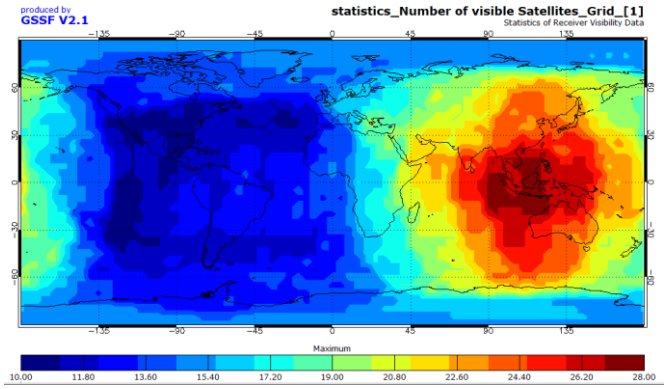

Figure. 3.27 Maximum number of visible Beidou satellites

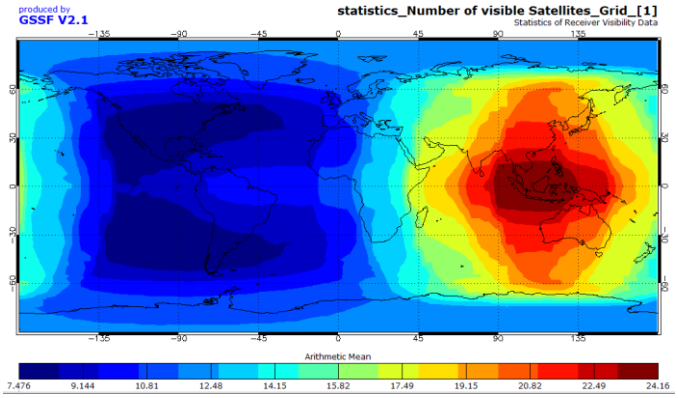

Figure. 3.28 Average number of visible Beidou satellites

To assess the availability of a full-scale warehouseGNSS with all Galileo, GPS, and Beidou satellites will be loaded into the GSSF scenario with a common almanac of these systems (Fig. 3.29).

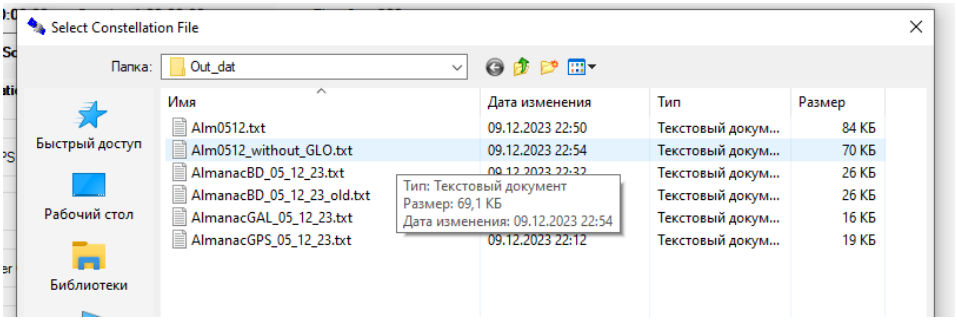

Figure. 3.29 Selection in the file system of the shared GNSS almanac

As a result, the common constellation contains 102 satellites, of which 25 belong to the Galileo system, 31 to GPS, 46 to Beidou.

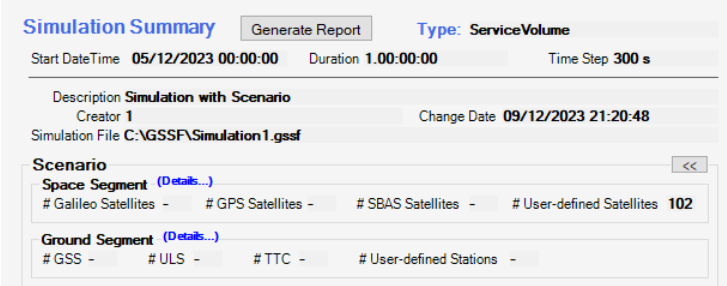

Figure. 3.30 Scenario with a constellation of 102 satellites

Results of the assessment of the availability of the combined satellite systemGNSS are shown in fig. 3.31 - 3.33.

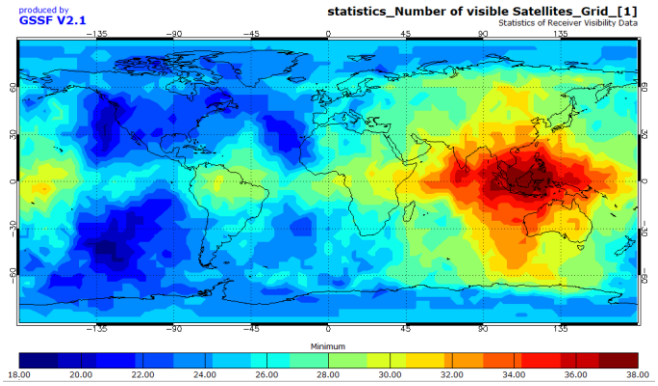

Figure. 3.31 Minimum number of visible GNSS satellites

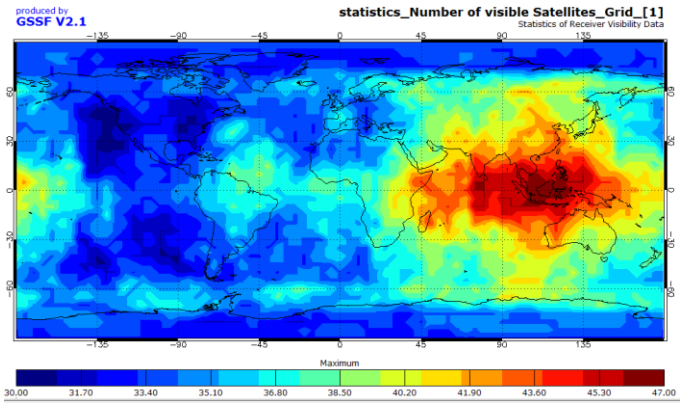

Figure. 3.32 Maximum number of visible GNSS satellites

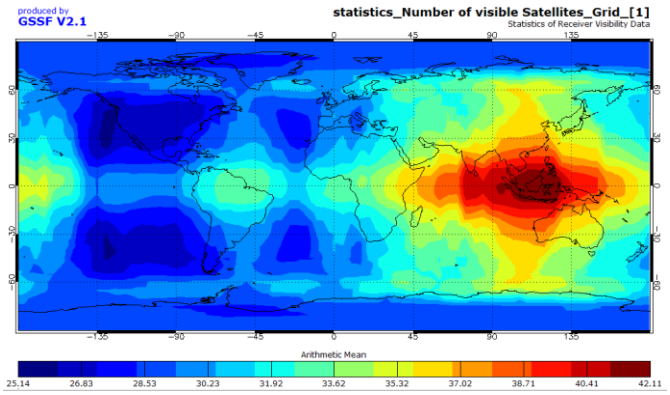

Figure. 3.33 Average number of visible GNSS satellites

The obtained results demonstrate a global assessment of the availability of each of the satellite systems separately and in case of joint use. Also inGSSF has the ability to reproduce the graph of changes in the number of satellites in the sky above the user for a given geographical position (Figs. 3.34 and 3.35).

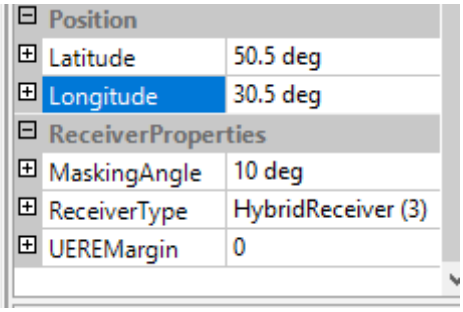

Figure. 3.34 Establishing a point to assess the change in availability of GNSS satellites

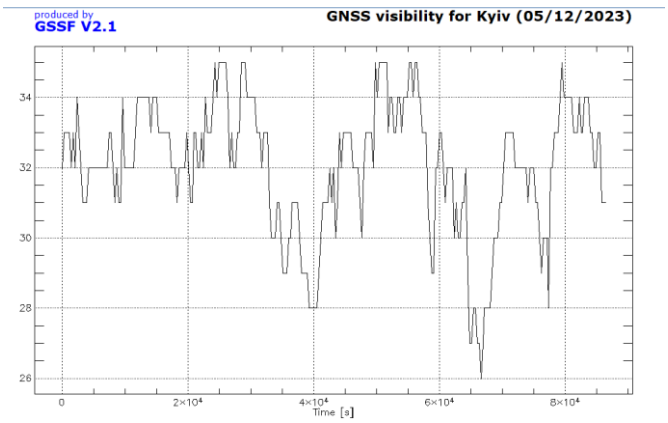

Figure. 3.35 Change in the number of visible satellites over Kyiv during 12/5/2023

3.4 Experimental assessment of accuracy

The accuracy of determining the coordinates of the user depends both on factors related to the type of equipment used by him and the method of determining the coordinates (two-frequency or single-frequency measurements are performed, phase or code ranges are determined), and on factors that are common to all users and which are collectively included in such a parameter as UERE - the total error of determining the range to the navigation satellite. The final connection between a specific UERE (which

for modeling tasks can be set at a certain level) and the accuracy of the navigation system is established through the geometric accuracy degradation factor - GDOP.

The results of the study of the geometric accuracy factor and the final accuracy of the Galileo navigation system are shown in Fig. 3.36-3.37.

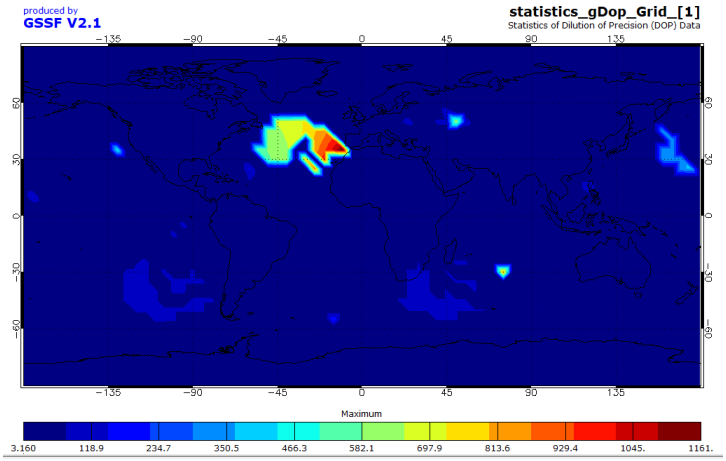

Figure. 3.36 Maximum GDOP for the Galileo system during 12/5/2023

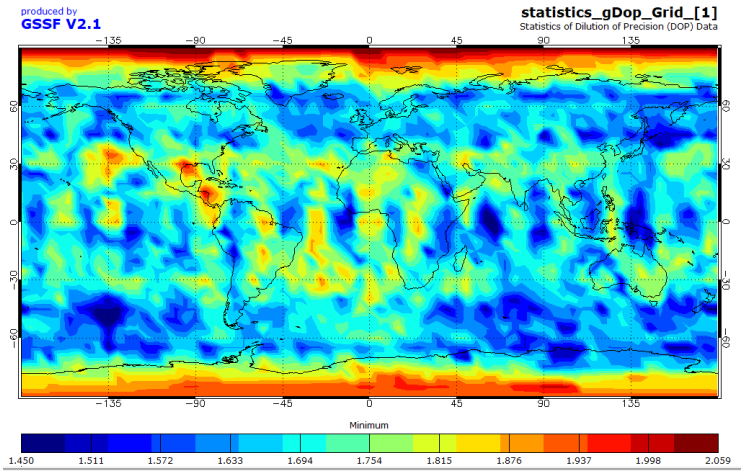

Figure. 3.37 Minimum GDOP for the Galileo system during 12/5/2023

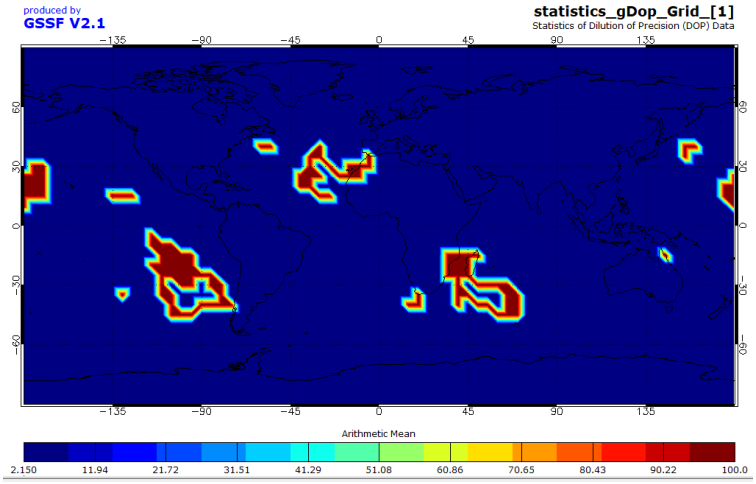

Figure. 3.38 Average GDOP score for the Galileo system during 12/5/2023

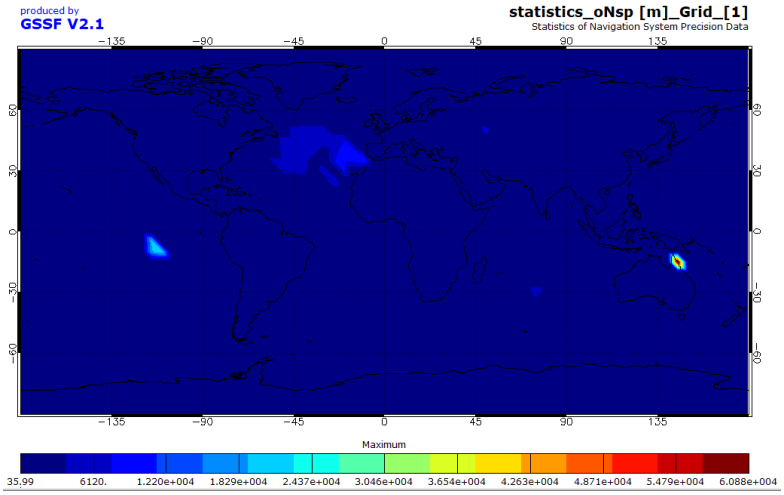

Figure. 3.39 Maximum Galileo error value during 12/5/2023

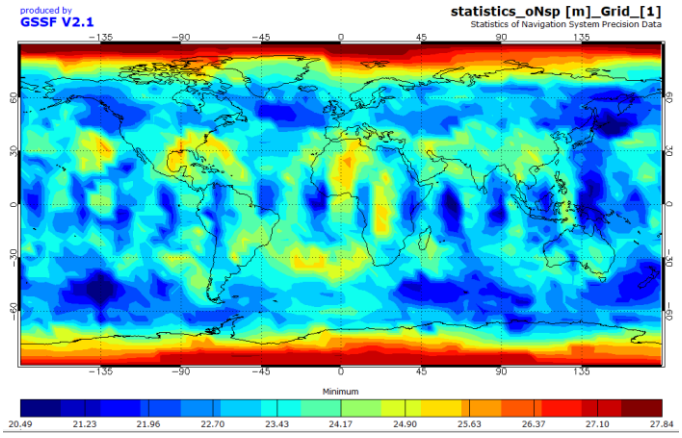

Figure. 3.40 Minimum Galileo error value during 12/5/2023

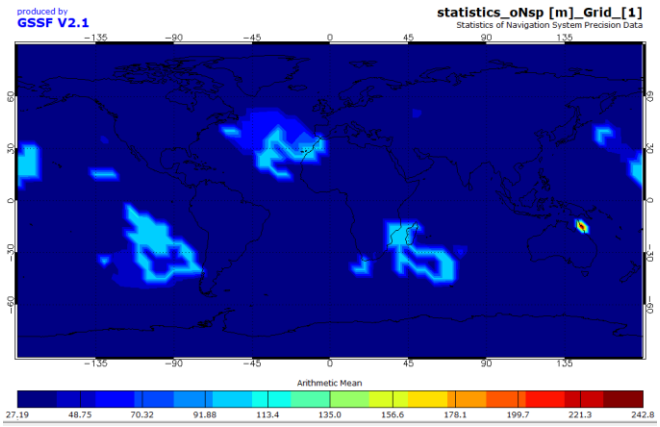

Figure. 3.41 Average error of the Galileo system during 12/5/2023

The results of the study of the geometric accuracy factor and the final accuracy of the GPS navigation system are shown in Fig. 3.42-3.47.

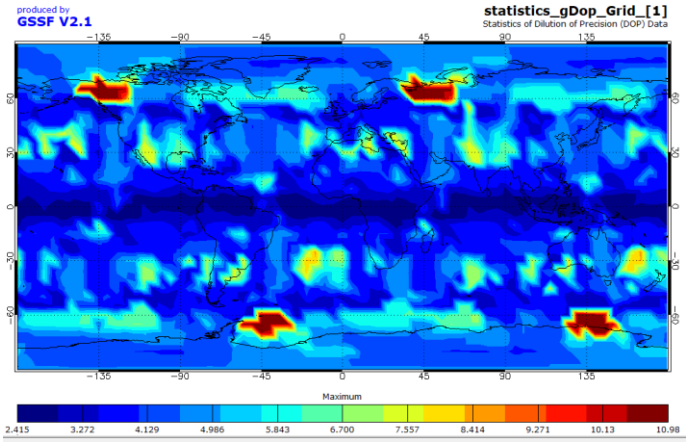

Figure. 3.42 Maximum GDOP for the GPS system during 12/5/2023

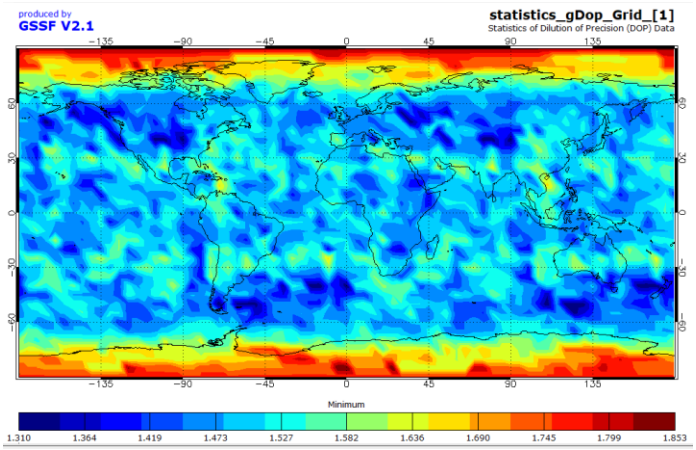

Figure. 3.43 Minimum GDOP for GPS system during 12/5/2023

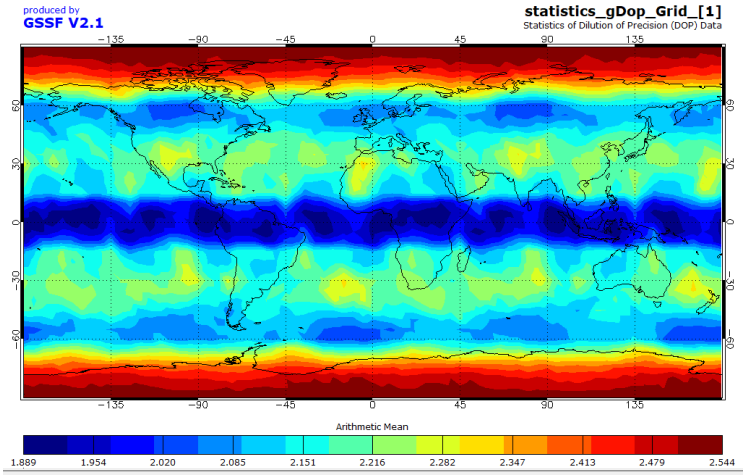

Figure. 3.44 Average GDOP for GPS during 12/5/2023

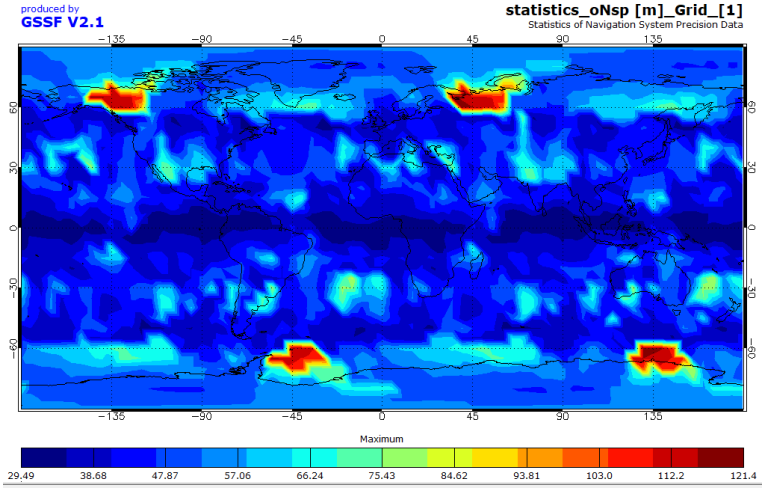

Figure. 3.45 Maximum GPS error value during 12/5/2023

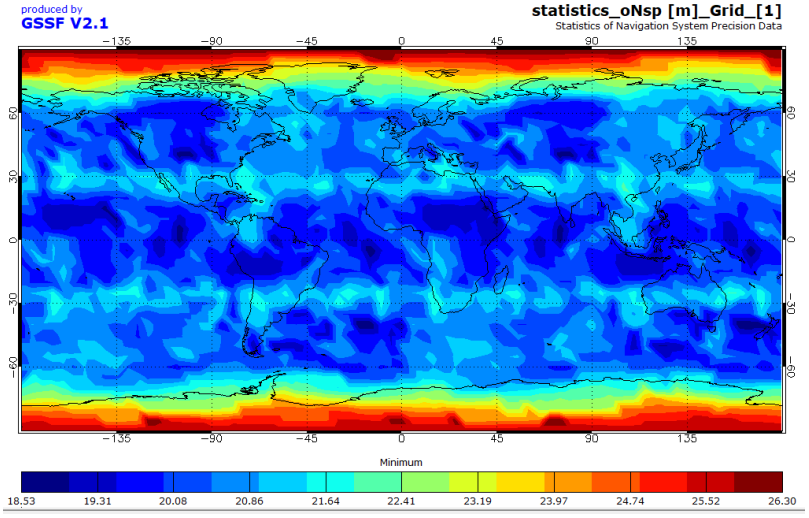

Figure. 3.46 Minimum GPS error value during 12/5/2023

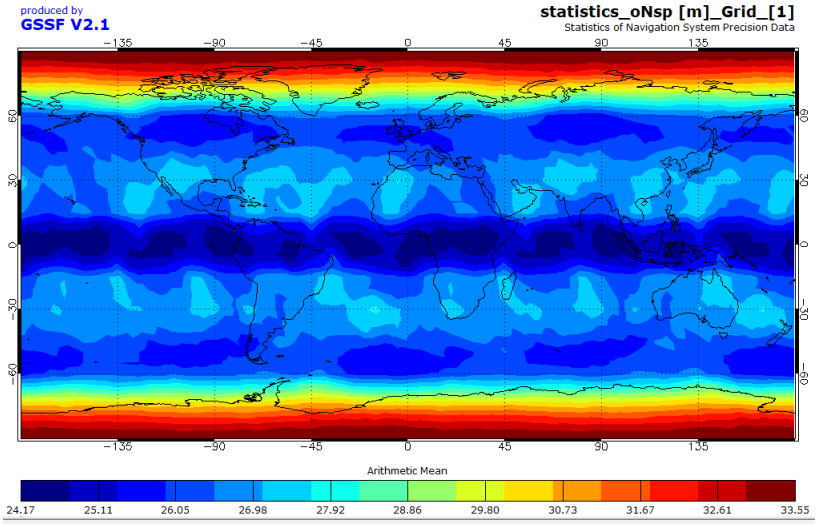

Figure. 3.47 Average GPS error during 12/5/2023

The results of the study of the geometric accuracy factor and the final accuracy of the Beidou navigation system are shown in Fig. 3.48-3.53.

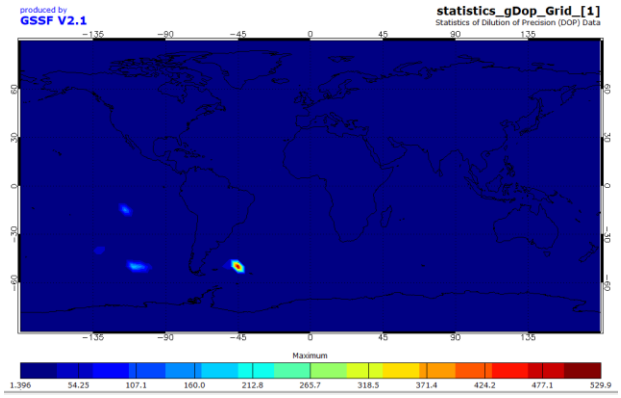

Figure. 3.48 Maximum GDOP for Beidou system during 12/5/2023

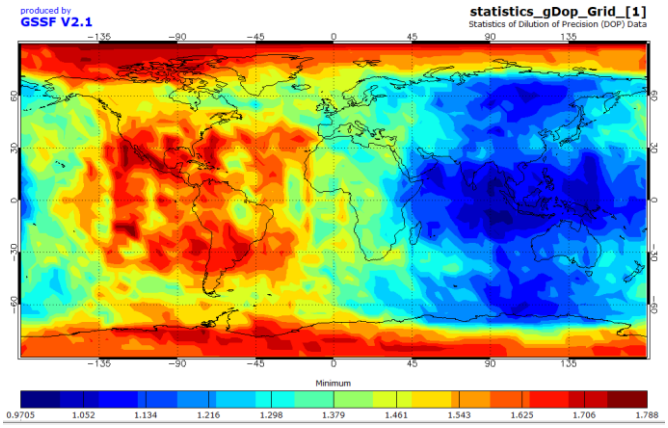

Figure. 3.49 Minimum GDOP for Beidou system during 12/5/2023

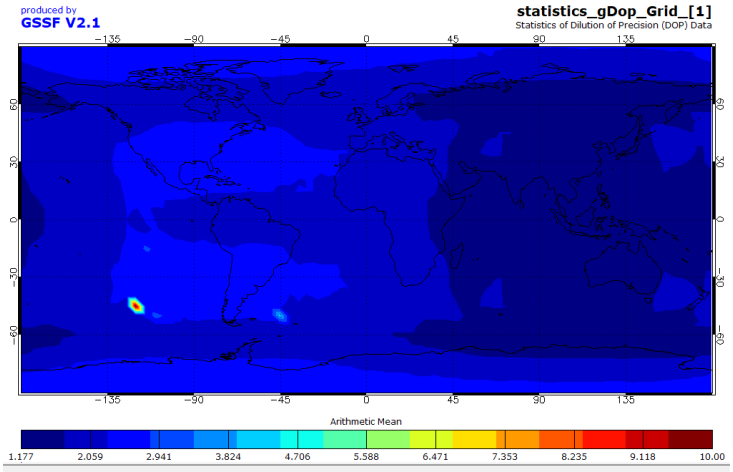

Figure. 3.50 Average GDOP for Beidou system during 12/5/2023

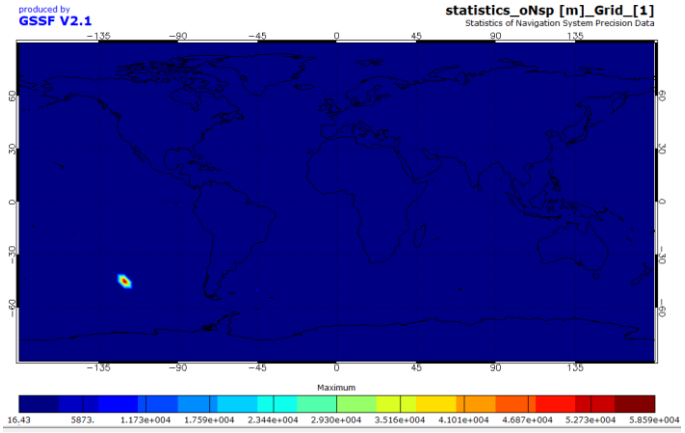

Figure. 3.51 The maximum error of the Beidou system during 12/5/2023

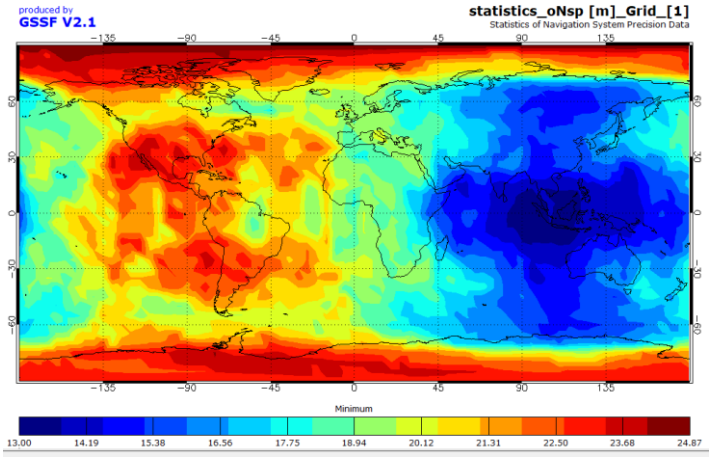

Figure. 3.52 The minimum error of the Beidou system during 12/5/2023

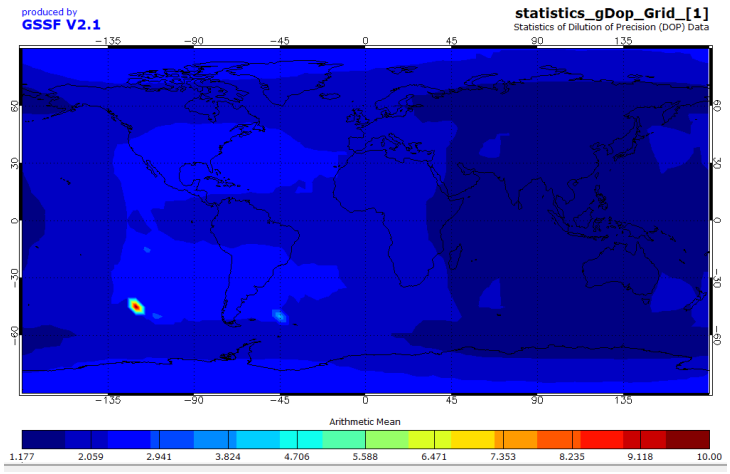

Figure. 3.53 Average error of Beidou system during 12/5/2023

The results of the study of the geometric accuracy factor and the final accuracy of the GNSS navigation system, which includes all satellites of the Galileo, GPS, and Beidou systems, are shown in Fig. 3.54-3.60.

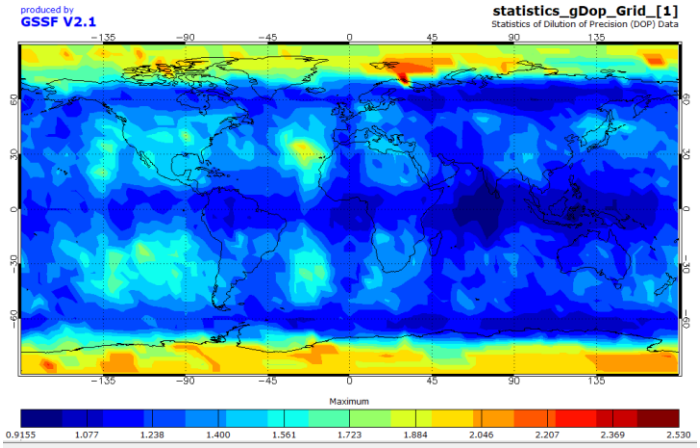

Figure. 3.54 Maximum GDOP for the GNSS system during 12/5/2023

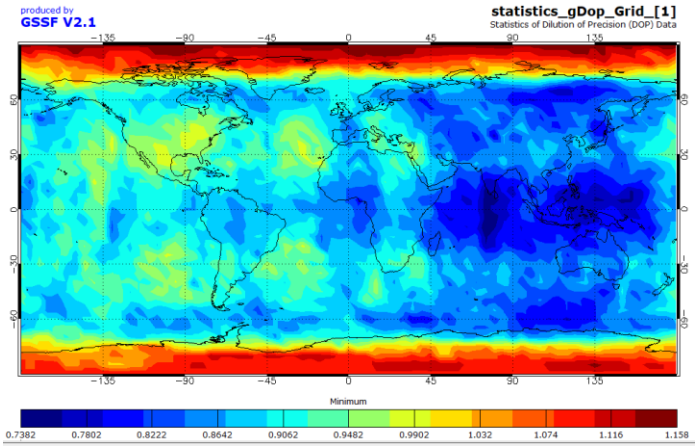

Figure. 3.55 Minimum GDOP for the GNSS system during 12/5/2023

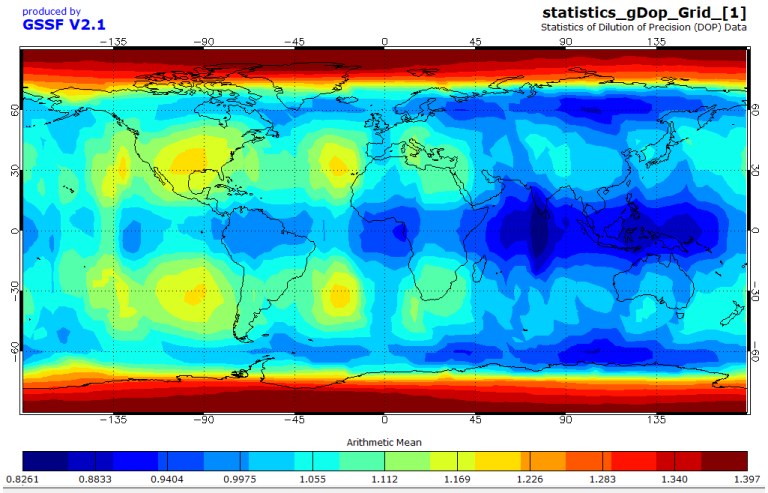

Figure. 3.56 Average GDOP for the GNSS system during 12/5/2023

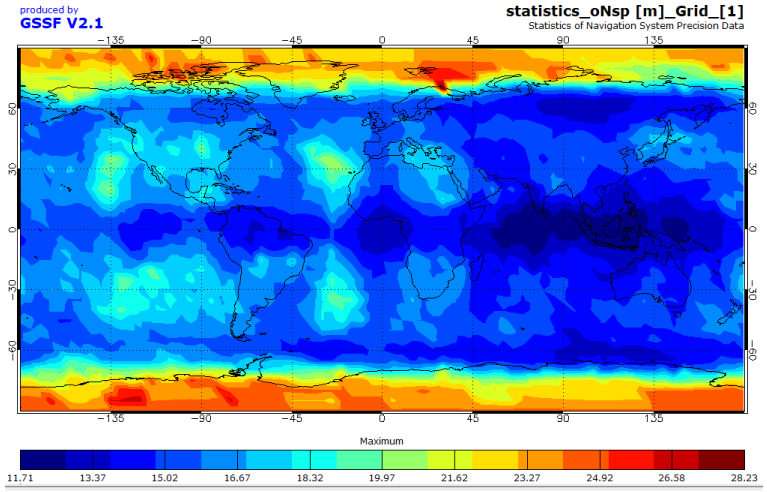

Figure. 3.57 Maximum error of the GNSS system during 12/5/2023

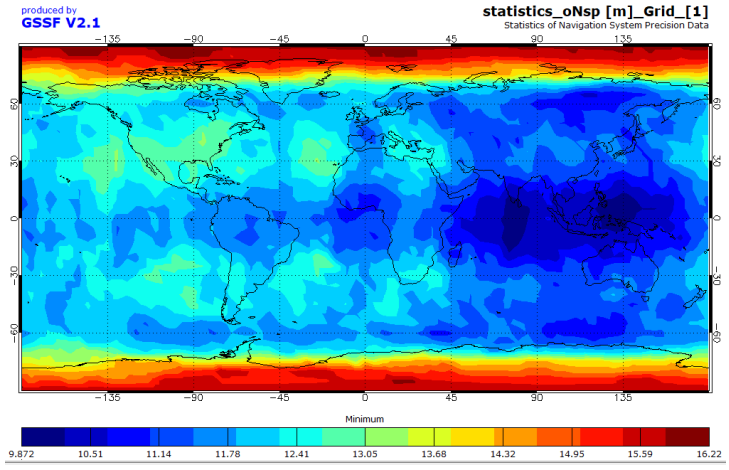

Figure. 3.58 Minimum error of the GNSS system during 12/5/2023

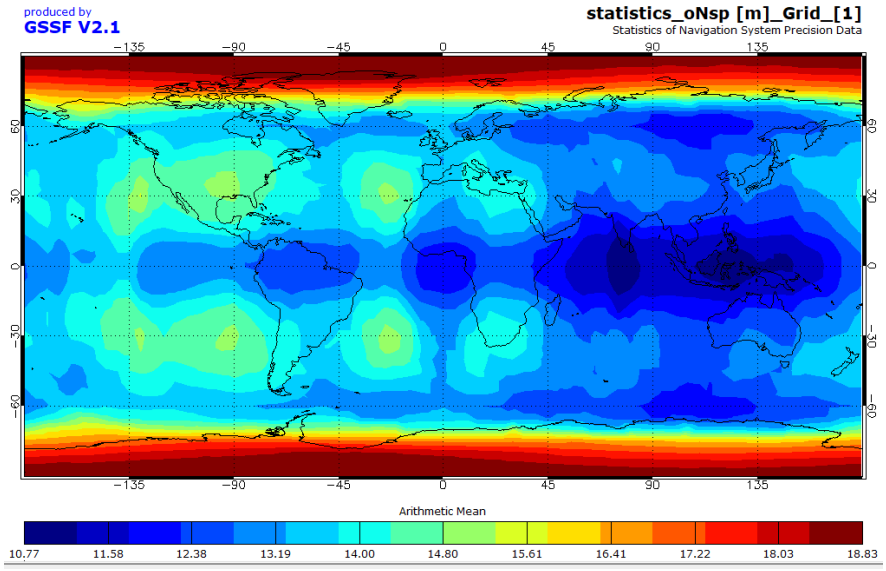

Figure. 3.59 Average error of the GNSS system during 12/5/2023

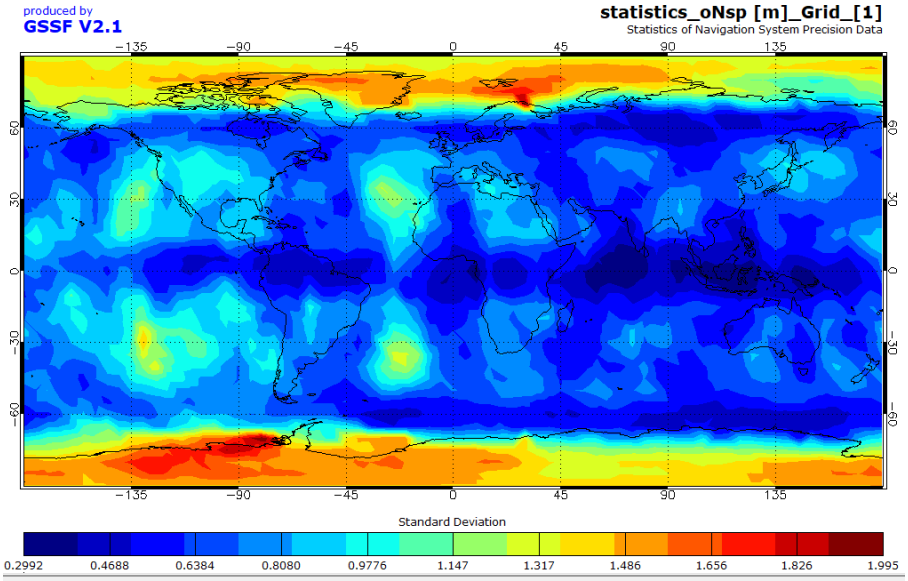

Figure. 3.60 SCV of GNSS errors

Conclusion

1. An analysis of the requirements for performance indicators of existing satellite navigation systems, which are present in the ICAO documentation, was carried out. He showed that the effectiveness of GNSS is evaluated by accuracy, reliability, operational readiness and coverage area.

2. A method of conducting a study on the evaluation of the effectiveness of satellite navigation systems is proposed. For its implementation, up-to-date information on the current state of various satellite systems that are part of the Global Navigation Satellite System (GNSS) was taken and converted into separate GPS, Galileo, Beidou almanacs by the special programs of the satellite systems laboratory of the ANS department.

3. At the research stage, an assessment of GNSS performance indicators was performed under several scenarios, which differed in the list of systems included in its composition. The obtained results demonstrated that the best results are obtained in multi-system processing scenarios.

CHAPTER 4. CALCULATION OF THE ECONOMIC EFFICIENCY OF THE DEVELOPMENT OF OPTIMIZATION AND IMPROVEMENT OF SATELLITE SYSTEMS

Under efficiency in the framework of the calculation, it is appropriate to consider the ratio of estimated (expected) profit in relation to the amount of resources spent on development and implementation. Economic efficiency is not the only type of possible efficiency. We will also pay attention to the synergistic result due to the system integration of various types of efficiency, among which the following are present:

- Economical
- Technical
- Informational
- Mathematical modeling and decision-making
- Psychological
- Social
- Cultural
- Ecological
- Ergonomic

Systemoptimization and improvement of efficiency of satellite systemsmust be cost-effective, at the same time it must satisfy the diverse interests of the community of providers of educational services and those who form a demand for them. The cost of services for students should always be taken into account when evaluating any proposals to provide an opportunity to exercise the right to education enshrined in the Constitution of Ukraine. The market economy, the implementation of which is accepted as a basis in modern Ukraine, provides economic stimulation of any kind of creative, scientific, technical activity by requesting payment for services rendered or work performed.

At the same time, the high cost cannot become a barrier that cannot be overcome by a person who seeks to realize the right granted by the Law of Ukraine on Education.

The general algorithm for calculating the profitability of the project involves taking into account such components as the costs of the main version of the final system

implementation (aviation simulator), as well as its alternative version. Here it is appropriate to recall the well-known truth of the opposition of such categories as Fast-High-Quality-Cheap. Of these three components, it is possible to implement only two at the same time due to the transformation of the third into its complete opposite.

Thus, it is possible to create aviation quickly and qualitatively, but it will be expensive. You can choose High-quality and Cheap, but the time to create it can approach Infinity.

The methodological basis of the calculation consists in the use of the following calculation algorithm, represented by the sequence of formulas 4.1 - 4.4.

1. Costs for the main option:

$$З_{прб} = С_б + Е_н \cdot К_б \quad (4.1)$$

2. Costs for an alternative (new) option:

$$З_{пра} = С_а + Е_н \cdot К_а \quad (4.2)$$

Sat - basic costs;

KB - capital investment;

En - standard of investment efficiency ratio, En = 0.15.

1. Payback period of additional capital investments

$$Т_{ок} = \frac{К_а - К_б}{С_б - С_а} \quad (4.3)$$

2. Annual economic effect of the implementation of the new system

$$Е_г = З_{прб} - З_{пра} = (С_б + Е_н \cdot К_б) - (С_а + Е_н \cdot К_а) \quad (4.4)$$

To perform the calculation of the effectiveness of the development of the aviation simulator system for training on a contract basis, we will set the following initial data in Ukrainian hryvnias.

For the main option, which will be performed according to the Fast and Quality approach:

$С_б$= 1,500,000

$К_б$= 1,000,000

Then the costs for the basic option, taking into account the norm of the investment efficiency ratio at the level of En = 0.15, will be according to (4.1):

$$З_{прб} = С_б + Е_н \cdot К_б = 1500000 + 0{,}15 \cdot 1000000 = 1650000$$

*An alternative option*we plan to implement according to the High Quality and Cheap scheme with the following input data:

$С_а$= 500,000

$К_а$= 800,000

Then the costs for the basic option, taking into account the norm of the investment efficiency ratio at the level of En = 0.15, will be according to (4.2):

$$З_{пра} = С_а + Е_н \cdot К_а = 500000 + 0{,}15 \cdot 800000 = 620000$$

For the obtained results, we will calculate the payback period of additional capital investments according to the formula (4.3):

$$Т_{ок} = \frac{К_а - К_б}{С_б - С_а} = \frac{800000 - 1000000}{1500000 - 500000} = -0.2$$

At the same time, the annual economic effect, which is calculated according to formula (4.4), will be as follows:

$$Е_г = З_{прб} - З_{пра} = (С_б + Е_н \cdot К_б) - (С_а + Е_н \cdot К_а) =$$

$$= 1650000 - 620000 = 1030000$$

The obtained results are fully confirmed during the automation of calculations by using an Excel file, the results in the form of a print-screen from which are shown in fig. 4.1

Summarizing the calculation, it is advisable to once again pay attention to the fact that economic efficiency, despite all its obviousness, is not the only option for assessing the overall level of efficiency, as is stated at the beginning of this section.

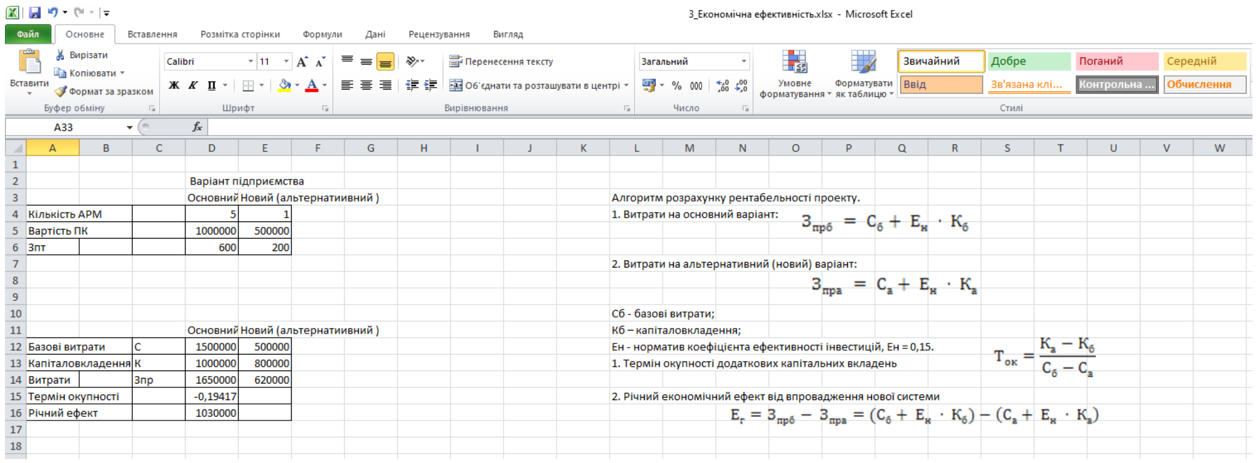

Figure 4.1 – Automation of economic calculation efficiency by means of Excel

CHAPTER 5. LABOR PROTECTION AND ENVIRONMENTAL PROTECTION

5.1 Calculation of the illumination of the working area

When working on a computer that includes an improved and optimized satellite system, the level of illumination should be optimal. Excessive lighting causes rapid fatigue of workers, which can lead to loss of work capacity and injury. Natural lighting of the room is carried out by side light through holes in the outer walls or through transparent parts of the walls.

The main value for calculating lighting is KPO. It depends on the latitude of the area, the season and the weather. It is used to regulate natural lighting.

With one-sided side lighting, the minimum value of KPO is normalized at a point located at a distance of 1 meter from the wall farthest from the light holes, at the intersection of the characteristic size of the room and the conventional working surface.

The calculation method is described in [8]. According to SNiP II-4-79/85, the normalized value of KPO for high-precision works (object of distinction from 0.3 to 0.5 mm) with the average contrast of the object of distinction and the average background for the III-th belt $e_H^{III} = 2.0\%$. For the city of Kyiv (IV zone of the world climate) KPO:

$e_H^{IV} = e_H^{III} \cdot m \cdot c$, where (5.1)

e_H^{IV} -KPO forIII belt

m –global climate factor; according to table 1.2 from [8], we find m=0.9

c- coefficient of solar climate according to table. 1.3 from [8], for light holes oriented along the azimuth of 70 degrees. coefficient c=0.8

$e_H^{IV} = 2 \cdot 0.9 \cdot 0.8 = 1.44$ (5.2)

The actual value of KPO for side lighting is calculated using the formula

$e_P^{б} = (\varepsilon_{б} \cdot q + \varepsilon_{ЗД} \cdot R) \cdot r_1 \cdot \tau_0 / K_З$, where (5.3)

$\varepsilon_б, \varepsilon_{ЗД}$ - geometric KPO at the point of calculation with side illuminationlighting, taking into account the direct light of the sky and the light reflected from the opposite building, respectively;

n1,n1`,n2,n2`- the number of rays according to schedules I and II[8] passing from the sky and the opposite building to the point of calculation in the cross-section and plan of the room;

$$\varepsilon_б = 0.01(n1 \cdot n2) \quad (5.4)$$

$$\varepsilon_{ЗД} = 0.01(n1` \cdot n2`) \quad (5.5)$$

q– the coefficient that takes into account the uneven brightness of the cloudy sky from Table 2.4 [8] for the angular height of the middle of the light hole above the working surface (Fig. 4.1).

R– the coefficient that takes into account the relative brightness of the opposite building, for a brick building, taking into account the indices of the opposite building in plan Z1 and in section Z2.

$$Z1 = \frac{l_n \cdot l}{(p+l)a}; Z2 = \frac{H \cdot l}{(p+l)a}; \quad (5.6)$$

l_n, H - the length and height of the opposite building, respectively;

l - distance from the calculation pointindoors to the outer surface of the outer wall;

p– the distance between the buildings under consideration;

and– window width in plan;

r1- the coefficient that takes into account the increase in KPO with side lighting due to reflection from the surfaces of the room and the underlying layer.

Depends on the ratio of the depth of B to the height of the window mount to the level of the working surface h1, the ratio of l to B, and the ratio of the length of the room $l_{ПОМ}$ to its depth B, the weighted average reflectance of the surfaces of the room $\rho_{СР}$:

$$\rho_{СР} = \frac{\rho_1 S_1 + \rho_2 S_2 + \rho_3 S_3}{S_1 + S_2 + S_3} \quad (5.7)$$

ρ_1, ρ_2, ρ_3-reflection coefficients, respectively, of the ceiling, walls, and floor from [8]

S_1, S_2, S_3- areas of the ceiling, floor and walls, respectively;

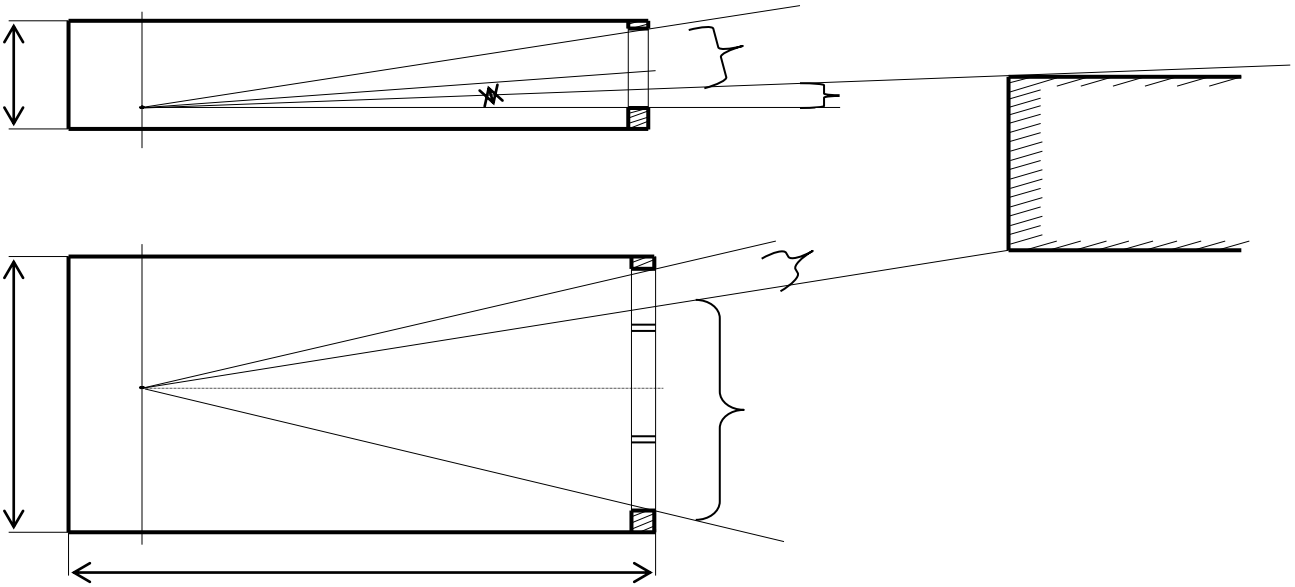

Figure 5.1 - Cross section and room plan

τ_0 - total light transmission coefficient;

$$\tau_0 = \tau_1 \tau_2 \tau_3 \tau_4 \tau_5 \quad (5.8)$$

τ_1 - the light transmission coefficient of the glazing material from table 1.8[8] for double window sheet glass;

τ_2 - the coefficient that takes into account the losses in the window frames from table 1.9.[8]

K_3 -the reserve ratio is determined according to Table 1.12 [8].

The values of the parameters determined according to the tables [8], as well as according to the plan and section of the room, the results of intermediate calculations are summarized in the table. 5.1, substituting numerical values we find:

$$\varepsilon_б = 0.01(4 \cdot 31) = 1.24$$

$$\varepsilon_{ЗД} = 0.01(1 \cdot 19`) = 0.19 \quad Z1 = \frac{30 \cdot 4.25}{(40 + 4.25)3.6} = 0.8 \quad Z2 = \frac{10 \cdot 4.25}{(40 + 4.25)3.6} = 0.27$$

Table 5.1 - Initial data and values of coefficients for calculating KPO.

Output data and coefficients	Value	Output data and coefficients	Value
n1	4	ρ_2	0.7
n1`	1	ρ_3	0.1
n2	31	S_1	$25\,m^2$
n2`	19	S_2	$49\,m^2$
$\varepsilon_б$	1.24	S_3	$25\,m^2$
$\varepsilon_{ЗД}$	0.19		
α	14	ρ_{CP}	0.55
q	0.64	*B/h1*	2.4
l_n	30 m	$l\ /B$	0.8
H	10 m	$l_{ПОМ}/B$	1
l	4.25 m	r_1	2.5
p	40 m		
a	3.6 m	τ_1	0.8
h1`	2.8 m	τ_2	0.7
h1	2.1 m	τ_3	1
B	5 m	τ_4	1
$l_{ПОМ}$	5 m	τ_5	1
		τ_0	
Z1	0.8	$K_З$	0.56
Z2	0.27	*R*	1.5
ρ_1	0.7		0.25

$$\rho_{CP} = \frac{0.7 \cdot 2.5 + 0.7 \cdot 49 + 0.1 \cdot 25}{25 + 49 + 25} = 0.55, \tau_0 = 0.8 \cdot 0.7 \cdot 1 \cdot 1 \cdot = 0.56$$

As a result, we get:

$$e_P^{\delta} = (1.24 \cdot 0.64 + 0.19 \cdot 0.25) \cdot 2.5 \cdot 0.56/1.5 = 0.79$$

The calculated KPO is 2 times less than the norm. This means that workplaces must be located near the windows of the room, so that they are located in a zone within which the actual value of KPO is greater than or equal to the norm, or it is necessary to use common lighting with the corresponding KPO norm $e_H^{III} = 0.9$ at the same time, using formula (4.2), we determine:

$$e_H^{IV} = 0.9 \cdot 0.8 \cdot 0.75 = 0.55$$

At the same time, the norms of SNiPII-4-79/85 will be observed within the entire premises.

We will carry out a verification calculation of artificial lighting according to the method described in [9]. Figure 4.2 shows the scheme for determining the conditions for applying calculation methods. With rows of small length (ln/n <3), the actual illumination of the working surface is determined by the formula

$$E = \frac{N \cdot n \cdot \Phi_{Л} \cdot \mu \cdot \sum_{i=1}^{m} \varepsilon_i \cdot \varphi_i}{1000 \cdot K_З \cdot h^2 \cdot l_p} \quad (5.9)$$

N- the number of lamps in the room;

n- the number of lamps in the lamp;

$\Phi_{Л}$ - luminous flux of the lamp, lm;

μ - the coefficient that takes into account the increase in illumination;

ε_i - relative illumination at the point of calculation, pcreated by the i-th half-row of lamps.

φ_i - reserve factor;

h- the height of the lamp suspensions; h=3-0.3-0.8=3m

lp- the length of a row of lamps; lp=3.4 m

For lamps of the LB40 type, used for lighting this room, the luminous flux is according to table 1.1.[9] $\Phi_{Л}$ =3120*lm*

We have n=4, N=4, $K_З = 1.5, \mu = 1.2, m = 2$

To determine the table value of the function ε we find the relationship $p`=p/n$,

where p is the distance from the calculation point to the projection of a row of lamps on the horizontal plane.

$l`=l2/n$, $l2$ is the distance from the calculation point to the wall.

$p'=1/4=0.25$ $l'=2.5/4=0.62$

For the corner α=25 under which the light U falls α= *162 lm*. According to table 1.10 [9] according to U α, for lamps of the 9th group, we determine f(p`,l`)=0.55 Then ε *=f(p`,l`) U* α*=0.55*162=89*

By substituting numerical data, we get:

$$E = \frac{4 \cdot 4 \cdot 3120 \cdot 1.2 \cdot 8.9}{1000 \cdot 1.5 \cdot 4 \cdot 3.4} = 560 лк$$

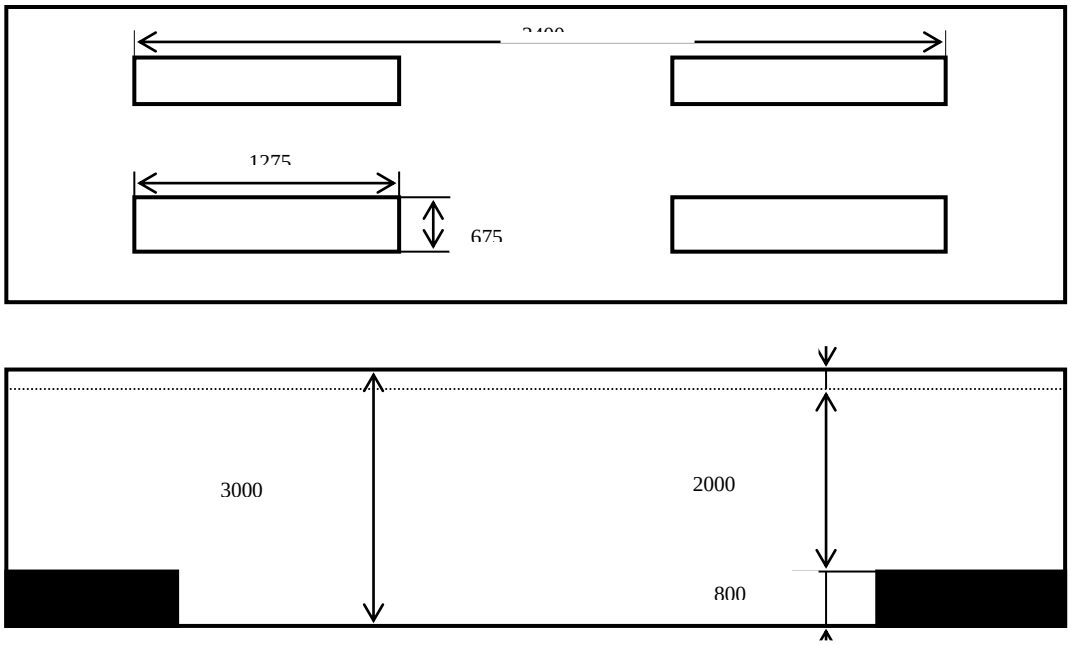

Figure 5.2 – Scheme for applying the calculation method

a) location of lamps

b) determination of the distance from the lamps to the surface of the tables (1 – workplaces)

According to the table, we determine the value of normalized illumination. For high-precision works (object of resolution from 0.3 to 0.5 mm) with an average contrast

of the object of resolution with the background with an average background, we find En=500lux.

Due to the fact that the calculated actual value of illumination is greater than the norm, we conclude about the suitability of the lighting system in the room.

5.2 Fire and explosion safety

Some substances and materials used at the installation site are fire-explosive. These substances and some of their characteristics, as well as fire extinguishing agents are listed in the table. 5.2.

Table 5.2 - Fire-hazardous substances used during the production of the printed unit.

The name of the substance	Ignition temperature	Temperature of self-occupation	Explosive limits		Fire extinguishing means
			Lower	Upper	
Rosin	-	850 ^{o}C	12.6 $г/м^3$	-	Chemical and air-mechanical foam, sprayed water
Ethyl gasoline alcohol	8 ^{o}C	104 ^{o}C	3.6%; 68 $г/м^3$	19%; 340 $г/м^3$	Chemical foam, water, inert gases
Gasoline	7-44 ^{o}C	255-474 ^{o}C	0.76-1.1%	5.16-8.12%	Foam, water vapor, inert gases
Glass-textolite	-	-	-	-	Water, chemical foam

In order to determine the category of the room according to explosion and fire hazard in accordance with ONTP 24-86, it is necessary to calculate the excessive pressure of the explosion in the room. The overpressure of the explosion is determined by the following formula:

$$\Delta P = [P_{MAX} - P_0] \frac{m \cdot Z}{V_{CB} \cdot \rho_{ГП}} \cdot \frac{100}{C_{CT}} \cdot \frac{1}{K_u} \quad (5.9)$$

P_{MAX} -the maximum explosion pressure of a stoichiometric gas-air or vapor-air mixture in a closed volume (P_{MAX} *=750kPA);*

P_0 - initial pressure, P_0 *=101 kPa;*

m – mass of combustible substance, kg;

Z is the evaporation area, m^2;

V_{CB} -free volume of the room;

$\rho_{ГП}$ - steam and gas density ($\rho_{этилового\_спирта\_по\_воздуху} = 1.6 кг/м^3$)

St– stoichiometric concentration of combustible gas or vapors, %;

Ky- the coefficient that takes into account the leakiness of the room and the non-adiabatic nature of the combustion process, Ki=3;

Free volThe volume of the room is determined by the formula:

$$V_{CB} = 0.8 \cdot V_{ПОЛН} \quad (5.10)$$

The stoichiometric concentration is determined by the formula

$$C_{CT} = \frac{100}{1 + 4.84 \cdot \beta} \quad (5.11)$$

β - stoichiometric coefficient of oxygen in the combustion reaction.

$$\beta = n_e + \frac{n_n + n_x}{4} - \frac{n_0}{2} \quad (5.12)$$

n_0, n_x, n_n, n_e - the number of C, H, O atoms and halides in the fuel molecule;

We calculate ΔP according to the above method, accepting $V_{ПОЛН} = 75 м^3$

0.3 liters of alcohol is consumed daily at the installation site; the worst-case calculation has been made; all contents enter the room (for 0.3 l of flammable liquid, the spill area is $0.3 м^2$);

The mass of liquid vapor is determined by the formula

$$m = W \cdot S \cdot T$$

W - intensity of evaporation, $кг \cdot с^{-1} \cdot м^{-2}$;

S - evaporation area, m^2;

T - duration of evaporation ($T = 3600c$)

We will determine the intensity of evaporation as follows

$W = 10^{-6} \cdot \eta \cdot \sqrt{M} \cdot P_H$ (5.13)

η - coefficient chosen from[8] depending on the speed and temperature of the air above the liquid surface ($\eta = 3.5$);

M - molecular weight ($M = 46 г/моль$);

P_H - steam pressure C_2H_5OH ($P_H = 5.85 кПа$);

From reference data for C_2H_5OH :

$W = 1.38 \cdot 10^{-6} кг \cdot с^{-1} \cdot м^{-2}$

Then:

$m = 1.38 \cdot 10^{-6} \cdot 0.3 \cdot 3600 = 0.15 кг$, $\beta = 2 + \frac{5}{4} - \frac{1}{2} = 2.75$,

$C_{CT} = \frac{100}{1 + 4.84 \cdot 2.75} \approx 7.0\%$, $V_{CB} = 0.8 \cdot 75 = 60 м^3$,

$\Delta P = [750 - 101] \frac{0.15 \cdot 0.3}{60 \cdot 1.6} \cdot \frac{100}{7} \cdot \frac{1}{3} = 1.4 кПа$

As a result of the calculation, we make a conclusion about assigning the room to the B fire hazard category.Since explosive mixtures of combustible gases and vapors with air are not formed in the premises, but are formed only as a result of an accident or malfunction, the premises can be classified as class B-lb explosive zones.

The main causes of fire are:

-violation of accepted fire safety rules and dangerous handling of fire;

- malfunction and overload of electrical devices (short circuit);

- malfunction of the ventilation system, which causes self-occupation or dust explosion;

- careless and dangerous handling of fire;

-self-use of cotton tissue impregnated with oil, gasoline or alcohol;

- static electricity generated by the friction of dust or gases in ventilator installations;

- lightning discharges in the absence or malfunction of lightning rods.

In the premises where the installation of printed circuit boards takes place, we provide an electric fire alarm system (five POST-1 type annunciators), which serves to quickly notify the firefighting service about the occurrence of a fire.

The number of located fire extinguishers in the working room meets the requirements of ISO 3941-77.

All fire safety requirements are met in the workplace in accordance with the requirements of NAPB A.01.001-95 "Fire Safety Rules in Ukraine".

It is not allowed to block the entrance to the room, the passages between the tables and the corridors with various things and equipment. Special cabinets and containers are provided for storing all substances and materials.

We plan to conduct fire prevention briefings, classes and discussions with workers and service personnel.

General conclusions

1. In the course of the analytical review performed in the first section of the work, it is shown that satellite communication, navigation and surveillance technologies are widely used today in the aviation industry. In the future, their application will become even more extensive, as it is laid down in the concept of CNS/ATM.

2. A feature of the implementation of satellite systems for various purposes is the need to take into account the physics of the movement of artificial satellites, which leads to the emergence of different classifications of these systems according to the method of implementing orbits and broadcasting radio signals from space. These questions are explained in detail in the second chapter of the work.

3. In the third section, the method of conducting a study on the evaluation of the effectiveness of satellite navigation systems is proposed. For its implementation, up-to-date information on the current status of various satellite systems included in the Global Navigation Satellite System (GNSS) was taken. After converting these data into a unified Yuma format, several scenarios with different combinations of satellite systems as part of the GNSS were formed. The obtained graphic and calculation results clearly showed the superiority of multi-system data processing methods over single-system ones.

4. In the fourth chapter, the economic efficiency of the computerized information system, which uses satellite data during its operation, is calculated.

5. The fifth section of the work is devoted to occupational health and safety issues.

REFERENCES

1. [Electronic resource]. – Access:https://earthobservatory.nasa.gov
2. [Electronic resource]. – Access:https://www.esa.int
3. [Electronic resource]. – Access:https://www.rfwireless-world.com/Terminology/Advantages-and-Disadvantages-of-LEO-orbit.html
4. access mode: https://lotusarise.com/satellite-frequency-bands-upsc/
5. ORBCOMM satellite systems [Electronic resource]. – Access:https://www.orbcomm.com/en/networks/satellite
6. "Iridium satellites". N2yo.com. [Electronic resource]. – Access:https://www.n2yo.com/satellites
7. Order Starlink https://www.starlink.com
8. WorldVu Satellites Limited, OneWeb Ka-band NGSO constellation FCC filing SAT-LOI-20160428-00041.
9. Mishne, D. Formation Control of Satellites Subject to Drag Variations and J2 Perturbations. J. Guid. Control. Dyn. 2004, 27, 685–692.
10. Wertz, JR Orbit and Constellation Design and Management. Space Technology Library, Microcosm Press and Springer: Berlin, Germany, 2001.
11. Ferdowsi, A.; Challita, U.; Saad, W.; Mandayam, NB Robust Deep Reinforcement Learning for Security and Safety in Autonomous Vehicle Systems. In Proceedings of the 2018 21st International Conference on Intelligent Transportation Systems (ITSC), Maui, HI, USA, November 4–7, 2018; pp. 307–312.
12. Green, JC; Likar, J.; Shprits, Y. Impact of space weather on the satellite industry. Space Weather. 2017, 15, 804–818.
13. The Impact of the Space Environment on Space Systems [Electronic resource]. – Access:https://apps.dtic.mil/sti/citations/ADA376872
14. Curzi, G.; Modenini, D.; Tortora, P. Large constellations of small satellites: A survey of near future challenges and missions. Aerospace 2020, 7, 133.

15. Jakob, P.; Shimizu, S.; Yoshikawa, S.; Ho, K. Optimal Satellite Constellation Spare Strategy Using Multi-Echelon Inventory Control. J. Spacecr. Rocket. 2019, 56, 1449–1461.

16. C. Poivey. Radiation Hardness Assurance for Space Systems. In NASA Report.

17. Gogoi, B.; Kumari, A.; Nirmala, S.; Kartik, A. IRNSS Constellation Optimization: A Multi-objective Genetic Algorithm Approach. In Advances in Intelligent Systems and Computing. Springer: Singapore, 2020; Volume 1025, pp. 19.

18. [Electronic resource]. – Access:https://www.mdpi.com/2326- 4310/7/9/133

19. Cornara, S.; Beech, T.; Bello-Mora, M.; Martinez de Aragon, A. Satellite Constellation Launch, Deployment, Replacement and End-of-Life Strategies. Small Satellite Conference. 1999.

20. Alkadi, R.; Alnuaimi, N.; Yeun, C.; Shoufan, A. Blockchain Interoperability in Unmanned Aerial Vehicles Networks: State-of-the-art and Open Issues. IEEE Access 2023, 10, 14463–14479.

21. Maeng, SJ; Yapici, Y.; Guvenc, I.; Bhuyan, A.; Dai, H. Precoder Design for Physical-Layer Security and Authentication in Massive MIMO UAV Communications. IEEE Trans. Veh. Technol. 2021, 1.

22. Ralegankar, VK; Bagul, J.; Thakkar, B.; Gupta, R.; Tanwar, S.; Sharma, G.; Davidson, IE Quantum Cryptography-as-a-Service for Secure UAV Communication: Applications, Challenges, and Case Studies. IEEE Access 2023, 10, 1475–1492.

23. Taxonomy and Definitions for Terms Related to Driving Automation Systems for On-Road Motor Vehicles Society of Automotive Engineers. 2021.

24. Lim, H.; Ryu, H.; Rhudy, MB; Lee, D.; Jang, D.; Lee, C.; Park, Y.; Youn, W.; Myung, H. Deep Learning-Aided Synthetic Airspeed Estimation of UAVs for Analytical Redundancy With a Temporal Convolutional Network. IEEE Robot.

25. Yeong, DJ; Velasco-Hernandez, G.; Barry, J.; Walsh, J. Sensor and Sensor Fusion Technology in Autonomous Vehicles: A Review. Sensors 2021, 21, 2140.

26. Lai, Q.; Yuan, H.; Wei, D.; Wang, N.; Li, Z.; Ji, X. A Multi-Sensor Tight

Fusion Method Designed for Vehicle Navigation.

27. Reid, TG; Chan, B.; Goel, A.; Gunning, K.; Manning, B.; Martin, J.; Neish, A.; Perkins, A.; Tarantino, P. Satellite Navigation for the Age of Autonomy. In

28. Proceedings of the 2020 IEEE/ION Position, Location and Navigation Symposium (PLANS), Portland, OR, USA, April 20–23, 2020; pp. 342–352.

29. Garcia, AE; Ozger, M.; Baltaci, A.; Hofmann, S.; Gera, D.; Nilsson, M.; Cavdar, C.; Schupke, D. Direct Air to Ground Communications for Flying Vehicles: Measurement and Scaling Study for 5G. In Proceedings of the 2019 IEEE 2nd 5G World Forum (5GWF), Dresden, Germany, 30 September–2 October 2019; pp. 310–315.

30. Gaber, A.; ElBahaay, MA; Maher Mohamed, A.; Zaki, MM; Samir Abdo, A.; AbdelBaki, N. 5G and Satellite Network Convergence: Survey for Opportunities, Challenges and Enabler Technologies. In Proceedings of the 2020 2nd Novel Intelligent and Leading Emerging Sciences Conference (NILES), Giza, Egypt, 24–26 October 2020; pp. 366–373.

31. Kohani, S.; Zong, P. LEO Hybrid Satellite Constellation Design Based on Multi-purpose Genetic Algorithm to Optimize Cost and Reliability of Global Coverage. Wseas Trans. Commun. 2020, 19, 71–80.

32. Deng, R.; Di, B.; Zhang, H.; Song, L. Ultra-Dense LEO Satellite Constellation Design for Global Coverage in Terrestrial-Satellite Networks. In Proceedings of the GLOBECOM 2020-2020 IEEE Global Communications Conference, Taipei, Taiwan, December 7–11, 2020; pp. 1–6.

33. Kak, A.; Akyildiz, IF Designing Large-Scale Constellations for the Internet of Space Things With CubeSats. IEEE Internet Things J. 2021, 8, 1749–1768.

34. Amit, RA; Mohan, CK A Robust Airport Runway Detection Network Based on R-CNN Using Remote Sensing Images. IEEE Aerosp. Electron. Syst. Mag. 2021, 36, 4–20.

35. Niu, Z.; Shen, XS; Zhang, Q.; Tang, Y. Space-air-ground integrated vehicular network for connected and automated vehicles: Challenges and solutions. Intel. Converg. Netw. 2020, 1, 142–169.

36. Juan, E.; Lauridsen, M.; Wigard, J.; Mogensen, PE 5G New Radio Mobility Performance in LEO-based Non-Terrestrial Networks. In Proceedings of the 2020 IEEE Globecom Workshops (GC Wkshps), Taipei, Taiwan, 7–11 December 2020.

37. Tan, L.; Yu, K.; Lin, L.; Cheng, X.; Srivastava, G.; Lin, JCW; Wei, W. Speech Emotion Recognition Enhanced Traffic Efficiency Solution for Autonomous Vehicles in a 5G-Enabled Space-Air-Ground Integrated Intelligent Transportation System. IEEE Trans. Intel. Transp. Syst. 2021, 1–13.

38. Li, K.; Li, Y.; Qiu, Z.; Wang, Q.; Lu, J.; Zhou, W. Handover Procedure Design and Performance Optimization Strategy in LEO-HAP System. In Proceedings of the 2019 11th International Conference on Wireless Communications and Signal Processing (WCSP), Xi'an, China, 23–25 October 2019; pp. 1–7.

39. He, S.; Wang, T.; Wang, S. Load-Aware Satellite Handover Strategy Based on Multi-Agent Reinforcement Learning. In Proceedings of the GLOBECOM 2020-2020 IEEE Global Communications Conference, Taipei, Taiwan, December 7–11, 2020; pp. 1–6.

40. [Electronic resource]. – Access:http://www.celestrak.com/NORAD/documentation/ tle-fmt.php)

41. Space Connected. 2019. Access:https://audacy.space/

42. SK Rao, ``Advanced antenna technologies for satellite communications payloads," IEEE Trans. Antennas Propag., vol. 63, no. 4, pp. 1205–1217, Apr. 2015.

43. Xuanfeng Tong, Zhi Hao Jiang, Yuan Li, Fan Wu, Ronan Sauleau, Wei Hong, "Dual-Wideband Dual-Circularly-Polarized Shared-Aperture Reflectarrays With a Single Functional Substrate for K-/Ka-Band Applications", IEEE Transactions on Antennas and Propagation, vol.70, no.7, pp.5404-5417, 2023.

44. A. Babuscia, T. Choi, J. Sauder, A. Chandra and J. Thangavelautham, "Inflatable antenna for CubeSats: Development of the X-band prototype", 2016 IEEE Aerospace Conference, pp. 1-11, 2016.

45. CA Balanis, Antenna Theory: Analysis and Design, USA, NJ, Hoboken: Wiley-Interscience, 2005.

46. R. Sandau, "Status and trends of small satellite missions for earth observation", Acta Astronautica, vol. 66, no. 1–2, pp. 1-12, 2010.

47. H. Zhang, H. Herdian, AT Narayanan, A. Shirane, M. Suzuki, K. Harasaka,

48. K. Adachi, S. Yanagimachi, and K. Okada, "29.4 ultra-lowpower atomic clock for satellite constellation with 2.2×10−12long-term Allan deviation using cesium coherent population trapping," in IEEE Int. Solid-State Circuits Conf. (ISSCC) Dig. Tech. Papers, Feb. 2019, pp. 462–464.)

49. Chobotov, VA Orbital Mechanics; Aiaa: Reston, VA, USA, 2002.

50. Mortari, D.; Wilkins, MP; Bruccoleri, C. The Flower Constellations. J. Astronaut. Sci. 2004, 52, 107–127.

51. Avendaño, ME; Davis, JJ; Mortari, D. The 2-D lattice theory of Flower Constellations. Celeste. Mech. Dyn. Astron. 2013, 116, 325–337.

52. Davis, JJ; Avendaño, ME; Mortari, D. The 3-D lattice theory of Flower Constellations. Celeste. Mech. Dyn. Astron. 2013, 116, 339–356.

53. Satellite radio navigation systems/V.V. Konin, V.P. Harchenko; National Aviation University. - K.: Holtech, 2010. -233.

54. [Electronic resource]. – Access: https://gisgeography.com/gps-accuracy-hdop-pdop-gdop-multipath/

55. H. Benzerrouk, Q. Nguyen, F. Xiaoxing, A. Amrhar, AV Nebylov, and R. Landry, “Alternative PNT based on Iridium Next LEO satellite-lites Doppler/INS integrated navigation system,” in 2019 26th SaintPetersburg International Conference on Integrated Navigation Systems (ICINS), 2019, pp. 1–10

56. H. Benzerrouk, Q. Nguyen, F. Xiaoxing, A. Amrhar, H. Rasaee, andR. J. Landry, “LEO satellites based doppler positioning using distributed nonlinear estimation,” IFAC-PapersOnLine, vol. 52, no. 12, pp. 496 –501, 2019, 21st IFAC Symposium on Automatic Control in Aerospace.

57. J. Wertz, Mission Geometry: Orbit and Constellation Design and Management: Spacecraft Orbit and Attitude Systems. Portland, OR, USA: Microcosm

Press, 2001.

58. Al-Hourani, A. Optimal Satellite Constellation Altitude for Maximal Coverage. IEEE Wirel.